2016

Variations of the Subclavian Arterial Branching Pattern and Maximization of its

Juwan Ryu
Western University, jryu22@uwo.ca

Variations of the Subclavian Arterial Branching Pattern and Maximization of its Supraclavicular Surgical Exposure

(Project format: Integrated)

by

Juwan Ryu

Graduate Program in Anatomy and Cell Biology
Division of Clinical Anatomy

A project submitted in partial fulfillment
of the requirements for the degree of
Master's of Science

The School of Graduate and Postdoctoral Studies
The University of Western Ontario
London, Ontario, Canada

Abstract

The subclavian artery (SCA) is an important vessel with several branches. However, significant pattern variations exist. Characterizing SCA branches and its relationships to landmark structures like the anterior scalene muscle (ASM) is important in surgery. Computed Tomography Angiograms from 55 patients were retrospectively analyzed using Aquarius iNtuition. Measurements were taken of: distance of origin of SCA branches from the aorta and the ASM-VA origin distance. Only 13 SCAs (12.9%) exhibited the highest prevalence in typical branching pattern. VA originated 1st in 80.2% of SCAs, with ITA arising 2nd (41.3%), TCT 3rd (47.3%), CCT 4th (43.6%) and DSA 5th branch (56.9%). Average VA-ASM distance was 14.14mm with 94.9% of VAs originating within 30mm proximal to the medial border of ASM. The subclavian artery branching order and pattern may present significant variation from the typical order. ASM is reliably positioned proximal to VA and may be used as a landmark for VA.

Keywords

Subclavian artery, Morphological variations, Anterior scalene muscle landmark, Branching patterns, Vertebral artery, Supraclavicular triangle, Shoulder manipulations

List of Abbreviations

SCA	Subclavian Artery
CCA	Common Carotid Artery
VA	Vertebral Artery
ITA	Internal Thoracic Artery
TCT	Thyrocervical Trunk
CCT	Costocervical Trunk
DSA	Dorsal Scapular Artery
CTA	Computed Tomography Angiogram
ASM	Anterior Scalene Muscle
SCT	Supraclavicular Triangle

Acknowledgments

First and foremost, I would like to thank Dr. Adam Power. I still remember what you told me: *"There are those who crumble under the face of hardship and harsh words. And there are those who face defeat, say "I got to do better", and pick themselves up."* During the times when I had misplaced my focus, your words of motivation helped to set my course straight and take ownership of this project. You have inspired me beyond words, gave me a chance to reflect on myself, and pushed me to become better. I will continue to remember the lessons that you've taught me as I step forward as a student, and a person.

Secondly, I would like to give tremendous thanks to Oonagh Scallan. From the outset, you have been a wonderful source of help, and your enthusiasm and eagerness have inspired me to strive to become a student of your caliber. This project would not be complete without you!

Third, I want to express my sincere gratitude to my supervisory committee, Dr.Marjorie Johnson and Dr.Tim Wilson. You have both welcomed my questions with open doors and smiling faces at all times, and guided me within this research project, as well as outside, in the classroom and in the anatomy lab.

Lastly, I want to thank the Department of Clinical Anatomy. Kevin Walker and Haley Linklater, thank you for keeping me company and your enormous help down in the morgue. To the second year graduates, especially Jackie Yang, there is no other group of people that I would rather choose to work alongside if I had to do it all over again. A big thank you to my mom, dad and sister for your encouragement and support throughout this program, both financially, and morally. ☺

Table of Contents

List of Tables

List of Figures

List of Appendices

Chapter 1
Introduction and Literature Review

1.1 Introduction

The human body presents itself with countless differences in structure and many of these variations have been documented in anatomical literature. One such case is the subclavian artery (SCA) and the numerous arterial branches that originate from it. The SCA and its branches are documented in literature to present significant variation in pattern and origin, however, there is no consolidated study describing the prevalence of these different variations. As these branches present much variation, they are not well described in their relationships to surrounding structures and may be difficult to locate with ease in a given anatomical space. The vertebral artery (VA), an important branch of the SCA, is one such example and has been studied little in its relationship to neighboring anatomical structures for identification and acquisition. To complicate matters further, the SCA and its variations in branching reside in a compact and complex anatomical space. SCA's particular location presents much difficulty in its exposure during surgery, in addition to its variability with patient positioning during operative procedures. All in all, there is much uncertainty and variability in literature surrounding the subclavian artery and its exposure, and examination of these differences may prove to be beneficial.

1.2 Anatomical Introduction

1.2.1 Aorta and Supra-Aortic Vessels

The aorta is the largest artery in the human body. The aorta arises from the left ventricle of the heart to deliver oxygenated blood throughout the systemic circulation. It is situated in the chest cavity throughout the mediastinum and is divided into three anatomical sections: ascending aorta, arch of aorta, and descending (thoracic) aorta.

The ascending aorta spans superiorly from its origin at the left ventricle to the arch of aorta at the level of the thoracic plane (level of T4-T5). The arch of aorta is located in the superior mediastinum, beginning and ending its arch at the level of the thoracic plane, eventually progressing posteriorly to the posterior mediastinum as the descending aorta (also known as thoracic aorta).

The arch of aorta usually gives off three major vessels, from proximal to distal: brachiocephalic artery (BCT), left common carotid artery (LCCA), and left subclavian artery (LSCA). The BCT branches distally to become right subclavian artery and right common carotid artery and supply the right side of the upper extremity, neck and head. Subsequently, the LCCA provides blood supply to the left neck and head, and originating most distally, the LSCA supplies the left upper extremity, neck and head. These supra-aortic vessels are extremely important in providing vascularization to the upper body and occlusion of any of these vessels may lead to an impairment of neurological functioning (Moore et al., 2013).

1.2.2 Prevalence of Subclavian Arterial Branches

The subclavian arteries begin their course posterior to the sternoclavicular joints and within the boundaries of the superior thoracic aperture from their respective supra-aortic origins (left from aorta; right from BCT). Bilaterally, these vessels ascend superolaterally, arching posterior to the clavicle and descending on the superior surface of the first rib prior to becoming axillary arteries at the lateral edges of the ribs (Moore et al., 2013).

The subclavian artery is a substantial vessel with several branches. Most commonly reported branches originating from the SCA are, in no particular order: vertebral artery (VA), internal thoracic artery (ITA), thyrocervical trunk (TCT), costocervical trunk (CCT), and dorsal scapular artery (DSA).

1.2.2.1 Vertebral Artery

The vertebral artery (VA) is characteristically illustrated as the first branch of the SCA. Following its origin, VA ascends along the cervical vertebrae to typically enter the 6th transverse foramen and proceeds superiorly to the cranium where it enters through the foramen magnum prior to forming basilar artery with the contralateral VA (Matula et al., 1997). Vertebral artery is a vessel of great importance for its contribution to the posterior brain circulation through the vertebrobasilar system, which accounts for approximately 30% of the blood to the brain (Dodevski et al., 2012). There have been a number of anomalous variations in the VA origin reported in literature, some of which are origins from the aortic arch (Matula et al., 1997), common carotid artery (Matula et al., 1997), and brachiocephalic trunk (Bhatia, 2005). Despite the relatively low frequency of anomalous VA origins, the incidence of variation has been reported to be higher on the left than the right SCA (Poonam & Sharma, 2010). In a study by Yamaki et al., the prevalence of VA origin from the SCA was reported to be 94.2% (left) and 100% (right), presenting a high degree of reliability in its origin from the SCA (Yamaki et al., 2006).

1.2.2.2 Thyrocervical Trunk

The thyrocervical trunk (TCT) is typically comprised of four arteries: ascending cervical artery, inferior thyroid artery, suprascapular artery and transverse cervical artery. The thyrocervical trunk has been extensively reported in literature for its high variation in branching patterns and arterial contribution (Huelke, 1958; Lischka et al., 1982; Weiglein et al., 2005). Generally, it arises from the anterosuperior side of the SCA immediately proximal to the medial border of the anterior scalene muscle, and supplies the thyroid gland, upper neck and shoulder muscles (Moore et al., 2013).

1.2.2.3 Internal Thoracic Artery

The internal thoracic artery (ITA) arises on the anteroinferior aspect of the SCA, coursing inferiorly along the anterior thoracic wall to segmentally branch into intercostal arteries at each rib level to supply the thorax. ITA has been reported to originate directly from SCA with high prevalence (left=70%, right=95%), (Henriquez-Pino et al., 1997).

1.2.2.4 Costocervical Trunk

The costocervical trunk (CCT) originates on the posterior aspect of the SCA and generally gives off two branches: deep cervical artery and superior intercostal artery, which supply deep neck muscles and first two intercostal spaces, respectively (Moore et al., 2013). It has also been reported that an accessory ascending cervical artery may arise independently from the SCA in the absence of CCT and may represent a variation of the deep cervical artery of the CCT (Su et al., 2000).

1.2.2.5 Dorsal Scapular Artery

The dorsal scapular artery (DSA) often arises from the transverse cervical artery (~25%), a branch of the TCT, but has been reported to originate on the SCA with a much higher frequency (~75%), (Reiner & Kasser, 1996; Huelke, 1958). The DSA courses posterolaterally towards the scapulae, along with the dorsal scapular nerve to supply the levator scapulae, rhomboids and contribute to the anastomosis of the shoulder (Moore et al., 2013; Reiner & Kasser, 1996).

1.2.3 Subclavian Arterial Branching Pattern

The prevalence of subclavian arterial branches is well documented in literature. In addition, the variation patterns of branches arising from thyrocervical trunk (Lischka et al., 1982), costocervical trunk (Su et al., 2000) and dorsal scapular arteries (Reiner & Kasser, 1996) are well documented. However, with respect to the subclavian artery, there has been consolidated literature on the prevalence of variations in the relative pattern and order of its branches. In reference to some of the widely used anatomy atlases in medical education, Cunningham's (1818) (Figure 1B), Grant's (Drake et al., 2014) (Figure 1C), Moore's (Moore et al., 2013) (Figure 1D), and Netter's (2014) (Figure 1E) all illustrate differing subclavian arterial branching patterns from one another and do not provide evidence to their prevalence. A sample legend has been provided (Figure 1A).

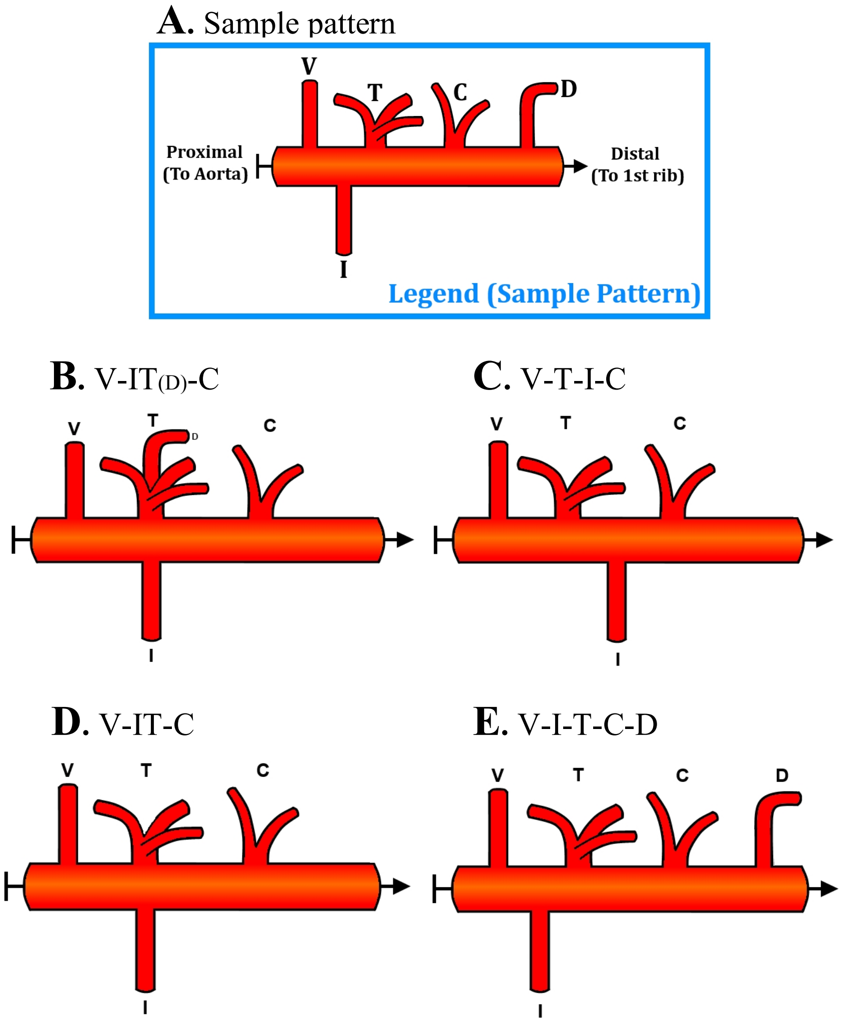

Figure 1 Illustration of differing subclavian arterial branching patterns found in some of the popular medical textbooks: Cunningham's (B), Grant's (C), Moore's (D) and Netter's (E). Figure 1A has been included as as legend. Vessel branches are: vertebral (V), internal thoracic (I), thyrocervical (T), costocervical (C) and dorsal scapular (D).

1.3 Aortic Aneurysms and Stent-Graft Interventions

1.3.1 Introduction to Aortic Aneurysms

Aortic aneurysms (AA) are abnormal, balloon-like enlargements of the aorta which impede blood flow and lead to an increasingly weakening of the aortic wall. AAs can occur in any segment of the thoracic aorta, with the sites of common incidence being the ascending aorta (60%), arch of the aorta (10%), and descending aorta (40%) (Isselbacher, 2005). The incidence is estimated to be approximately six out of 100,000 per year (Bickerstaff et al., 1982), but trends in population studies indicate annual increases in AA prevalence (Coady et al., 1999). There seems to be a strong genetic component in the formation of an AA, in addition to atherosclerosis, hypertension, hypercholesterolemia, and smoking (Klein, 2005).

If remained untreated, it results in a progressive widening of aortic lumen size with an average increase of 0.29cm in diameter annually, with the risk of rupture increasing with the aneurysm size (Coady et al., 1997). Aortic rupture has been shown to occur in diameters as small as 4.0-4.9cm, with the highest occurrence in sizes larger than 6.0cm (Davies et al., 2002). The rates of rupture in patients without surgical intervention ranges between 21-74% (Clouse et al., 1998; Bickerstaff et al., 1982), with the mortality rate for an aortic rupture event being extremely high, ranging from 97-100% (Johansson, 1995).

The cause for concern is compounded by the finding that over 95% of TAAs are asymptomatic (Elefteriades & Rizzo, 2007) and tend to be overlooked in many clinical situations until incidentally discovered.

1.3.2 Interventions to Aortic Aneurysms

Current AA interventions are categorized into an open surgical repair (SR) or endovascular repair (EVAR). Surgical repair involves an open-chest approach where the affected segment of the aorta is replaced with a synthetic polyester tube called a “graft”. In EVAR, a long delivery catheter containing an expandable “stent-graft” is inserted into the arterial lumen and moved up until it is deployed at the affected site, reinforcing the aortic wall and allowing blood flow without exerting pressure on the aneurysm. It is minimally invasive and eliminates the need for thoracic surgeries

SR has been the predominant surgical intervention for aortic aneurysm in the past 50 years and was considered the gold standard for aortic repairs. However, meta-analysis of comparative studies assessing SR and EVAR post-operative complications have shown that EVAR is associated with a significantly lower mortality, morbidity, and risk of neurologic deficits (Xenos et al., 2008). For these reasons, EVAR has been emerging as a safer and preferred therapeutic alternative to open aortic surgery (Goodney et al., 2011; Schouchoff, 2000).

There are different types of EVAR procedures, each characterized by the type of stent-graft device and the technique employed: Fenestrated stent-graft (Oderich & Ricotta, 2009), branched stent-graft (Saito et al., 2005), retrograde stent-graft (Baldwin et al., 2008), etc. In all cases of stent-graft deployment in EVAR, an adequate proximal and distal “landing zones” along the length of the aorta are required.

1.3.3 Landing Zones and SCA Coverage

Landing zones are pre-defined regions of the aortic wall where a stent-graft will contact the wall of the normal aorta to anchor itself and create a seal in order to prevent the interaction of blood flow and pressure with the affected aneurysmal wall. Possible stent-graft deployment failures include “endoleaks” (leakage of blood around the stent-graft into the aneurysmal sac) and “migration” (slippage of stent-grafts down the length of the aorta) which may be fatal (Chaikof et al., 2009). To prevent this, adequate thought must be given to appropriating a landing zone for an EVAR stent-graft based on the location and type of AA.

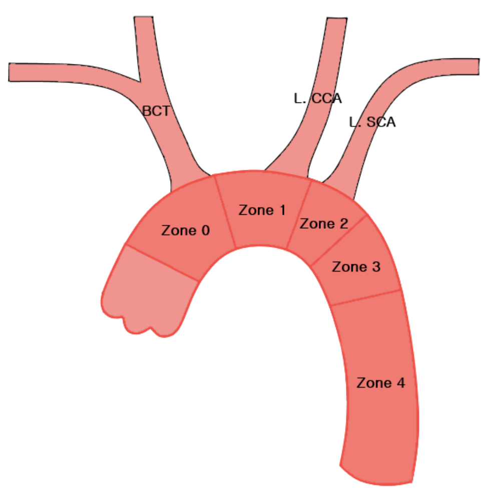

Figure 2 Landing zones (0-4) of the aorta. BCT=brachiocephalic trunk; L.CCA=left common carotid artery; L.SCA=left subclavian artery

There are a number of set proximal landing zones of the ascending, arch, and descending portions of the aorta (Zone 0-Zone 4, refer to Figure 2). Landing zones 0-2 overlap the origins of the supra-aortic vessels (brachiocephalic, left common carotid, and left subclavian artery) and an aortic stent-graft positioned in these zones results in the blockage of normal blood flow in endovascular surgeries of aortic aneurysms (Figure 3). In studies where landing zone 2 has been used, the resulting blockage of the origin of the LSCA and its branches has been shown to cause significant morbidity, some of which include paraplegia, stroke, spinal cord ischemia, upper extremity ischemia and vertebrobasilar insufficiency (Sze et al., 2009; Feezor & Lee, 2009).

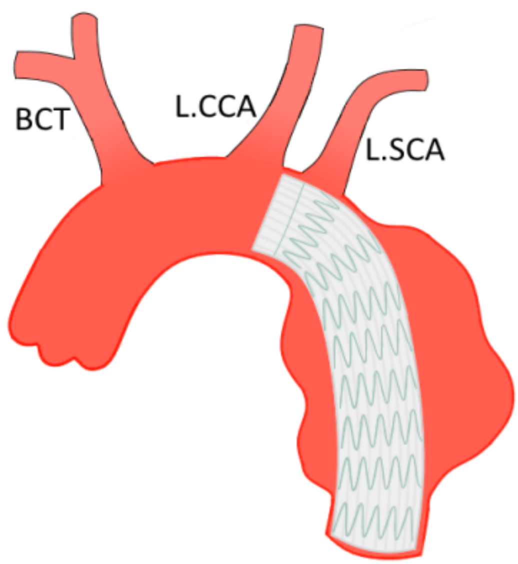

Figure 3 Thoracic Aortic Aneurysm (TAA) with a stent-graft intervention utilizing landing zone 2 resulting in L.SCA coverage. BCT=brachiocephalic trunk; L.CCA=left common carotid artery; L.SCA=left subclavian artery

There are a number of cases describing an absence of complication following an intentional blockage of LSCA. From careful reviewing of literature characterizing the perioperative complications from LSCA coverages, the most important factors which indicate possibility of developing morbidities include the presence of a dominant vertebral artery on the operative side, coronary artery to internal thoracic artery bypass, and incomplete circle of willis and vertebrobasilar circulation. Also, operative duration may play a critical role in the risk of developing a stroke (Buth et al., 2007).

Surgical treatments to LSCA coverage involve vascular reconstruction through LSCA-LCCA bypass or transposition.

1.3.4 Subclavian Reconstruction

In bypass, SCA is clamped proximal to the origin of the VA prior to excising an opening on the vessel wall and sewing on a prosthetic graft and establishing an end-to-end anastomosis with the LCCA. Following the clamp release, blood flow to the SCA and its branches is preserved through the anastomosis of the LCCA. Transposition is similar to bypass in that SCA is ligated proximal to the origin of the VA, however, the SCA is also divided at this point and the resulting stump is sutured to the LCCA to create an anastomosis (Ouriel, 1998).

In both surgical procedures, LSCA and its branches are revascularized and blood flow is maintained through the anastomosis with the LCCA to reduce risk of complications and morbidity (Holt et al., 2010; Matsumura et al., 2009). However this task becomes increasingly challenging with proximal variations in the origin of the vertebral artery.

1.3.5 Difficulties with SCA Reconstruction

The compact anatomy of the supraclavicular region presents a difficulty in manoeuvering through the operative area during surgical procedures. The vertebral artery lies deep within the supraclavicular fossa and requires a deep exposure of the SCA for its acquisition. In the proximal anatomical variations of the vertebral artery where the vertebral artery originates extremely proximal on the SCA near its origin on the aorta or on the arch of the aorta, LSCA reconstruction becomes a difficult task as the SCA cannot be accessed at its origin on the aorta through a supraclavicular incision. Exposure of the SCA at the aortic origin would require elaborate and high morbidity-associated procedures such as sternotomy.

As mentioned previously, vertebral artery provides an important blood flow to the vertebrobasilar circulation and its occlusion has been shown to present with severe morbidities. For this reason, VA origin is the crux of SCA reconstruction procedures and extreme care must be taken to preserve and maintain its vascularization along with the SCA.

1.4 Anatomical Boundaries of the Supraclavicular Triangle

The regional anatomy of the neck is divided into two, anterior and posterior triangles, using superficial landmark muscles and bones. The anterior triangle is formed by the medial margin of the sternocleidomastoid (SCM) muscle laterally, inferior margin of the body of the mandible superiorly, and the midline of the neck following a sagittal plane along the trachea. The posterior triangle is the area formed by the lateral margin of the sternocleidomastoid (SCM) medially, medial margin of the trapezoid laterally, and its base by the middle third of the clavicle (Ihnatsenka & Boezaart, 2010). Current literature describes an additional regional classification termed supraclavicular triangle (Hirokawa et al., 2010), subclavian triangle (Wechsler et al., 1989), and omoclavicular triangle (Chung et al., 2011) which overlaps—at least in part—the anatomical boundaries of the posterior triangle. Among these, the term supraclavicular triangle (SCT) has been used most often in literature.

Supraclavicular triangle is an anatomical region of interest for its importance in containing vascular, neural and muscular structures within a small area above the clavicles. However, there has been little consensus on distinguishing its boundaries in addition to a number of classification terms currently in use. Haapaniemi (1973) described the limits of SCT using: the medial border as the lateral margin of SCM, lateral border as anterior margin of trapezius, the middle 1/3 of clavicle being the inferior border, and the floor comprising of ASM and SCA. Description by Wechsler (1989) depicted an even smaller area called the subclavian triangle, bounded superiorly by the inferior belly of the omohyoid, laterally by trapezius, medially by ASM, inferiorly by clavicle and the floor comprising of middle and posterior scalene muscles. Alemanno & Vigl (2014) represented SCT boundaries to be formed by SCM (medially), trapezius (laterally) and clavicle (inferiorly), however, further subdivided SCT into two smaller triangles: omotrapezoid triangle and omoclavicular triangle. The latter was described as being bounded superiorly by the omohyoid, laterally by trapezius, medially by SCM and inferiorly by the clavicle, similar to the description of SCT by Wechsler (1989).

An inherent difficulty in utilizing the inferior belly of the omohyoid muscle to describe the upper border of the SCT is that it presents some variability in its course. The inferior belly of the omohyoid usually courses approximately 2.5cm superior to the clavicle, however, it has been reported to be posterior to the clavicle (Rai et al., 2008). The passage of the omohyoid behind the clavicle has not been associated with functional complications, however, the classification of the supraclavicular triangle becomes indiscernible (Alemanno & Vigl, 2014). Current anatomical descriptions and subdivisions of the posterior triangle of neck, especially with regards to the supraclavicular triangle, presents with conflicting boundaries and limitations in its superior border and additional thought may be required in establishing more reliable boundaries.

1.4.1 Anatomical Contents

On gross surface examination, SCT forms a depression within the limits of the clavicular head of the SCM medially, trapezius laterally and superior to the clavicle. This area is termed the supraclavicular fossa (SCF) where it houses complex anatomical contents within a narrow space (Hirokawa et al., 2010). Superficially, the SCF is covered by the platysma, a thin, flat sheet of muscle which has supraclavicular and infraclavicular attachments. Exposing this muscle reveals the SCF. On the medial aspect, SCM is usually observed forming its border through its two head attachments, clavicular and sternal heads, which attach to the proximal 1/3 of the clavicle and manubrium, respectively. The SCT is covered by the investing fascia, a superficial layer of the cervical fascia, which extends and splits to envelop the SCM and trapezius. The external jugular vein (EJV) normally descends to mid-clavicular level on the surface of SCM to pierce the investing fascia drain into the subclavian vein either lateral or anterior to the ASM, located in the SCF. The intersection of the EJV and posterior border of SCM has been reported to correspond to the level of the brachial plexus as it exits between the anterior and middle scalene muscles (Cousins et al., 2009). There are reported variations of the EJV draining into IJV, being duplicate, or draining superiorly into a distal portion of IJV (Balachandra, 2012). The subclavian vein (SCV) is positioned anterior to the ASM and drains the axillary vein as it courses over the lateral edge of the first rib to join in drainage with the EJV and IJV (Rozing, 1993). In the majority of cases, the SCV is situated posterior to the clavicle (60%), however, it isn't uncommon to observe SCV coursing superior to the clavicle (30%) (Land, 1971). The SCF is usually filled by a variable amount of scalene fat pad which contains supraclavicular lymph nodes, arterial branches from the SCA (specifically, suprascapular and transverse cervical arteries), adipose tissue and thoracic duct as it drains lymph into the junction of IJV and SCV on the left side of the body (Bentel et al., 2000).

The omohyoid muscle is categorized into three portions: inferior belly, intermediate tendon, and superior belly (Rai et al., 2008). The inferior belly usually originates from the upper border of the scapula and travels anteriorly to attach to the lateral aspect of the clavicle through a fibrous expansion (Standring et al., 2015). The inferior belly may be used as a landmark to the brachial plexus trunks (Chung et al., 2011). It ascends superomedially approximately 2.5cm superior to the clavicle to become a tendinous sling on the anterior aspect of the IJV (Kasapoglu & Dokuzlar, 2007) but posterior to the belly of the SCM. Omohyoid and IJV are attached through the pretracheal fascia of the deep cervical fasica, and the contraction of the omohyoid muscle has been reported to lead to an enlargement of the IJV lumen (Ziolkowski et al., 1983). The intermediate tendon ascends superiorly to attach on the hyoid bone.

Posteriorly to the fat pad lies the scalene muscles, anterior (ASM), middle (MSM) and posterior (PSM) scalenes, respectively encased in prevertebral fascia, a deep layer of the cervical fascia.

The phrenic nerve arises primarily from C4 cervical root with contributions from C3 and C5 (Paraskevas et al., 2011). It descends inferiorly along the anterior surface of the ASM in an oblique, lateral-to-medial direction to enter the thoracic cavity posterior to the SCV. In 2.38% of cases, phrenic nerve has been reported to descend anterior to the SCV (Paraskevas et al., 2011). There is also evidence of an accessory phrenic nerve arising from C5-C6 roots (Bigeleisen, 2003) and crossing anterior to the SCV to form a loop with the phrenic nerve inferiorly in 61.8-75% of individuals (Bergman et al., 1988). The accessory phrenic nerve acts to preserve diaphragmatic function in cases where the main phrenic nerve becomes damaged (Loukas et al., 2006).

ASM originates from the transverse processes of C3-C6 vertebrae and proceeds inferiorly to attach on the scalene tubercle of the 1st rib with a reported with between 12.7-16.1mm (Rusnak-Smith et al., 2001). Situated posterior to the ASM, the MSM originates from C2-C6 transverse processes in 80% cases to attach on the 1st rib posterior to the ASM (Rusnak-Smith et al., 2001). ASM and MSM form an interscalene triangle through which the trunks of the brachial plexus (BP) and SCA at the level of the 1st rib emerge. In 10% of individuals, a scalene minimus has been reported to be present inserting on the 1st rib between the lower trunk of the BP and SCA (Makhoul & Machleder, 1992). It has been hypothesized to be a persisting residual ligament and abnormal in variation. The ASM is positioned anterior to the SCA as it inserts on the 1st rib to divide the artery into three portions: 1st portion is proximal to the ASM and usually gives off vertebral artery and thyrocervical trunk; 2nd portion is behind the ASM and may have origins of thyrocervical trunk and costocervical trunk; 3rd portion is lateral to the ASM and may display the origin of the dorsal scapular artery. The SCA usually lies on the surface of the 1st rib, however, may be positioned 3-4cm above (Sanders & Raymer, 1985).

The C5-T1 nerve roots of the brachial plexus originate from the cervical transverse foramina of C5-C7 and T1 vertebrae. The anterior rami of these roots are positioned posterior to the vertebral artery as it ascends through the transverse foramen, and these roots unite to form upper, middle and lower trunks prior to emerging from the interscalene triangle (Rozing, 1993). The lower trunk is closely associated with the SCA, and the midpoint of the clavicle has been shown to be associated with the position of the BP (Ihnatsenka & Boezaart, 2010). As these trunks continue laterally, they unite to form anterior and posterior divisions distal to the lateral edge of the 1st rib. The BP is situated more laterally than SCA as they emerge in the interscalene triangle, and the superior trunk of BP has been reported to be as close as 1cm beneath the skin (Hirokawa et al., 2010). Cutaneous branches of the cervical plexus (C1-C4) emerge between ASM and MSM superior to the BP and SCA to supply sensory innervation of the SCT through supraclavicular nerves.

1.4.2 Bony Landmarks and features

The clavicle, manubrium, acromion process of the scapula, first rib and first thoracic vertebra form much of the osteological features of the thoracic inlet, and are associated with the structures of the supraclavicular triangle and fossa. The clavicle is a long, S-shaped bone connecting proximally to the clavicular notch of the manubrium by the sternoclavicular joint and extending distally to attach to the acromion process of the scapula by the acromioclavicular joint. Proximally, the clavicle is thick and displays an anteriorly convex curvature while distally, it is thin and presents a concave curvature. The transition point between two curvatures is considered to be an anatomic midpoint. The medial third portion of the clavicle are attached to the clavicular head of the SCM, while the lateral third are attached to the trapezius and fibers from the deltoid muscle. Throughout the length of the clavicle, it is covered by skin, platysma and sensation is provided by supraclavicular nerves arising from the cervical plexus (Moore et al., 2013).

The first rib limits the superior aspect of the thoracic inlet. It articulates with the manubrium anteriorly and curves laterally on its posterior course to attach to the transverse process of the 1st thoracic vertebra. Two depressions on the superior surface of the 1st rib near its lateral aspect are associated with the groove for the SCA (posteriorly) and SCV (anteriorly). In between the two depressions are Lisfrac's tubercle to which ASM inserts. The medial curvature of the 1st rib is associated with the apex of the cervical pleura of the lung. (Moore et al., 2013; Alemanno & Vigl, 2014). The first rib is divided into a head, neck, tubercle, angle and body portions. Of these, the head and tubercle articulate with the vertebrae and the proximal portion of the body attaches to the costal cartilage prior to its articulation with the manubrium.

The first thoracic vertebra is the vertebral level at which ribs begin their articulation. A rare exception would be in the presence of cervical ribs which arise in less than 1% of cases and may attach to cervical vertebrae (Sanders & Hammond, 2002). The 1st thoracic vertebra joins to the 1st rib through the articular facet on its vertebral body (joining with the head) and a whole facet on the transverse process (joining with the tubercle).

1.4.3 The Effect of Positioning on the Supraclavicular Window

The supraclavicular surgical technique involves performing a careful incision above the clavicle to gain access to the contents of the supraclavicular fossa, such as the subclavian artery, brachial plexus, 1st rib and scalene muscles. This surgical approach requires a thorough understanding and knowledge of possible vascular, neural and muscular variations due to the compact anatomy of the supraclavicular fossa and the presence of essential anatomical structures which may be inadvertently injured.

In current literature on supraclavicular procedures, operative techniques employ a variety of patient positioning in its methodology with little consensus or rationale. Contemporary and past supraclavicular techniques have employed various positioning such as shoulder manipulations, neck rotations, manipulations of the upper extremity, body positions and a mix-and-match of the previous in their operative methodology.

1.4.3.1 Protraction & retraction of shoulders in addition to neck extensions and body positioning

Sanders & Raymer (1985) in their study of 1st rib resections have placed patients in a supine position with a rolled towel running vertically under the spine to extend the neck and retract the shoulders (Sanders & Raymer, 1985). In a comparative study by Donahue (2011) examining the transaxillary versus the supraclavicular approach of 1st rib resection, Donahue took a different approach and set patients in a supine, semi-Fowler's position with the operative shoulder side elevated by approximately 6 inches. Additionally the head was rotated 45 degrees to the non-operative side (Donahue, 2011). It was stated that this particular shoulder positioning opened up the costoclavicular space and enabled a greater exposure of the first rib. In a supraclavicular surgical treatment of thoracic outlet syndrome, a reverse Trendelenburg position was employed with a 30 degrees elevation at the head of the table, in addition to neck extension and rotation to the non-operative side (Thompson et al., 1997). A Trendelenburg position is an overall body positioning maneuver where the patient is laid supine with the feet of the operating table raised by 15-30 degrees (Appelboam et al., 2015).

There was also variability in subclavian vein catheterization procedures using the supraclavicular approach. Traditional positioning of retracted shoulders using a towel roll between scapulae and contralateral head rotation was employed in some studies due to the compression and identification of the subclavian vein between the clavicle and the first rib (Shires, 1984; Kim, 2013), whereas other studies recommended flat patient position with head and shoulders in a neutral position (Jesseph et al., 1987). In a different SCV catheterization procedure, Trendelenburg position with no shoulder and head manipulations was employed (Fortune & Feustel, 2003). In a study by Land (1971), it was reported that a maximal contralateral head rotation did not change SCV relationship to the clavicle (Land, 1971).

1.4.3.2 Elevation & depression of shoulders

Study by Kang et al. (2011) reported an increase in contact of SCV with the clavicle with shoulder depression, resulting in a decrease in SCV diameter and narrowing of the costoclavicular space (Kang et al., 2011). A similar finding was found by Kitagawa et al. (2005) where shoulder depressions up to 5cm didn't significantly affect SCV diameter but increased its exposure through increasing contact with the clavicle (Kitagawa et al., 2005). It was additionally reported that in a lowered shoulder position, the mean distance between SCA and SCV were significantly different at the level of the sagittal plane of the clavicular head of SCM (1.6mm vs. 3.1mm separation observed in depression) due to a greater inferior shift of the SCV than the SCA. Shoulder elevation was described to result in a decreased overlap of the clavicle with the medial portion of the SCV to decrease its exposure (Tan, 2000) and was reported to have increased separation from the clavicle (Kitagawa et al., 2005).

1.4.3.3 Positioning of the upper extremity

Park et al. (2013) has demonstrated that arm abductions of 90 degrees with slight external rotation induces a 40% decrease in diameter of the SCA and compression of the brachial plexus in the costoclavicular space (Park et al., 2013). This finding was supported by Matsumura et al. (1997) where significant reductions in costoclavicular distance and ASM-clavicle distance were observed with arm abduction on computed tomography (Matsumura et al., 1997). Remy-Jardin (2000) reported similar findings of SCA and SCV compression observed with abduction of the upper extremity (Remy-Jardin, 2000). Stapleton et al. (2009) demonstrated using sonographic analysis that the clavicle performs a scissor like action on the first rib to reduce the costoclavicular space during arm abduction and horizontal extension. Topographical anatomy of the supraclavicular fossa described by Alemanno & Vigl (2014) reported that shoulder depression may lead to a shallower depth of the fossa resulting in a more superficial exposure of anatomical contents due to the downward rotation action of the distal clavicle (Alemanno & Vigl, 2014).

1.5 Rationale of Study

The main goals of this integrated project aims to achieve three objectives through three separate sub-studies:

1. To characterize the variations in the subclavian arterial branching pattern by prevalence through retrospectively examining patient computed tomography angiograms and categorizing each observed pattern. In light of the plethora of subclavian branching patterns currently described in literature, this study aims to answer whether these depictions are accurately or falsely represented, and to examine which pattern presents the highest prevalence. Medical education and textbooks draw their understanding from anatomical literature, and this study hopes to improve current understanding and knowledge of subclavian branching pattern for an up-to-date awareness of medical students, anatomists, and surgeons alike.

2. To examine the relationship of the origin of the vertebral artery to anterior scalene muscle through retrospectively examining patient computed tomography angiograms and measuring the distance of separation along the subclavian artery. The vertebral artery can be considered the most important vessel as it supplies substantial blood flow to the brain, and subclavian surgeries take careful considerations to preserve its origin. This study aims to characterize the distance of each VA origin from the anterior scalene muscle in order to assist surgeons by providing an easy estimation of the proximity of VA origin during surgical operations. Through the findings of this study, we hope to update ASM as a reliable landmark to locate the VA origin proximally and to improve surgeons' ease of VA acquisition and avoid complications pertaining to VA injury due to difficulties in its preservation.

3. Lastly, to investigate the effect of shoulder positioning on the exposure area of the supraclavicular triangle using dissections of fresh cadavers, emulating protraction

and retractions, and measuring the resulting changes in area. Protraction and retraction are patient positioning most frequently utilized in surgical literature, and evaluating their effectiveness in maximizing the exposure of the supraclavicular contents is the primary goal of this study. Through the findings of this study, we aim to understand which shoulder movement will deliver the maximal exposure area and provide the highest ease of access for surgeons in their operations on the subclavian artery and its branches, and may assist in reducing inadvertent damage to structures due to poor visualization of the operative area. This study hopes to improve the understanding of current procedural techniques on the supraclavicular area, and provide empirical evidence to the benefit of employing certain patient positioning over others. *** need to update your table of contents

Chapter 2

Retrospective Computed Tomography Angiogram Characterization on the Subclavian Arterial Branching Pattern

2.1 Introduction

The subclavian artery (SCA) is characteristically thought to have origins of multiple branches. Most typically, these include vertebral, internal thoracic, thyrocervical, costocervical and dorsal scapular arteries. However, there are significant variations reported in the branches that originate from the SCA. These variations include abnormal subclavian origins of the branches of the thyrocervical trunk (Huelke, 1958), costocervical trunk (Su et al., 2000), and an absence of the dorsal scapular artery (Reiner & Kasser, 1996). Anatomically, in a proximal-to-distal direction, these branches may originate in various orders relative to the other branches of the SCA. The prevalence in the origin of the typical SCA branches is reported in literature (Yamaki et al., 2006; Henriquez-Pino et al., 1997; Weiglein et al., 2005; Huelke, 1958). The vertebral artery is an important vessel supplying the posterior brain circulation and has been reported to most often originate as the first branch of the SCA (Sci et al., 2012). Despite the well described vertebral artery, there is a surprisingly little amount of literature published studying the variations in the prevalence in the order of the other SCA branches. Understanding the order of the SCA branches may be important as the variations in the SCA branching pattern is knowledge crucial to surgeons.

2.1.1 Purpose of Study

The purpose of this study aims to fulfill two goals. The first is to provide a description of the prevalence in the order of each arterial branch as they originate from the subclavian artery (VA, ITA, TCT, CCT, and DSA). Current literatures on the branching descriptions of the SCA only describe their prevalence of origin, and provide no evidence on the prevalence in the order of origin of the SCA branches. Characterization of the order of these branches and their prevalence may add to the current anatomical knowledge and aid vascular surgeons in their awareness of SCA branch variations.

The second aim is to categorize and schematically represent the most common branching patterns of SCA branches through combining the prevalence of individual arterial branches from the first aim of the study. Despite some reported literature on the variation patterns of certain subclavian arterial trunks, there has been no study examining the overall branching patterns of the subclavian arterial branches. Categorizing these vascular patterns may help to explore possible anatomical variations and distinguish common variations from abnormal, uncommon variations.

2.1.2 Objectives

Through the use of Computed Tomography Angiograms, the objectives of this study are:

1. To provide a description of the branching order characteristics of individual arterial branches and their prevalence originating from the SCA
2. To organize and schematically represent the branching pattern variations of the subclavian arterial branches into distinct categorizations

2.2 Methods and Materials

2.2.1 Patient Selection

The vascular anatomy of the subclavian artery and it branches was retrospectively analyzed in a series of patient computed tomography angiograms (CTA). Patient CTA scan acquisition privileges were granted through Dr. Adam Power of the London Health Sciences Center (LHSC), and all scans were uploaded onto the TeraRecon server of LHSC network, and analyzed on a computer located at Victoria Hospital, London, Ontario.

Patient upper limb and head & neck CTAs taken during the periods of January 2008 to January 2015 and stored in the LHSC network were selected for scans displaying subclavian arterial anatomy. All CTAs displayed bilateral subclavian anatomy (Left and Right sides), although the resolution of one side did not always match the other.

Initially, 74 CTAs (148 bilateral sides) taken in the Jan. 2008-Jan. 2015 period were retrospectively examined. From this pool, CTAs (unilateral or bilateral sides) displaying a poor resolution and clarity of the subclavian arterial anatomy were excluded. The remaining scans created a pool of 55 CTAs scans displaying 101 SCAs (left=49 and right=52) from 55 patients.

2.2.2 Morphologic Analysis of the Subclavian Artery using Aquarius iNtuition

Aquarius iNtuition version 4.4.7 (TeraRecon Inc., San Mateo, California) is a 3D visualization workstation that provides a pre- and post-operative evaluation and processing of patient CT images [Lee, 2007]. It allows vasculature, osteology and musculature CT data to be reconstructed and presented in a 2D and 3D format for comprehensive analysis, where the user can freely view and rotate the model for evaluation and measurement.

The 3D visualized head & neck and upper limb CTA models on Aquarius iNtuition displayed intravenous contrast-filled lumens of the subclavian artery and its branches, rendering an accessible viewing of the patient's vascular anatomy.

This software allowed analysis of CTA scans with various program tools, in particular, the Curved Planar Reformation (CPR), a process where a longitudinal cross section is generated to measure a length along the centreline of the convoluted tubular pathway e.g. the length of the SCA [Kanitsar et al., 2002]. Other tools like 'distance' allowed for the measurement of distances along 2 points, and tools such as 'rotate', 'window/level', 'pan', 'zoom' and 'slab' assisted in view manipulation to identify and trace the path of various vasculature (Figure 4).

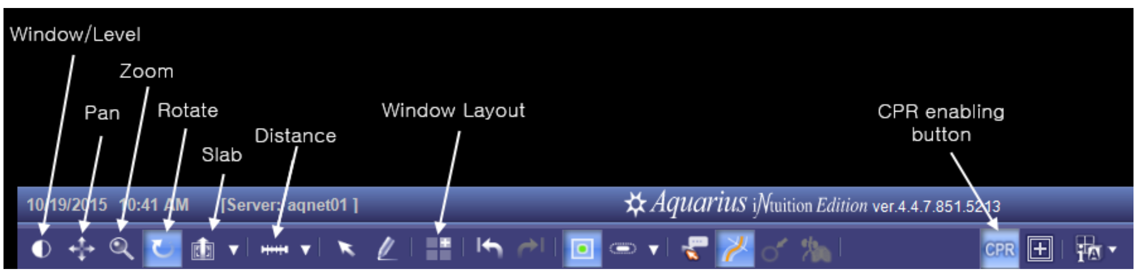

Figure 4 The toolbar of the 3D imaging platform, Aquarius iNtuition v.4.4.7. This screenshot shows the routinely utilized viewing manipulation tools (Pan, Zoom, Rotate, Slab, and Window Layout), measuring tools (Distance and CPR button) and adjustment tool (Window/Level).

Aquarius iNtuition's 2x2 Window Layout mode displays three 2D CT panels arranged in an orthogonal view of each other, and one panel showing the 3D reconstructed model (Figure 4). Each panel shows a transverse section (from the feet view), coronal section (anterior view) or a sagittal section (from the Left or Right side) with a crosshair marker indicating each of these planes on its neighboring panels that move real time corresponding to one another. Through the use of these crosshair markers, it allows a structure marked on one panel to be simultaneously indicated on the other panels.

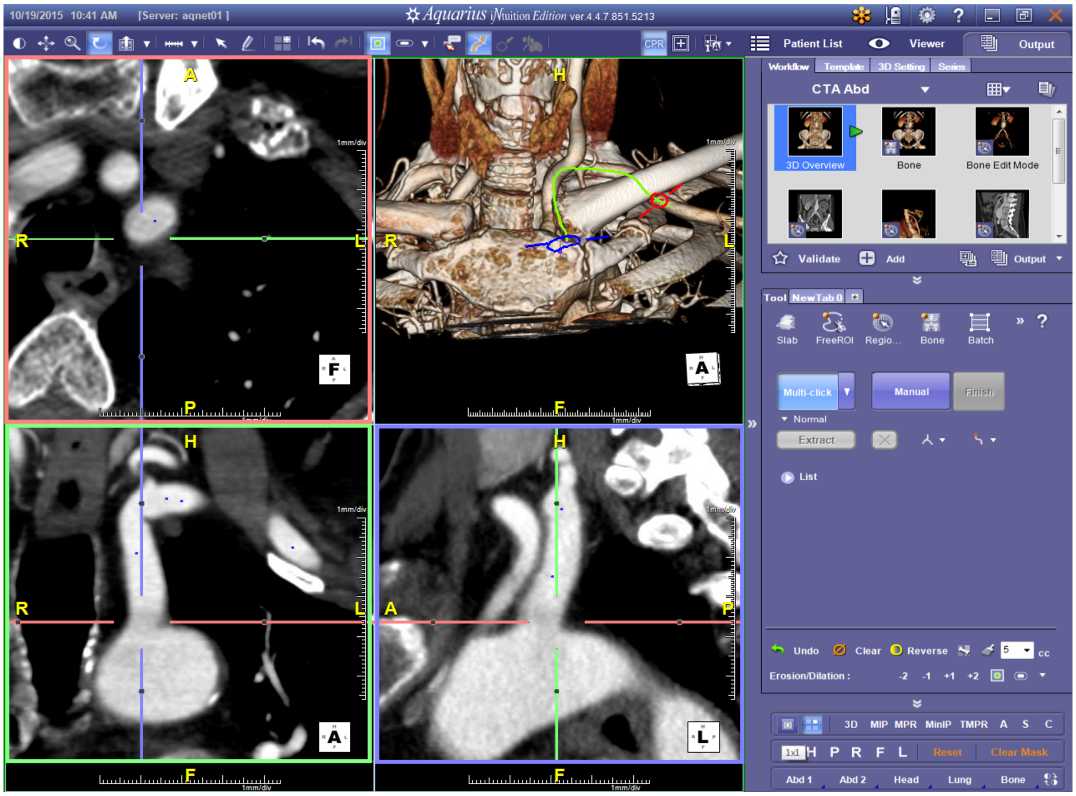

Figure 5 A screenshot of the 2x2 Window Layout view of Aquarius iNtuition v. 4.4.7 showing the subclavian artery. It displays the CT scan in a transverse section (pink box), coronal section (green box), and sagittal section (blue box), along with the crosshairs in each panel indicating the orthogonal sectional planes which move in real time corresponding to each other. The upper right panel shows the 3D reconstructed model of all these CT scans.

2.2.3 Patient Measurements

Prior to each measurement of a CT scan set, patient identification number (no personal information was recorded), age, sex and CTA side (left or right) was noted.

The length of the subclavian artery was measured by initially selecting the transverse section view and scrolling down the CT scans stacks using the 'slab' tool until the subclavian artery was observed originating off of the arch of the aorta (Figure 5, top left panel). From this view, CPR was selected (multiclick setting; manual mode) and a single 'point' was placed on the center of the subclavian artery's lumen in the cross sectional view of the transverse section panel by left clicking on the mouse.

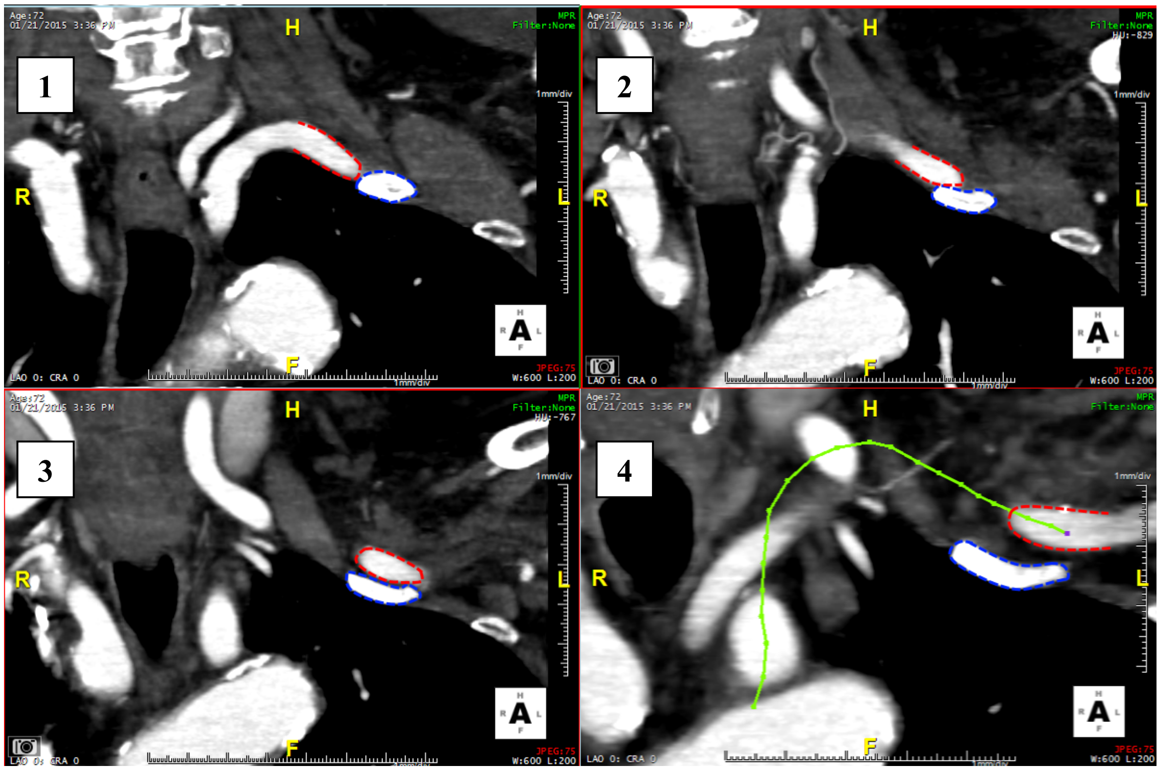

Figure 6 A collection of coronal section CTAs displaying the lateral course of the LSCA (red dashed line) over the first rib (encircled in blue) as the 'slab tool' was used to move in the anteroposterior plane (1-4). Measured course of SCA is displayed (green).

The lumen of the subclavian artery was continually traced along its path superolaterally and additional 'points' were placed along SCA's centreline of flow by 'shift + left clicking' the centre of the lumen. The coronal and sagittal sectional views were intermittently used throughout the CPR process to ensure the points were being placed on the center of the SCA. The 'point' placements continued along SCA's length until its termination at the anatomical end of the SCA at the lateral border of the 1st rib, as visualized best by the coronal section view) (Figure 6).

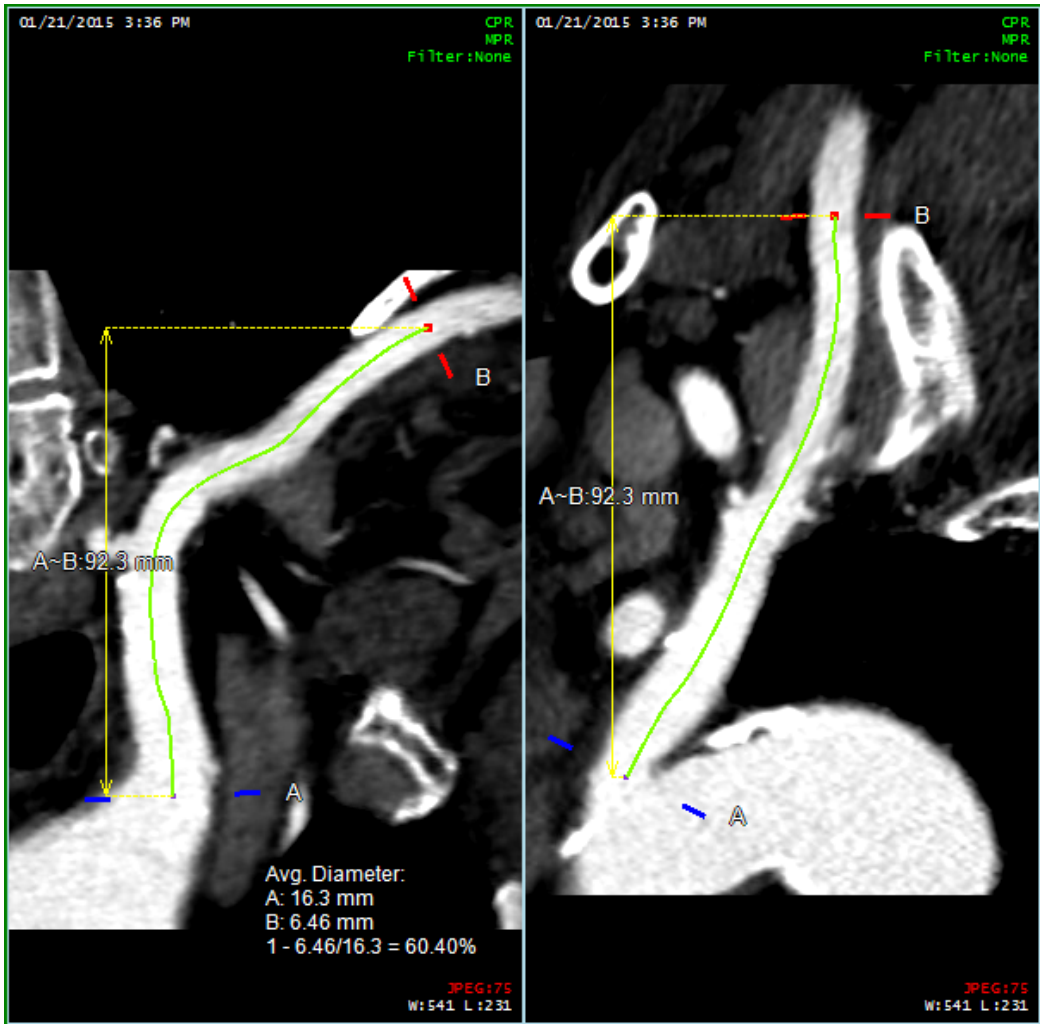

Figure 7 SCA length measurement displayed in the 2x2 CPR vertical layout.

CPR measurements were finalized by clicking 'Finish' and the centerline of the subclavian artery was automatically generated and displayed on a separate window layout mode. Using the distance tool, the full length of the centreline was measured and the value was recorded as the SCA length (Figure 7).

Following the establishment of the center through the length of the SCA, the window layout mode was switched to 'Vessel Track', where it displayed 3D reconstructed orthogonal panels of SCA and its branches using the measured centreline and CT scans. This layout mode permitted an accurate identification of subclavian branches based on 3D anatomy in space, compared to the limited views of 2D CT scans (Figure 8).

Figure 8 Vessel track layout displaying a 3D view of the SCA branches and their origin and course. SCA=subclavian artery; VA=vertebral; ITA=internal thoracic; TCT=thyrocervical; CCT=costocervical; DSA=dorsal scapular artery

The 'distance' tool was selected and the centreline of SCA was measured from its origin on the arch of the aorta (from the origin of the brachiocephalic trunk for the RSCA) and was set as the starting CPR point, to the first branch observed on the SCA. The arterial branch was identified based on its course and direction established from descriptions in literature. This measurement was repeated for each branch originating off of the SCA and the measured 'distance of origin' and the name of the vessel was recorded (Figure 9). The tool ‘window/level’ was seldom employed to increase the contrast of the vessels for better identification and measurement (Refer to Appendix A).

Following the measurement of all SCA branch distances, the number of branches that originated from the SCA was counted and recorded. Each distance of origin value was divided by the SCA length of the corresponding side and expressed as a fraction of the SCA length.

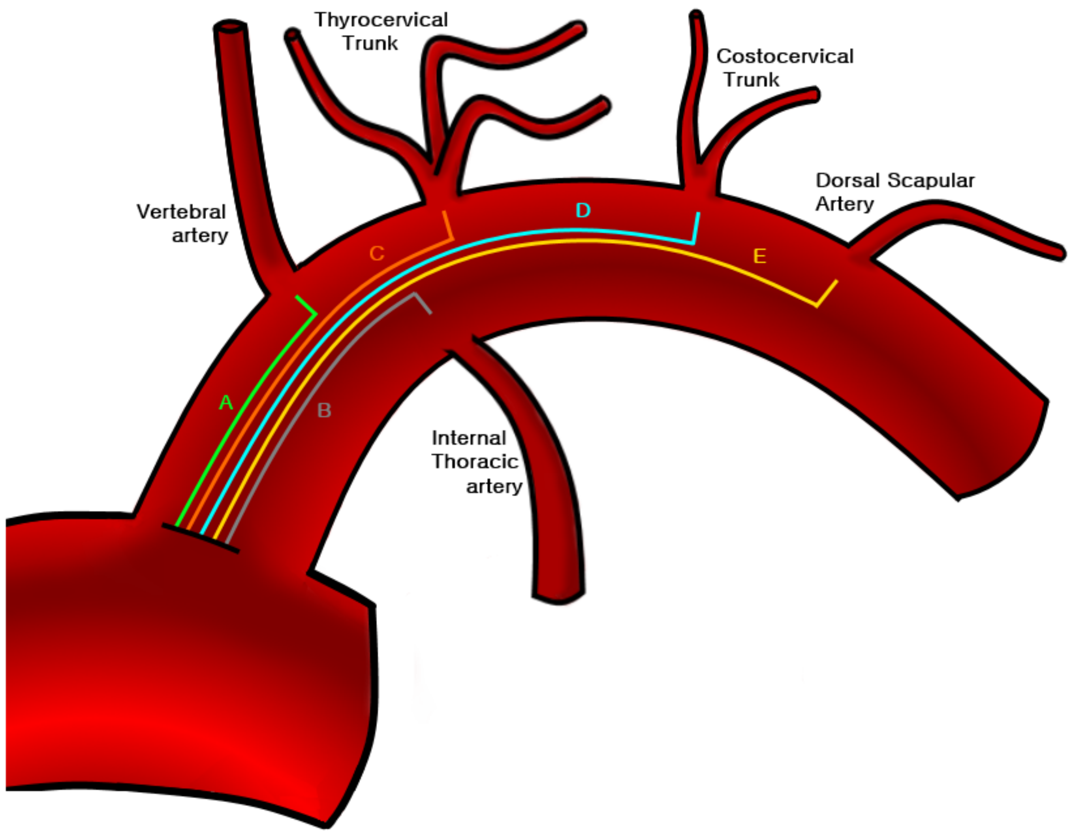

Figure 9 An illustration of the measurements taken of the branches of the left subclavian artery. Distances were measured from the aorta to their respective origins on both left and right SCA. Measurements: A=vertebral; B=internal thoracic; C=thyrocervical; D=costocervical; E=dorsal scapular

2.3 Results

2.3.1 Subclavian Arterial Branches

2.3.1.1 Prevalence of SCA branches

Each incidence of a unique arterial branch originating from the SCA was categorized, summed and divided by the total number of CTAs of the SCA measured (n=101) to calculate the prevalence of each vessel branch (Table 1). Branches of the highest prevalence were, in the order of most to least prevalent: vertebral, internal thoracic, thyrocervical, costocervical and dorsal scapular artery (>50% prevalence). Low prevalence (<10%) was observed in the following branches originating from the SCA: branches of the TCT (inferior thyroid, suprascapular, common origin of transverse cervical & suprascapular, ascending cervical), branches of the CCT (deep cervical, superior intercostal), accessory vertebral, common origin of internal thoracic & dorsal scapular, and common origin of internal thoracic, thyrocervical and costocervical trunk. All branches with an origin on the SCA were included. Three VA on the left side originated on the aorta and were excluded from the calculation of its prevalence, however, two LVAs with an extremely proximal origin on the LSCA were included.

Table 1 Prevalence of various arterial branches of the subclavian artery. Each branch was expressed as a percentage of the total SCA count (101).

SCA branch	Count (/101)	Prevalence
Vertebral	98	97.0%
Internal Thoracic	92	91.1%
Thyrocervical	91	90.1%
Costocervical	78	77.2%
Dorsal Scapular	58	57.4%
Inferior Thyroid	8	7.9%
Suprascapular	2	2.0%
TCA/SSA	1	1.0%
Ascending Cervical	5	5.0%
Deep Cervical	10	9.9%
Superior intercostal	9	8.9%
Accessory VA	1	1.0%
ITA/DSA	1	1.0%
ITA/TCT	7	6.9%
ITA/TCT/CCT	1	1.0%

2.3.1.2 L vs. R Differences in the number of SCA branches

The number of branches originating from each SCA (n=101) was categorized into their respective sides (Left or Right) and recorded (Table 2). The highest number of branches was observed for five branches category, followed by four branches. Data was imported into IBM SPSS Statistics version 23 and independent-samples T-test was performed to test for significant difference between number of SCA branches on the left and right SCA. The mean and SD for the left and right number of branches were calculated (left=4.53±0.91, right=4.84±0.75), and significant difference was observed (*p* value = 0.010). The summated values in the number of branches were used to graphically represent the number of SCA branches (Figure 10).

Table 2 Number of branches originating from the left and right sides of the SCA

# of branches	Left SCA	Right SCA
Three	6	1
Four	19	14
Five	16	31
Six	8	4
Seven	0	2
Total	49	52

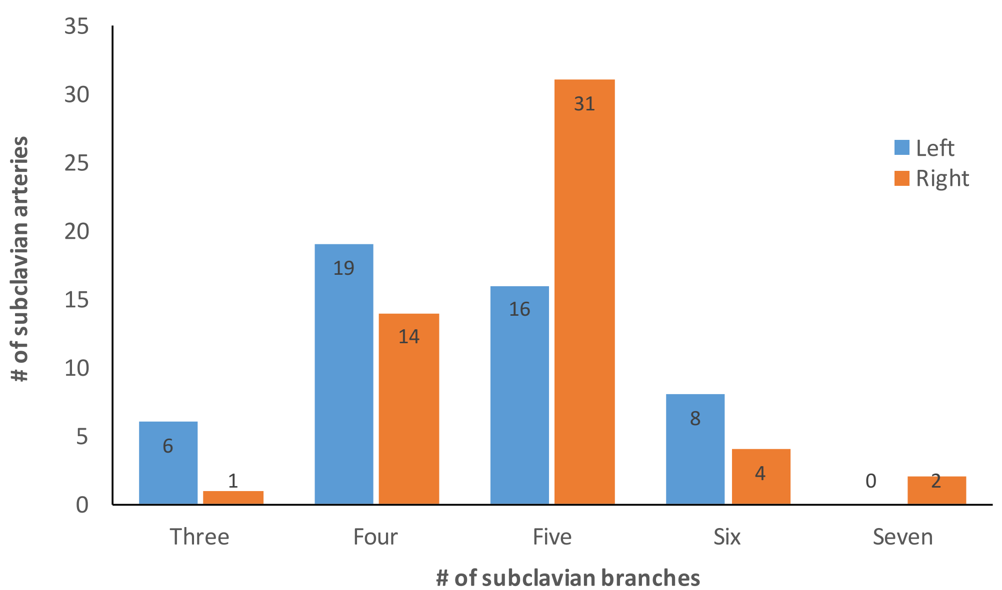

Figure 10 Graphical representation of the number of branches originating from the

2.3.1.3 Prevalence in the order of SCA branches

Branch origin distances (mm) were normalized to their respective SCA length and expressed as a percentage of SCA length. The distance percentages were arranged in a numerical order from lowest-to-highest and given a categorization of first, second, third, fourth, fifth, up to a maximum of seventh branch order. Branches originating within 0.5mm on the CTAs were considered to be from the same position, due to the difficulty in distinguishing the two origin positions. The branch categorizations were added and divided by its total prevalence and expressed as a percentage value. The prevalence in the order of typical branches in the SCA is shown in Table 3. The highest prevalence was observed in VA as the first branch (80.2%), ITA as the second branch (41.3%), TCT as the third (47.3%), CCT as the fourth (43.6%) and DSA as the fifth and last branch (56.9%). Vertebral artery was observed to have originated as the first branch with the highest prevalence.

Table 3 Prevalence in the order of origin of typical SCA branches, with highest prevalence in the order of VA (1^{st}), ITA (2^{nd}), TCT (3^{rd}), CCT (4^{th}), and DSA (5^{th})

Branch order	Typical SCA branches				
	VA	ITA	TCT	CCT	DSA
1	80.2%	9.9%	6.9%	2.0%	-
2	9.9%	41.3%	31.9%	25.6%	-
3	5.9%	32.6%	47.3%	23.1%	1.0%
4	1.0%	11.9%	10.9%	43.6%	31.0%
5	-	-	-	4.0%	56.9%

2.3.1.4 Subclavian Branching Pattern Variations

The numerical orders (first, second, third, etc) assigned to the typical branches of the SCA were grouped into similar branching patterns and categorized into 10 most common patterns (Table 4). The numbers 1,2,3,4 and 5 represent VA, ITA, TCT, CCT and DSA, respectively. The highest prevalence in branching pattern was observed in pattern I (1-2-3-4-5) in 13/101 SCAs (12.9%). Pattern II (1-3-2-4-(5)) varied in prevalence between 7.9-9.9% due to 8 SCAs displaying 1-3-2-4-5 pattern and two SCAs displaying a conserved 1-3-2-4 pattern with an absent '5' (DSA). Branches with a common origin position were seen in Pattern III, and V, where ITA/TCT and TCT/CCT, respectively, originated as the same trunk.

In total, 75 SCAs (74.1%) were categorized into 10 distinguishable branching patterns and illustrated (Figure 11). However, 26 SCAs (25.9%) exhibited an aberrant, abnormal and minor branching patterns which individually constituted <2% in prevalence. These branching patterns were deemed insignificant and were neither categorized nor illustrated.

Table 4 SCA branching pattern variations were categorized into 10 patterns of the highest prevalence constituting 74.1% of SCAs (75/101)

Color Code	Pattern	Count	Prevalence
I	**1-2-3-4-5**	13	12.87
II	**1-3-2-4-(5)**	8--10	7.9--9.9
III	**1-23-4-(5)**	7--9	6.9--8.9
IV	**1-3-4-2-(5)**	7	6.93
V	**1-34-2-(5)**	7	6.93
VI	**1-2-3-4**	7	6.93
VII	**1-4-2-3-(5)**	6	5.94
VIII	**1-2-3-(5)**	6	5.94
IX	**3-1-2-4-(5)**	4--6	3.9--5.9
X	**1-4-3-2**	3--4	2.9--3.9

Legend
1 = **V**A
2 = **I**TA
3 = **T**CT
4 = **C**CT
5 = **D**SA

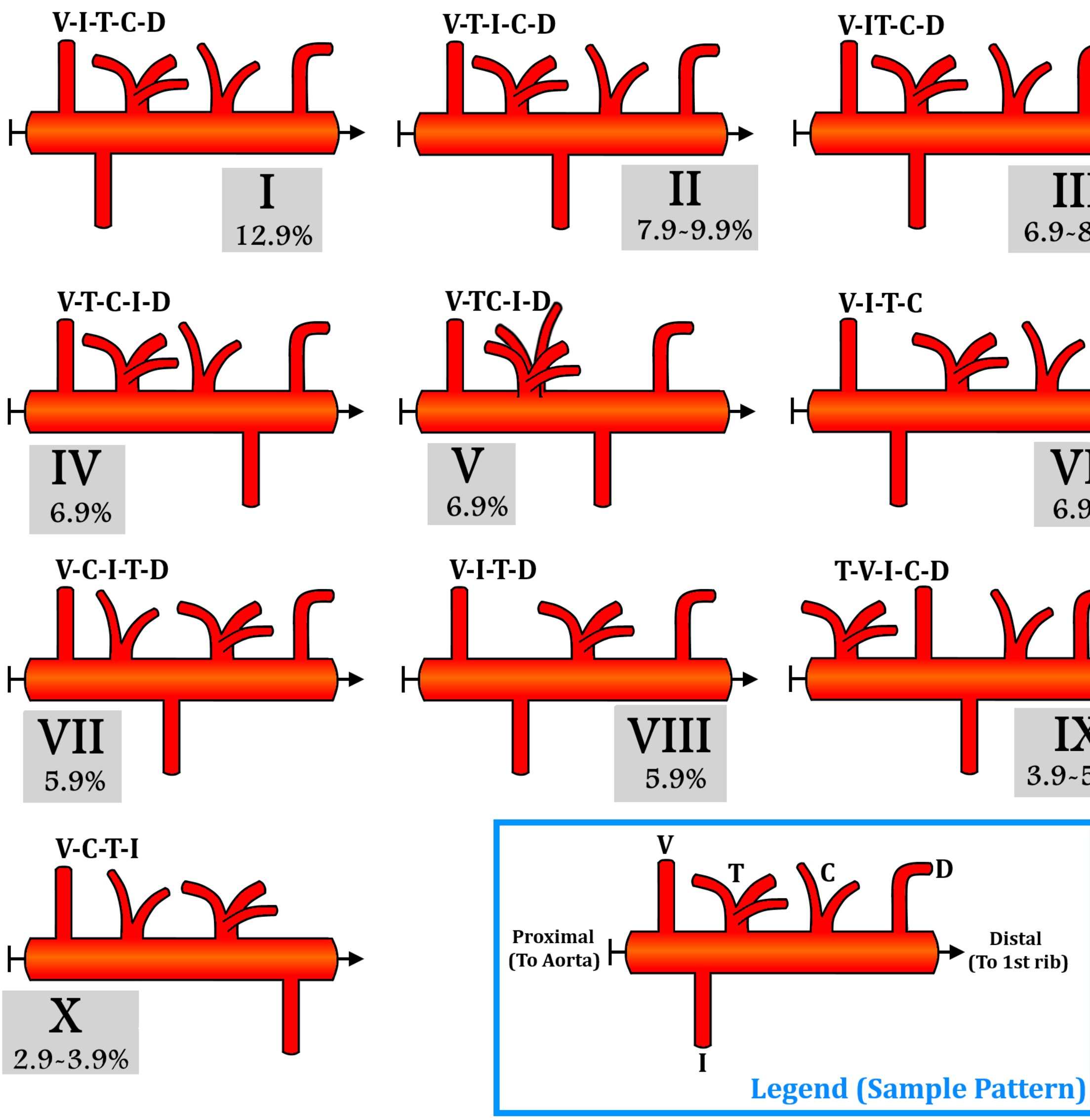

Figure 11 An illustration of the top 10 most prevalent SCA branching pattern variations observed in 101 SCAs

2.3.1.5 Inter-Rater Reliability

The total number of CT scans (101 CTAs, L=49; R=52) was measured by the primary examiner (JR, L=22; R=23) and secondary examiner (OS, L=27; R=29) on different occasions. Same measurement methods were used on Aquarius iNtuition by both examiners.

Following data acquisition, the patient PIN numbers of five CT scan sets (10 CTA sides) were randomly selected from the data of the second examiner and all measurements were repeated by the primary examiner to assess for inter-rater reliability (see Appendix I). Previous data was blinded to the primary examiner while measurements were being made. Using linear regression and line of best fit, interrater correlation coefficient was calculated from the data plot made on Microsoft Excel for the randomly selected measurements of 10 CTA sides (L=5; R=5), (Figure 12). The value was high (R^2=0.83861), permitting the merging and averaging of the data made by the primary and the secondary examiners.

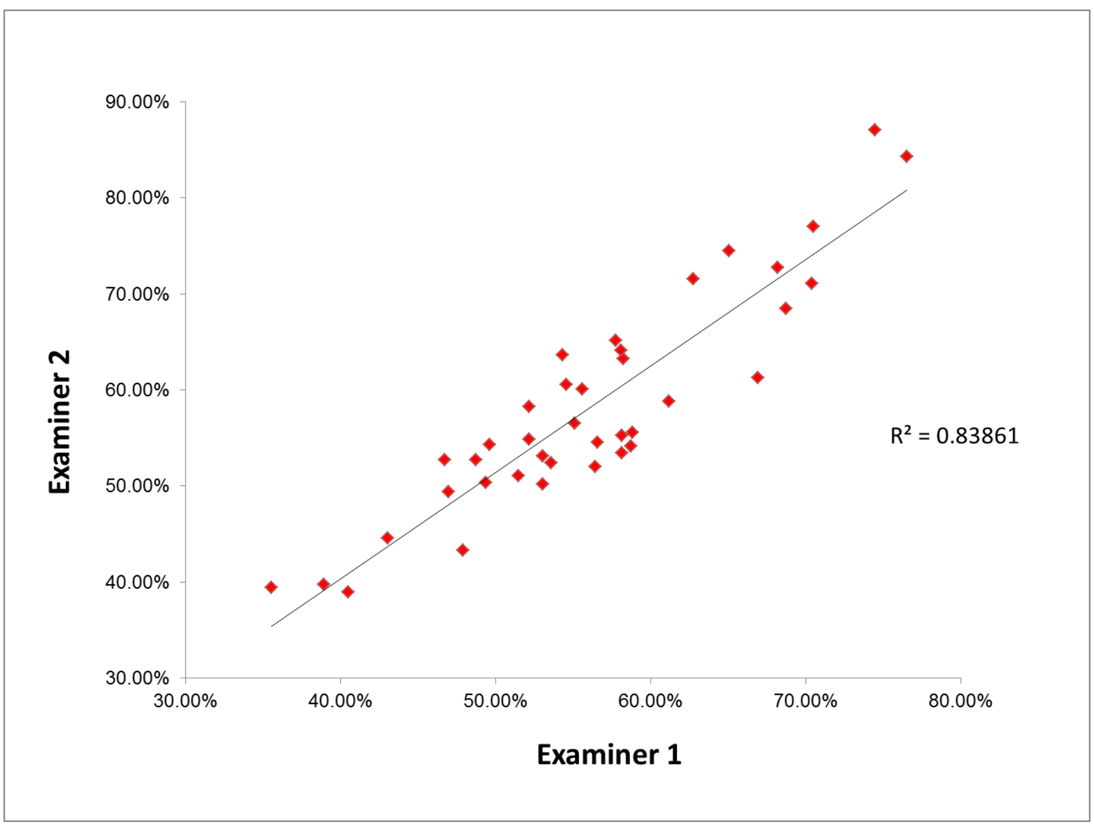

Figure 12 Inter-rater reliability plot on repeated measurements on 10 SCA CTAs

2.4 Discussion

2.4.1 Interpretation of Results

2.4.1.1 Subclavian branches and Clinical Significance

There is no consolidated literature review examining the prevalence of SCA branches and the prevalence in the branch order. However, studies of individual SCA branches investigating its prevalence and variability in branching from arterial trunks (e.g. TCT, CCT, etc) exist and are discussed in the following sections.

2.4.1.1.1 Discussion of the Vertebral artery

To date, the branch of SCA studied in most detail is the vertebral artery. Yamaki et al. (2006), through dissection of 515 human cadavers, reported 100% in RVA prevalence and 94.2% in LVA prevalence from the SCA. LVAs not originating from SCA (5.8%) were found to originate from the aortic arch, between the origin of the left common carotid and left subclavian artery. The findings of this study displayed a similar presentation: RVA prevalence of 100% (all 52 right sides displayed VA origin on SCA) and LVA prevalence of 93.9% (46/49 left sides displayed VA origin on SCA), with 6.1% of LVAs (3/49 left sides) originating on the arch of the aorta between the origins of LCCA and LSCA. However, unlike the findings by Uchino et al. (2013), there were no variations observed in the origin of the RVA. In this study, VA originated as the first branch in 80.2% of SCAs with the highest prevalence, which is supported by findings of different studies (Uchino et al., 2013; Yamaki et al., 2006; Yücel et al., 1999).

The variations in the VA origin can be explained by the embryological development of the aorta and its branches. A ‘double aortic arch’ model developed by Edwards (1948) offers an explanation for the VA origins on the aortic arch, in addition to the order of VA origin on SCA (Figure 13).

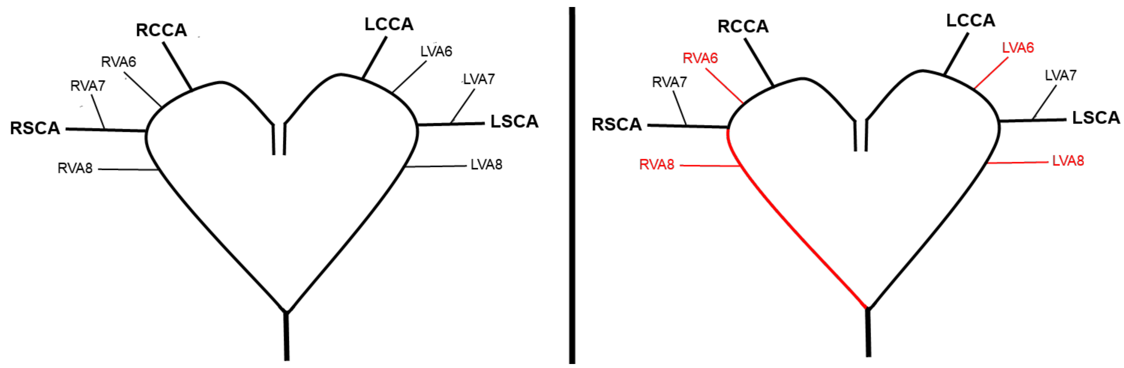

Figure 13 Double aortic arch developmental model (left image) displaying the eventual bilateral regression of the segmental vertebral arteries (VA6 & VA8) in addition to the aortic segment distal to the right subclavian artery (RSCA), (right image)

Bilateral regression of segmental VA branches with the exception of the 7th segmental VA branch originating on the SCA leads to the development of VA as the first branch of the SCA. Abnormal regression of these segmental branches or persistence of LVA6 results in VA originating on the aortic arch in between LCCA and LSCA. An accessory vertebral artery was found in the current study (1/101, 1.0%) where a VA originated from the SCA in addition to an origin on the aortic arch. This finding has also been shared by Satti et al. (2006), and its embryological development can be explained by the model above.

The role of sex in LVA and RVA differences in variation were not examined in this study, due to the findings of Uchino et al. (2013) where the authors retrospectively analyzed CTAs of 2,287 patients and displayed no sex differences in LVA and RVA variations.

2.4.1.1.2 Discussion of the Internal Thoracic artery

In past studies, internal thoracic artery has been shown to originate from SCA with a high prevalence. Henriquez-Pino et al. (1997) examined 100 cadavers and ITAs were found in all cases, however, 70% of ITAs originated directly from the SCA and 30% of prevalence was attributed to common origins with various arteries of the SCA (e.g. TCT, CCT, DSA). Similarly, ITA originated in all cases, directly from the SCA (92/101, 91.1%), in common origin with TCT, DSA, and/or CCT (combined = 9/101, 8.9%). However, the same degree of variation in common trunk origins was not observed in this study (Henriquez-Pino et al. (1997) = 30% vs. current study = 8.9%). Regardless, this supports the finding by Henriquez-Pino et al. (1997) that ITA always originates from the SCA, either as a direct branch or with a common trunk origin. ITA originated with the highest prevalence as the second branch of the SCA (41.3%), however, readily swapped in order to originate as the third branch (32.6%). There are little reports on the order of branching of ITA; however, ITA has been reported to be closely associated with the course of the phrenic nerve at the level of the ITA origin (Owens et al., 1994), leading to injury of the phrenic nerve resulting in diaphragmatic paresis following myocardial revascularization (Abd et al., 1989). Future studies may wish to characterize the distance in the course between the phrenic nerve and ITA to assess for their degree of association.

2.4.1.1.3 Discussion of the Thyrocervical Trunk

The prevalence of TCT originating from the SCA was 90.1% (91/101), and the highest prevalence in order was seen with TCT originating as the third branch (47.3%), but it also frequently swapped the order with ITA and presented a moderate prevalence as the second branch (31.9%). TCT is a complex arterial trunk with significant variations in its branching pattern. Despite current literature on the TCT branching pattern, there is still no consensus among studies (Huelke, 1958; Lischka et al., 1982; Weiglein et al., 2005). Yücel et al. (1999) reported TCT prevalence on SCA to be approximately 50%, which is far less than the prevalence observed in this study (90.1%). Most common variation observed for TCT branching in this study was the direct origin of the inferior thyroid (IT) from the SCA (8/101, 7.9%). Surgical complications may involve an accidental injury and cauterization of IT resulting in the compromise of blood flow to the thyroid gland. Developmental explanations are scant in literature (Lischka et al., 1982) and will not be discussed in this study.

2.4.1.1.4 Discussion of the Costocervical Trunk

Similar to the TCT, there are large variations in the categorization and branching patterns of the CCT (Weiglein et al., 2005). In the present study, CCT originated as the 4th branch with the highest prevalence (43.6%), and was observed to originate directly from SCA in 77.2% cases (78/101). Due to the extensive anastomoses of the intercostal arteries and cervical region, no documented or foreseeable complication is predicted following an injury to the CCT. Further studies may be required to elucidate the branching pattern variations and surgical importance of the CCT.

2.4.1.1.5 Discussion of the Dorsal Scapular artery

DSA is frequently omitted from the list of subclavian branches due to its low prevalence in direct origin from the SCA and high incidence of common origin with ITA, TCT and CCT. Huelke (1958) reported DSA prevalence of 33%, however, collective review of DSA prevalence studies by Lischka et al. (1982) presented the value to vary between 1.7-94% in prevalence. This study displayed DSA prevalence to be 57.4% (58/101 SCAs), and highest prevalence in the order was observed as the fifth branch (56.9%). With such a large variability in branching prevalence and pattern, DSA continues to be an arterial branch requiring much categorization and study.

2.4.1.2 Subclavian Branching Pattern Variations

There are no consolidated literatures categorizing SCA branching pattern variations. The most common SCA branching pattern observed was V-I-T-C-D (13/101 SCAs, 12.9%). This pattern is the most typical variation taught in the anatomical curriculum with the mnemonic "*VITamin C & D* branches". The findings of this study readdress the importance of emphasizing and increasing knowledge of anatomical variations in vascular patterns, especially in the characteristics of the branches of the subclavian artery in surgical practice and medical education. Cahill & Leonard (1999) reported that "10% of clinical malpractice is due to ignorance of anatomical variations." The extensive variation in the subclavian branching pattern reported by the current study may assist surgeons in increasing their awareness of variation patterns and may prevent complications in subclavian surgeries. Awareness of SCA branch variations may be useful in subclavian reconstruction surgeries following stent-graft coverage of the LSCA in aortic aneurysms, where the preservation of the VA origin is the crux of the operation. Although there are conflicting reports, damage to the VA due to iatrogenic injury as a consequence of malpractice and ignorance of the prevalence of VA origin variations may lead to severe neurological morbidities and complications.

The embryological basis of the variations observed in this study may be explained by the development of the subclavian artery from the 7^{th} intersegmental artery. A number of longitudinal anastomoses develop between intersegmental arteries arising from the developing aortic arch, and any rotations may result in the development of aberrant connections emerging on the 7^{th} intersegmental artery (soon to be SCA) and longitudinal arteries, which develop into VA and ITA (Yücel et al., 1999).

In addition to the high variation of subclavian branching pattern as found in this study, the variations in the branches of the trunks originating from the SCA (e.g. TCT, and CCT) present another added dimension of complexity and intricacy to the overall SCA branching pattern. Further studies will be needed to fully categorize the variations in the SCA branching pattern.

2.4.2 Limitations

In comparison to similar studies on vascular variations in literature, this study employed a relatively small sample size (101 CTAs of SCAs; L=49, R = 52). In other literatures, a minimum of 300 CTAs or cadavers were studied and analyzed. Due to this reason, sex differences were not statistically examined, and prevalence of variation seen in this study may have been higher than normal, and may not be fully representative of the percentage of variation observed in a population. In addition, CTAs retrospectively analyzed were of patients with acute and chronic vascular problems. Their state of vascular health may have affected the variations in vasculature through inducing angiogenesis or stenosis of SCA branches leading to a misrepresentative CTA.

2.5 Conclusions

The subclavian artery (SCA) and its branches (VA, ITA, TCT, CCT and DSA) are of great clinical importance as there are significant variations in its branching patterns and prevalence. SCA surgeries such as subclavian reconstruction require excellent knowledge of possible vascular variations and suboptimal knowledge may lead to severe morbidity and neurological damage. This study demonstrated that i) VA, ITA, TCT, CCT and DSA originated from the subclavian artery with the highest prevalence and ii) the most prevalent SCA branching variation is in the order of V-I-T-C-D. The findings of this study may help to increase awareness among vascular surgeons and increase the ease of operation, and provide better knowledge for surgical consideration on the subclavian artery to reduce morbidities associated with damages.

Chapter 3

Investigation of the Relationship of Vertebral Artery origin to the Position of the Anterior Scalene Muscle

3.1 Introduction

Anterior scalene muscle (ASM) serves as an important landmark to identify number anatomical structures. Most importantly, the surface of the ASM is used to identify the phrenic nerve as it courses obliquely to the thoracic inlet. The lateral border of the ASM is a key margin for identifying the subclavian artery and the trunks of the brachial plexus as it emerges laterally. Anteriorly the subclavian vein may also be identified using the ASM. It is also forms the floor of the supraclavicular triangle. For the following reasons, ASM is widely used as a surgical landmark for vascular surgeries of the subclavian artery to avoid damage to the phrenic nerve and identify the SCA.

With a particular importance and relationship to the subclavian artery, it separates SCA into three segments as it inserts on the 1st rib: segment I (from SCA origin to medial border of ASM); segment II (posterior to ASM); and segment III (distal to lateral border of ASM to lateral edge of 1st rib). Vertebral artery (VA) has been most commonly reported to originate from the SCA with the highest prevalence and this may be attributed to an origin on the 1st segment of the SCA, however, considerable variations in the origin of the vertebral artery exist. Extremely proximal origins on the SCA or aortic origins are a couple of the most common reported variations. In subclavian reconstruction surgeries, VA is considered the crux of the operation for its importance in providing bloodflow to the posterior circulation of the brain and reported morbidity following its coverage and injury.

However, there is no reported literature exploring the reliability of utilizing ASM as a landmark to estimate VA origin.

3.1.1 Purpose of Study

This study aims to describe the origin of the VA to the position of the ASM. The ASM is an important landmark for identifying a number of anatomical structures, however, current literature does not describe the prospect of using ASM to proximally identify and estimate the origin of the VA as it arises on the subclavian artery. Characterizing the distance of VA origin to the position of ASM on the SCA may assist surgeons in their decision-making and surgical considerations prior to operating on the VA and SCA.

3.1.2 Objectives

Using Computed Tomography Angiograms (CTA), characterize the relationship of the VA's distance of origin on the SCA to the position of the ASM. This will be accomplished through:

1. Identification of the anterior scalene muscle on the CTA as viewed on the software Aquarius iNtuition
2. Using the software's measurement tool, measuring the subclavian artery along its centerline of flow from the medial border of the ASM to the origin of the vertebral artery

3.2 Methods and Materials

3.2.1 Patient Selection

Same patient head & neck and upper limb CTAs and software (Aquarius iNtuition v4.4.7) used in Chapter 2 (*Retrospective Computed Tomography Angiogram Characterization on the Subclavian Arterial Branching Pattern*) were used to measure the relationship of the anterior scalene muscle to the vertebral artery. Measurements were made on the same computer at Victoria Hospital, London, Ontario.

From the same pool of CTAs used in the previous chapter, 51 CTAs (102 bilateral sides) were initially retrospectively examined. Of these, CTAs (unilateral or bilateral sides) displaying a poor resolution and clarity of the vertebral artery and the anterior scalene muscle were excluded. The remaining scans created a pool of 98 CTA scans comprising of bilateral sides (L=48; R=50) from 51 patients.

3.2.2 Patient Measurements

Similar to the pre-measurement methodology in the prior chapter, patient identification number (no personal information was recorded), age, sex and CTA side (left or right) was noted prior to each measurement of a given CTA scan set. No information on weight, height or BMI was provided.

In the coronal (anterior) view, the ‘slab’ tool was used to get to the depth of plane where the ASM was observed traveling inferiorly to attach to the 1st rib, with the orthogonal transverse and sagittal views assisting in its acquisition and identification (Figure 14, ASM outlined in dashed yellow). The ASM displayed a darker shade and was readily distinguishable over the lighter angiogram of the SCA. The SCA was rarely visible with the ASM at the same time due to the difference in plane position.

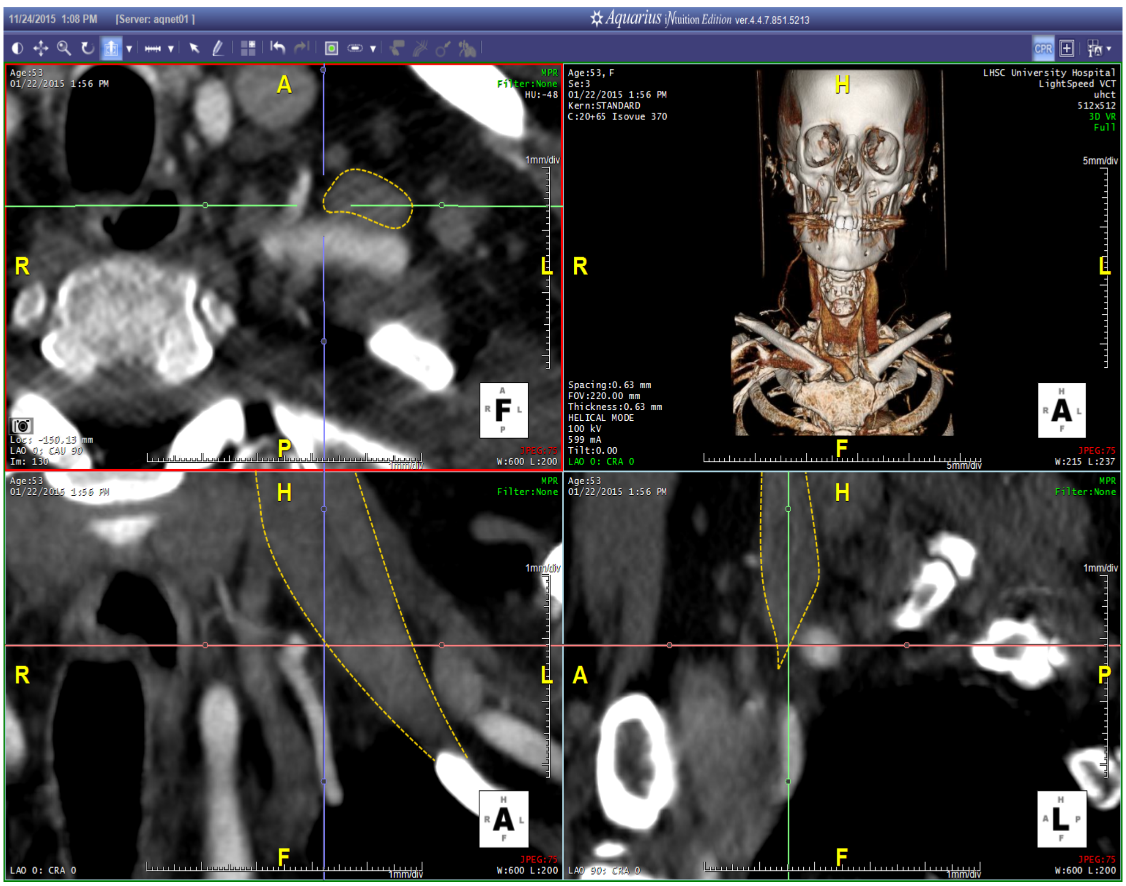

Figure 14 Screenshot of a 2x2 layout displaying the anterior scalene muscle in its depth of plane (outlined in yellow).

Following this, the centre of the crosshair indicator in the coronal view was positioned to overlie the medial border of the ASM (the intersection of the sagittal and transverse planes, represented by the blue and pink orthogonal lines, respectively). In the transverse view, the crosshair was placed anterior to the SCA and medial border of ASM (intersection of the sagittal and coronal planes, blue and green lines, respectively). Lastly, in the sagittal view, the crosshair was positioned anterior to the centerline of the SCA (the intersection of the coronal and transverse planes, green and pink lines, respectively).

In the coronal view, the 'slab' tool was scrolled to move the depth of plane posteriorly until the SCA was observed (Figure 15). 'CPR' tool (multiclick setting; manual mode) was selected and a point was placed on the SCA directly posterior to the medial border of ASM. From this point, the centreline path of SCA was traced proximally by placing more points until the origin of the VA, where it was set as the ending site. The VA and its origin on the SCA was ascertained and verified by its superior course on the CTA, orthogonal views and the measurements from methods 2.1. The CPR measurement was finalized by pressing 'finish' and the line from the medial border of ASM to the origin of VA along the centreline of the SCA was automatically generated and measured using the 'distance' tool (Figure 16). The value was recorded as the 'VA-ASM distance'.

Figure 17 displays the overall methodology and distances measured on the SCA.

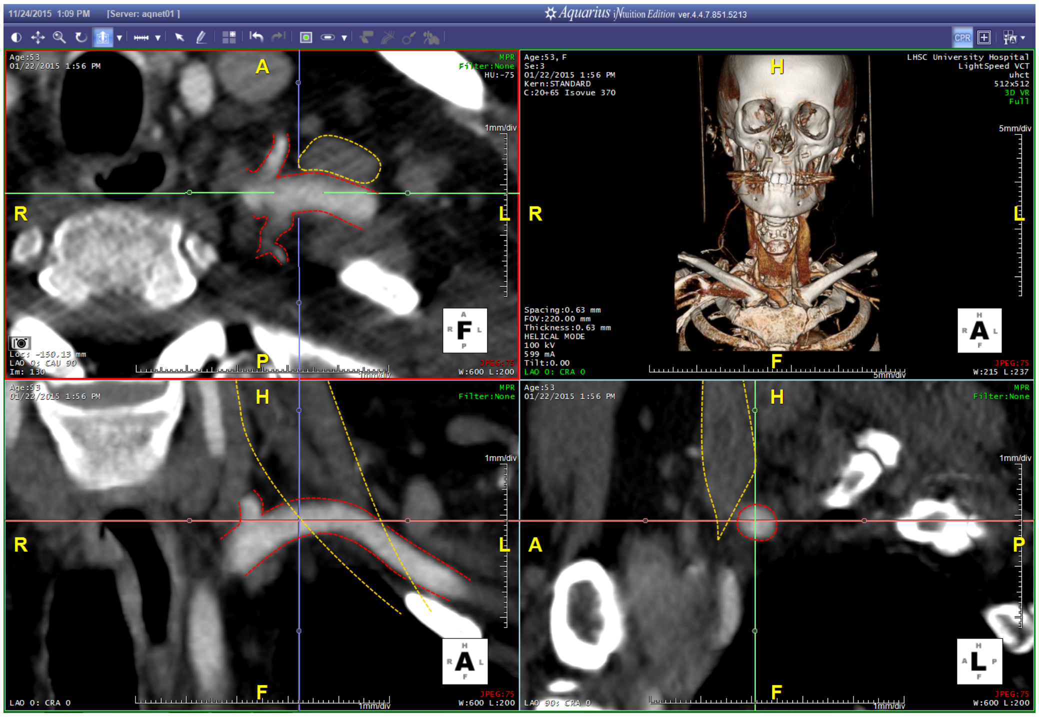

Figure 15 A posteriorly translated screenshot of Figure 9, displaying the SCA (outlined in red) coursing posterior to the ASM (yellow) on all orthogonal views.

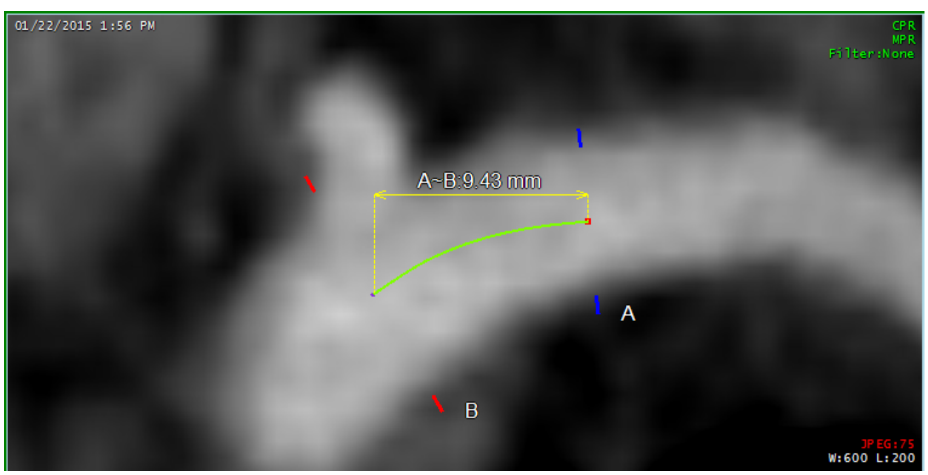

Figure 16 A screenshot of the CPR horizontal layout displaying the VA-ASM measurement distance (green)

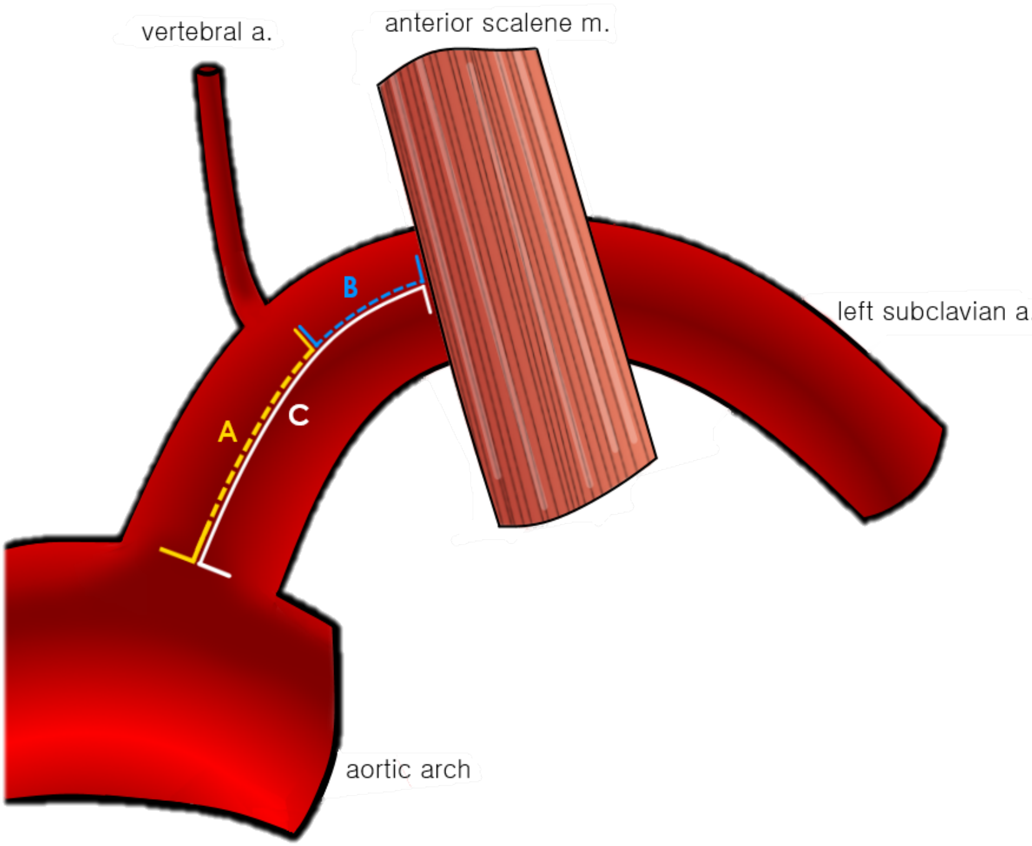

Figure 17 An illustration of the distances measured on the SCA. Measurement A represents the vertebral origin distance (from Chapter 2); B represents VA-ASM distance; and C represents the position of ASM on the SCA.

3.3 Results

3.3.1 Relationship of the VA origin to the ASM position

3.3.1.1 Statistical Analysis of L vs. R differences

Measurements were imported and analyzed using IBM SPSS Statistics software version 23. A Shapiro-Wilks test for normality was performed for normal distribution in all sample populations. An independent-sample t-test was performed to determine any left vs. right side differences, and *p* values <0.05 were considered to be significant. Differences were examined in the distances for VA-ASM, ASM position, and VA origin. Prior to running statistical analysis on the means above, outlier values were calculated (mean ± 2SD) and excluded.

3.3.1.2 Averages of measured distances (VA-ASM, ASM position and VA origin)

In all sample populations, Shapiro-Wilks test for normality displayed normal distribution ($p > 0.05$). The average VA-ASM distance (mm) was 14.14±5.30mm (L = 16.20±5.51; R = 12.25±4.43). There was a significant difference between left and right VA-ASM distance (*p* value = 0.000309). Average ASM position (mm) on the SCA was 68.67±17.74mm (L = 56.22±10.53; R = 81.11±14.60). Significance was found between left and right ASM position distances (*p* value < 0.05). Average distance of VA origin (mm) was 54.91±17.29mm (L = 40.81±9.31; R = 67.28±12.52). Significance was found between distances in the left and right VA origins (*p* value < 0.05).

Table 5 Mean distances (mm) of VA-ASM, ASM position and VA origin. Left and right side values are shown, and statistical difference was found in all left vs. right values

Average VA-ASM		Average ASM position		Average VA origin	
14.14 ± 5.30		68.67 ± 17.74		54.91 ± 17.29	
Left VA-ASM	Right VA-ASM	Left ASM position	Right ASM position	Left VA origin	Right VA origin
16.20 ± 5.51	12.25 ± 4.43	56.22 ± 10.53	81.11 ± 14.60	40.81 ± 9.31	67.23 ± 12.52
p = 0.000		p = 0.000		p = 0.000	

3.3.1.3 Ranges of VA-ASM distances

VA-ASM distances were categorized into 10mm ranges (Figure 17) and percentage calculations were performed. Values within 20mm (0 to 20mm range) comprised of 75.5% of VA-ASM distances, the majority of this percentage (68.9%) being attributed to the VA-ASM distances in the 10 to 20mm range. Expanding on this range, values within 30mm (0 to 30mm range) comprised of 94.9% of VA-ASM distances. Values beyond this range (40 to 50mm and 50 to 60mm range) constituted 5.1% of VA-ASM distances. The minimum VA-ASM distance was 0mm; maximum was 50.8mm.

Table 6 Categorization of all VA-ASM distances into 10mm ranges

Range (mm)	# of VA-ASM distances in this range
0 to 10	23
10 to 20	51
20 to 30	19
30 to 40	0
40 to 50	4
50 to 60	1
Total	98

3.4 Discussion

3.4.1 Relationship of Anterior Scalene to origin of Vertebral Artery

The findings of this study showed that ASM can be used as a reliable surgical and anatomical landmark to estimate the origin of the vertebral artery. Categorization of VA-ASM distances into ranges displayed that 94.9% of VA origins will be within 30mm proximal to the medial border of the ASM. The left VA-ASM distances (16.20±5.51mm) were shown to be significantly greater than the right VA-ASM distances (12.25±4.43mm), (p <0.05). The greater left VA-ASM distance may be explained by Uchino et al. (2013) whose findings reported a higher prevalence of LVA variation (6%) compared to the RVA (3.8%), among which was a common incidence in the proximal variations of the VA origin along the proximal length of the SCA, especially on the left side. In addition, the higher prevalence of proximal VA origins variations on the left side reported in literature (Poonam & Sharma, 2010) supports the significant difference observed between the left and right VA origin distances (L=40.81±9.31mm; R=67.23±12.52mm), where the LVA origin distance was smaller than the RVA origin.

The difference observed in the VA origin distances can be attributed to 1) measurement protocol followed in this study, and 2) difference in the origin of the supra-aortic vessels from the aorta. In the methodology of this study, RVA origin distance was measured from the origin of the brachiocephalic artery on the aorta, compared to the origin of the left subclavian artery on the aorta for the LVA origin distance. In addition, the brachiocephalic artery courses a longer distance to reach the right side prior to branching into the RSCA and RCCA in comparison to the distance LSCA must travel to reach the left side of the body. These reasons account for the difference observed in a shorter LVA origin distance than the RVA, as well as the consequential greater LVA-ASM distance being greater than RVA-ASM distance. ASM position was calculated as the sum of VA-ASM distance and its respective VA origin distance. The significantly greater right ASM position distance than the left can also be attributed to the reasons aforementioned above.

It's important to consider that in 5.1% of cases, VA origin will be located beyond 30mm. In the present study, 3.1% of LVA origins were located on the aortic arch between the origin of the LCCA and LSCA, and 2.0% of LVA origins were located extremely proximal on the LSCA (<10mm of the aortic arch).

In all the measured cases, no VA originated posterior or lateral to the ASM (minimum VA-ASM distance = 0mm). In other words, VA always originated proximal to the medial border of the ASM. This finding is important as it shows that VA origin may not be obscured by the ASM during surgical operation, and will be readily found, if the surgical estimation of 30mm holds true.

Overall, VA-ASM distance of 30mm may present as a useful surgical estimation during operations on the subclavian artery. This is especially true for SCA reconstruction procedures where the preservation of VA and identification of its origin may be considered the crux of the operation. Characterization of VA origin distance with respect to ASM position on the SCA may assist vascular surgeries in their considerations of surgical procedures on the subclavian artery, especially during instances of emergency where pre-operative CTAs are not performed. Although vascular variations of the subclavian arterial branches may be congenital, accurate understanding of potential variations are vital for reducing complications in surgeries of the supraclavicular region, and the knowledge may assist in selecting the choice of surgical approach.

3.4.2 Limitations

The limitations of this study are similar to those faced in Chapter 2. This study employed a relatively small sample size (52 CTAs of SCAs; L=48, R = 50) in comparison to other vascular variation studies, which prevented an accurate statistical analysis of sex differences. The prevalence of variation observed in this study may not have been fully representative of the percentage of variation observed in a population. In addition, CTAs retrospectively analyzed were of patients with acute and chronic vascular problems. Their state of vascular health may have affected the variations in vasculature through inducing angiogenesis or stenosis of SCA branches leading to a misrepresentative CTA.

3.5 Conclusions

This study demonstrated that VA reliably originates within 3cm proximal to the position of the ASM, and that ASM may be a useful surgical landmark to estimate the origin of the vertebral artery. The findings of this study may help to increase awareness among vascular surgeons and increase the ease of operation, and provide better knowledge for surgical consideration on the vertebral artery to reduce morbidities associated with inadvertent damage.

Chapter 4

Investigation on the Effect of Shoulder Manipulation on the Supraclavicular Window Exposure

4.1 Introduction

Supraclavicular triangle (SCT) is a small area above the clavicle containing important anatomical structures of surgical interest. Although its anatomical boundaries are still subject to much clarification, most commonly agreed upon understanding of the SCT lies within the clavicular head of the sternocleidomastoid muscle medially, inferior belly of the omohyoid superiorly, trapezius laterally, clavicle inferiorly, and the anterior scalene muscle forming the floor (Alemanno & Vigl, 2014). The SCT and its fossa represent an area of crowded and complex anatomy, enclosing essential structures like the brachial plexus, subclavian artery and phrenic nerve and are often presented with limited access and poor visualization during surgery, leading to inadvertent injury (Vanakesa & Goldstraw, 1999). Surgical operations of the SCT employ a variety of positioning and body manipulations with little consensus and rationale between, and even amongst the same procedures. However, shoulder manipulations appear to be most commonly changed across many of the operative guidelines in literature (Donahue, 2011; Sanders & Raymer, 1985; Kitagawa et al., 2005; Thompson et al., 1997). Shoulder protractions and retractions using towel rolls have been reported in a number of surgical guidelines, but a considerable variability in positioning exists along with manipulations of the upper extremity, neck rotation, and overall body position on the operating table.

4.1.1 Purpose of Study

This study aims to investigate the effect of shoulder manipulations, protraction and retraction specifically, on the dimensional area of the supraclavicular triangle. Despite the wide-spread knowledge and practice of the supraclavicular surgical approach, current literature on the practice of patient positioning to optimize the exposure of the supraclavicular triangle presents considerable variability among practitioners and little consensus has been shown. Examining the degree in which protraction and retraction of the shoulder changes the triangular exposure area may assist in elucidating an optimum position a surgeon should place a patient in order to maximize the ease of approach for a supraclavicular surgery.

4.1.2 Objectives

Through the use of fresh, unfixed cadavers the objectives of this study are to:

1. Dissect out key landmark structures outlining the boundaries of the supraclavicular triangle with adherence to the supraclavicular surgical procedures

2. Precisely measure the changes in the dimensions of the supraclavicular triangle with protraction of the shoulders using an electronic caliper

3. Precisely measure the changes in the dimension of the supraclavicular triangle with retraction of the shoulders using an electronic caliper

4.2 Methods and Materials

4.2.1 Subject Data

A total of nine fresh cadavers were examined. Of these, two (n=2, female, body #1945, &1956) fresh donor cadavers displaying intact anatomy were selected and their respective sides (L=2, R=2) were dissected. Donor bodies were provided by the Western University body bequeathal program in London, Ontario, Canada. Donor information (weight, age, and cause of death) were not known. The donor bodies were frozen prior to use and thawed for approximately 4 days before dissection was performed.

4.2.2 Exclusion criteria

Seven fresh cadavers were examined and excluded from the study. Cadavers with any prior dissection performed in the supraclavicular region, neck or sternum was excluded. In addition, cadavers with an absent head & upper extremity were also excluded.

However, cadavers with prior dissections on the abdominal region or lower extremity were included in the study.

4.2.3 Materials

The following tools were used in the measurements of the window:

- All measurements were taken using a Titan © digital caliper (range 0-150mm)
- Dissection labelling pins (A,B,C labels) were used to anchor landmark points
- Surgical scissors, foreceps, clamping scissors, probes, and scalpels were used to incise & blunt dissect the fresh cadaver and mobilize tissues to expose the area
- A stack(s) of Scott© multi-fold hand towel was used to manipulate the shoulder positions. Dimensions were 10cm in height, 9cm in width (Figure 18). After compression by both cadavers, the height of the towel stack measured 7cm.
- Wooden blocks were used to secure towel stacks in position

All materials and equipment were generously provided by the Anatomy & Cell Biology Department of Western University, London, Ontario, Canada.

Figure 18 Paper towel stack used to produce protraction and retraction of the shoulders

4.2.4 Dissection Protocol

Surgical procedures for supraclavicular incisions performed during scalenectomies (Sanders & Raymer, 1985), rib resections (Donahue, 2011; Thompson et al., 1997), brachial plexus surgeries (Chung et al., 2011) and subclavian reconstructions (Rutherford, 1993) were reviewed in literature and common operative methods were implemented on the two fresh cadaver dissections in addition to modifications to procedure to increase visualization.

a) A curved-linear incision at the level of the clavicle was made, extending medially from the clavicular head of the sternocleidomastoid muscle to the acromioclavicular joint laterally where label pin "C" was anchored (Figure 19, label pin C). Another incision was made extending superiorly along the lateral border of the SCM for approximately 6cm. Skin, platysma and subcutaneous tissue were retracted altogether as a flap (Donahue, 2011).

b) External jugular vein, supraclavicular nerves, clavicular head of SCM and inferior belly of the omohyoid (within scalene fat pad) were divided as per surgical guidelines (Chung et al., 2011; Sanders & Raymer, 1985). Internal jugular vein was observed coursing superiorly underneath the SCM. Label pin "A" was placed in the sternoclavicular joint at the proximal clavicle (Figure 19, label pin A)

c) Scalene fat pad located lateral to SCM was completely removed through blunt dissection and anterior scalene muscle was identified deep to it with the phrenic nerve coursing obliquely on its surface. Lateral to the ASM, trunks of the brachial plexus were observed. SCA was identified inferior to these trunks on the floor of the first rib, and SCV was identified coursing anterior to ASM, hidden posterior to the clavicle.

d) The 1st rib was observed at the insertion of the ASM and middle scalene muscle, and its bony structure was palpated along its curvature posteriorly to its articulation with the transverse process of the 1st thoracic vertebra. The posterior scalene muscle was divided at its insertion on the 2nd rib for better access to the lateral aspect of the T1 vertebra. Label pin "B" was placed at the costotransverse joint of T1 and 1st rib (Figure 19, label pin B).

e) Both left and right sides were dissected prior to measurements (Figure 20).

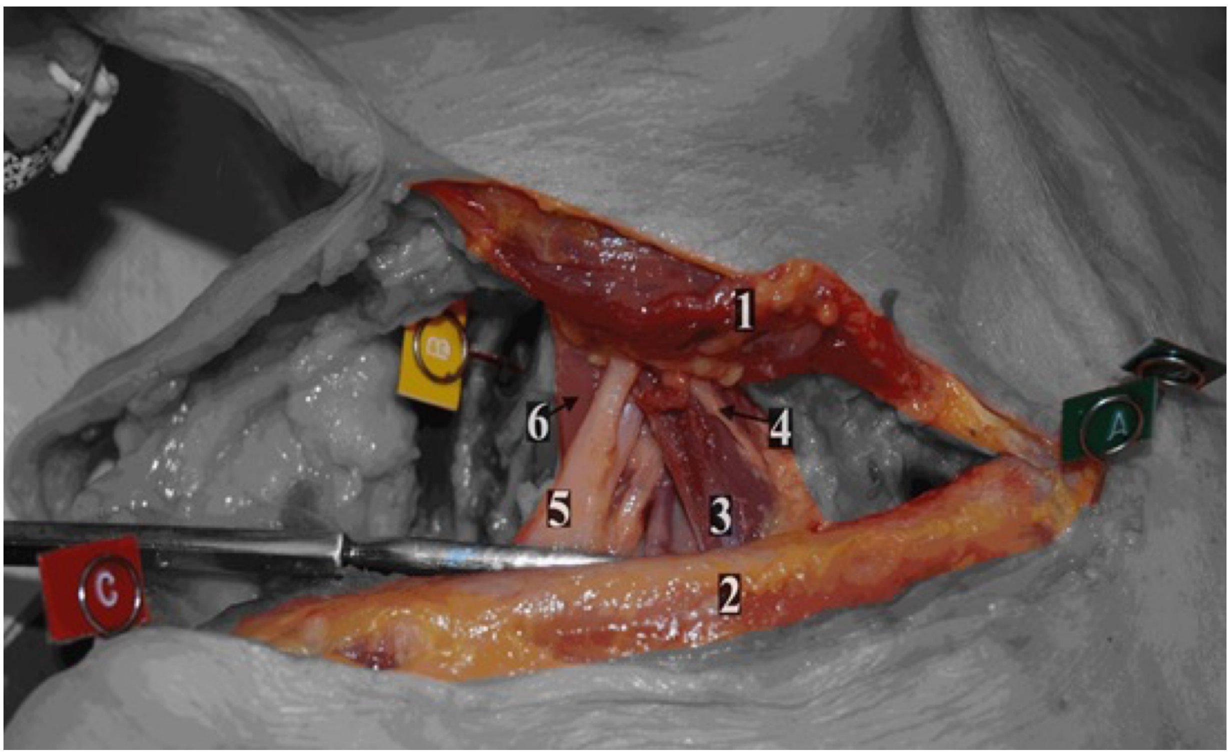

Figure 19 Right dissected supraclavicular triangle displaying important contents, landmark structures, and labelling pins (A,B,C) secured in place. (1) Reflected clavicular head of SCM, (2) clavicle, (3) anterior scalene, (4) phrenic nerve, (5) trunks of brachial plexus, (6) middle scalene.

Figure 20 Fully dissected supraclavicular triangles on both left and right sides. Labelling pins are secured in place and the cadaver has been manipulated in a retracted position (towel stack not clearly visible).

4.2.5 Shoulder Manipulation Protocol & Measurements

Both fresh frozen cadavers were thawed for approximately 4 days and were inspected for adequate gross movement of the shoulder and thorax with particular attention to protraction and retraction prior to dissection and manipulation. Following dissection and exposure of the landmark structures and anatomy, shoulder positions of both cadavers were manipulated into three positions using 1-2 paper towel roll stacks: 1) normal, 2) protracted, and 3) retracted.

Measurements were taken using a digital caliper once cadavers and the shoulder positions were securely positioned. The measurements were non-consecutively measured three times, the examiner was blinded to the previous dimension (each trial was recorded on a different sheet of paper), and all landmarked points were checked for secure placement prior to each recording.

4.2.5.1 Normal Positioning

All cadavers were laid supine on flat dissection tables with arms positioned along the side. Shoulders were placed in a relaxed position and allowed to rest freely on the table. Figure 21 is an illustration of the anatomical landmarks comprising the right supraclavicular triangle as seen from a head-down perspective of the donor lying supine. The head (not seen in figure 21) was not manipulated and gently rested on the table. Measurements were taken of AB, AC and BC dimensions using a digital caliper and recorded.

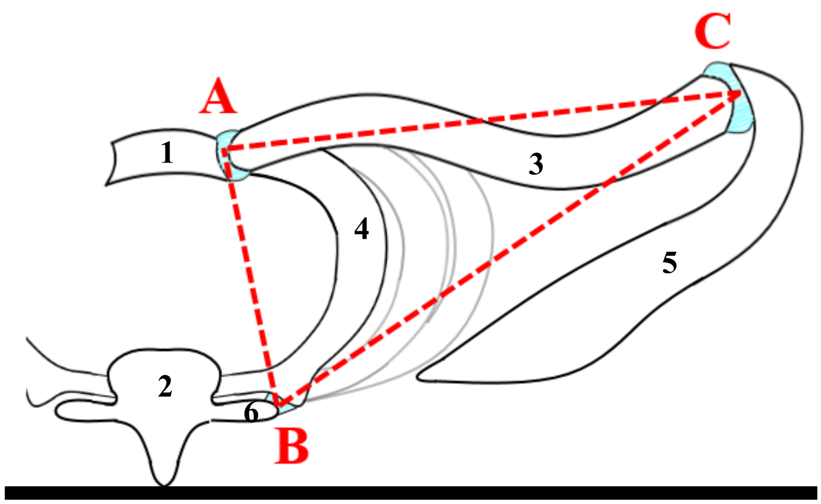

Figure 21 An illustration of the landmark points of a body in a normal, supine position, looking down from the head. A) Sternoclavicular joint, B) costotransverse joint, and C) acromioclavicular joint. The labelled structures are: (1) manubrium, (2) T1 vertebrae, (3) clavicle, (4) 1st rib, (5) scapula, and (6) transverse process of T1.

4.2.5.2 Protracted Positioning

Following the normal position recording, two Scott paper towel stacks measuring 10cm in height (prior to compression by the body) were placed longitudinally on the lateral aspect of each scapula such that the center of the paper stack was centered on the acromioclavicular joint to elevate it (Figure 22). Measurements were taken of AB, AC and BC dimensions as well as the height of the paper towel stack under the body using a digital caliper and recorded. The protracted position was secured by placing wooden blocks on the lateral sides of each towel roll to present any translational movement under the weight of the body.

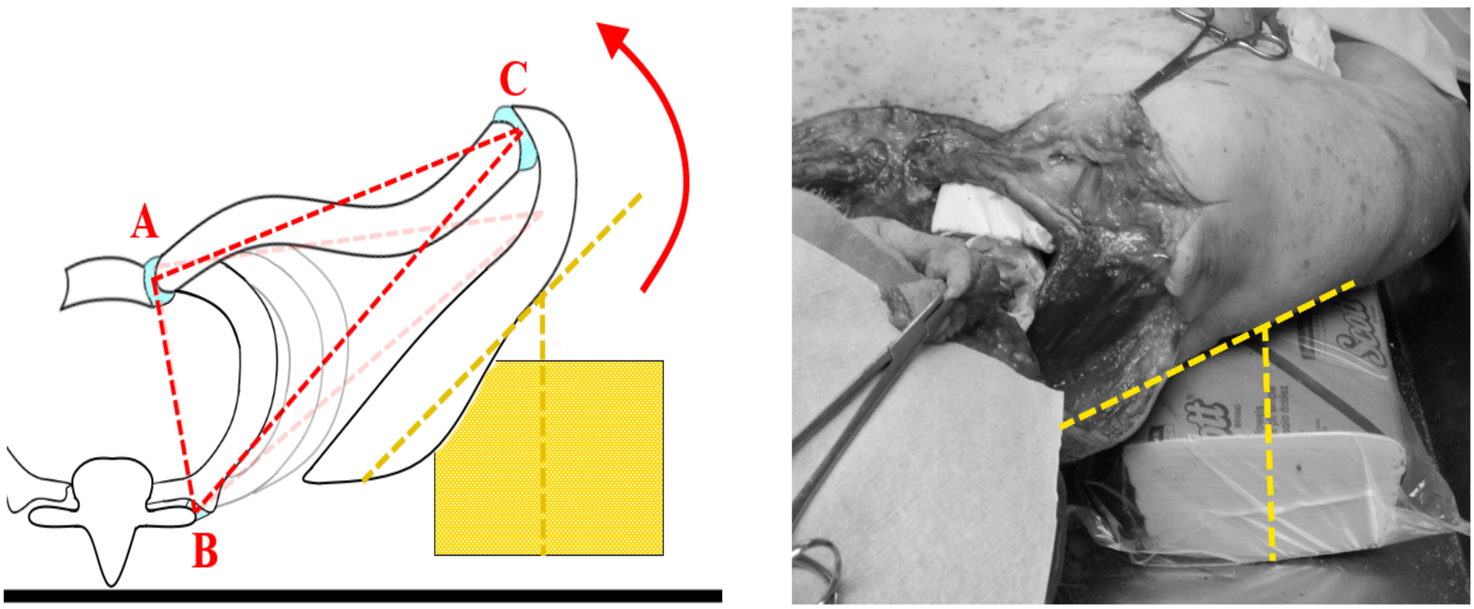

Figure 22 An illustrated view of the changes in dimension with a protracted shoulder position using a towel stack on the shoulders (Left=hypothesized; Right=image of the cadaver with the emulated position). Dashed yellow line outlines an approximate angle of protraction of the shoulders.

4.2.5.3 Retracted Positioning

Towel stacks used in protraction were removed and both cadavers were returned to normal position for approximately 30 minutes prior to retraction manipulations were performed. An unused paper towel stack measuring ~10cm in height was placed longitudinally along the T2-T7 vertebral level between the medial borders of the scapulae to emulate retraction (Figure 23). The head was supported from the table using a wooden block to prevent neck extension. Measurements were taken of AB, AC and BC dimensions as well as the height of the paper towel stack under the body using a digital caliper and recorded.

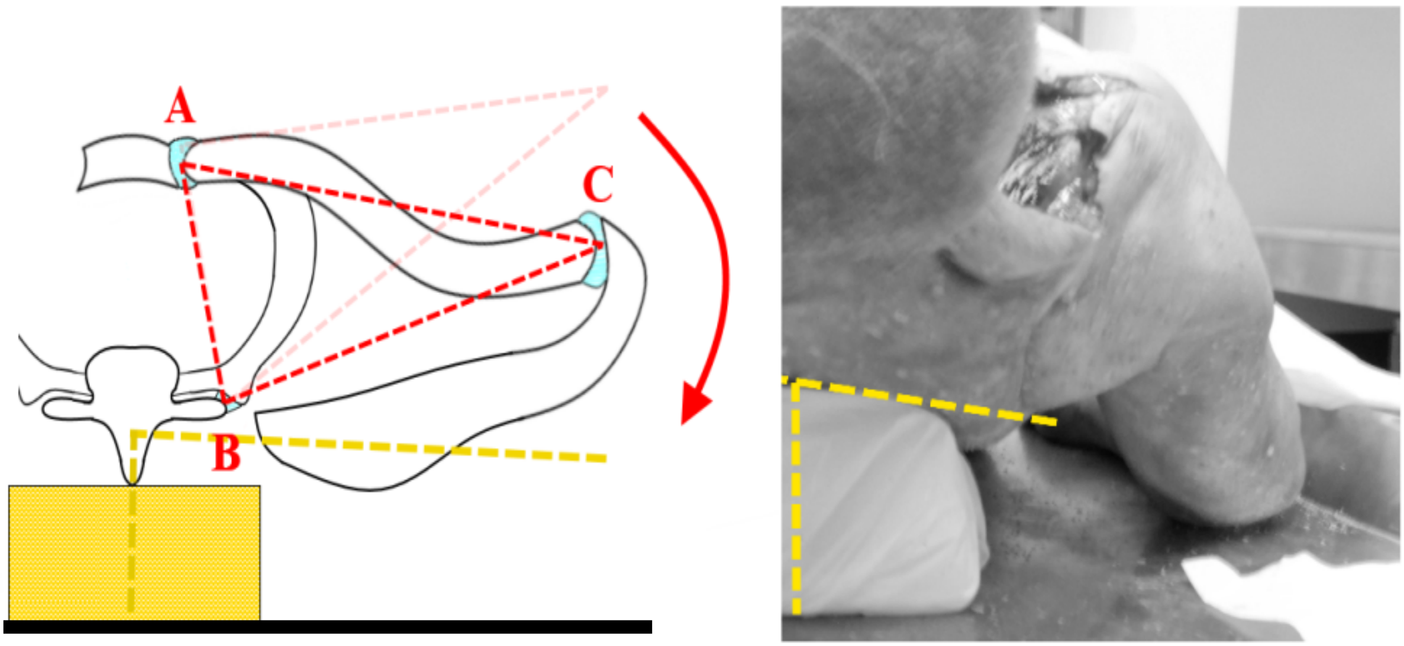

Figure 23 An illustrated view of the changes in dimension with retracted shoulder position using a towel stack along the vertebrae (Left=hypothesized; Right=image of the cadaver with the emulated position). Dashed yellow line outlines the approximate angle of retraction of the shoulders.

4.2.6 Calculations of the Supraclavicular Triangular Area

All three non-consecutively recorded measurements (AB, BC and AC) in each shoulder position group were used to calculate the triangular area of the supraclavicular triangle using Heron’s formula (Nelsen, 2001):

$$s = \frac{X+Y+Z}{2}$$

$$\text{Area} = \sqrt{s(s-X)(s-Y)(s-Z)}$$

X=AB dimension

Y=BC dimension

Z=AC dimension

s=intermediary value used to calculate the SCT area

Using this formula only the length of each of the sides of the triangle were needed. No angle measurements were required.

All measurements were transferred to Microsoft Excel and Heron's formula calculations were performed for each measurement set (AB, BC and AC) to calculate the area (mm^2) for the left and right sides of each shoulder position (normal, protraction and retraction).

4.3 Results

4.3.1 Statistical Analyses of Overall Shoulder Positioning Differences

Measurements were imported and analyzed using IBM SPSS Statistic software version 23. Initially, all measurements from cadaver dissections (#1945 and #1956) were categorized into their respective position groups for left and right sides. On SPSS, descriptive statistics was performed calculate mean, standard deviation, minimum and maximum values (Table 7), and to test for normality using Shapiro-Wilk test (Table 8). All categorizations were found to show normal distribution except Left Retraction (p = 0.011) and Right Normal (p = 0.023) groups.

Table 7 Mean±SD, minimum and maximum values of the supraclavicular area (mm^2) of each shoulder manipulation performed on the samples

#1945 & 1956 Descriptive Statistics

	N	Mean	Std. Deviation	Minimum	Maximum
LNormal	6	3647.36	545.57	3090	4307
LProtracted	6	4909.26	65.89	4818	4986
LRetracted	6	3196.90	767.08	2417.63	3904.95
RNormal	6	3886.65	900.06	2957.88	4758.36
RProtracted	6	5277.80	426.71	4844.71	5740.66
RRetracted	6	3758.16	787.12	2848.48	4526.46

Table 8 Shapiro-Wilk test of normality was performed on the SCT areas under each shoulder manipulation groups. All groups except left retraction and right normal displayed normal distribution, representing a non-normal distribution

Tests of Normality

Left/Right	Shoulder Position	Shapiro-Wilk		
		Statistic	df	Sig.
Left	Normal	.823	6	.094
	Protraction	.943	6	.687
	Retraction	.723	6	.011
Right	Normal	.756	6	.023
	Protraction	.819	6	.086
	Retraction	.800	6	.059

Following this finding, Friedman Test was performed (dependent group, non-parametric analysis) to examine for any significant differences. Friedman Test resulted in a significant difference ($p<0.05$) and a post-hoc Wilcoxon Signed Ranks test with Bonferroni correction was performed to find specific differences between groups. Using this test, all possible differences were examined between shoulder position groups and between left and right groups (Table 9).

Table 9 Post-Friedman test (which showed significance), Wilcoxon Signed Ranks test was performed to examine for statistical differences between shoulder manipulation groups of left and right sides

Wilcoxon Signed Ranks Test Statistics

	LProtracted - LNormal	LRetracted - LNormal	LRetracted - LProtracted	RProtracted - RNormal	RRetracted - RNormal	RRetracted - RProtracted	RNormal - LNormal	RProtracted - LProtracted	RRetracted - LRetracted
Asymp. Sig. (2-tailed)	0.028	0.028	0.028	0.028	0.173	0.028	0.249	0.116	0.028

Statistical differences were divided into position differences on left & right sides, and differences between sides. Left side displayed significant differences between all groups: Normal-Protraction, Normal-Retraction and Protraction-Retraction (p=0.028) (Figure 24A). Right side displayed significant differences between Normal-Protaction and Protraction-Retraction (p=0.028), except Normal-Retraction (p=0.173) (Figure 24B). Between left & right sides, no significant differences were observed in left & right Normal, and left & right Protraction groups, however, a difference was found between left & right Retractions (p = 0.028) (Figure 25).

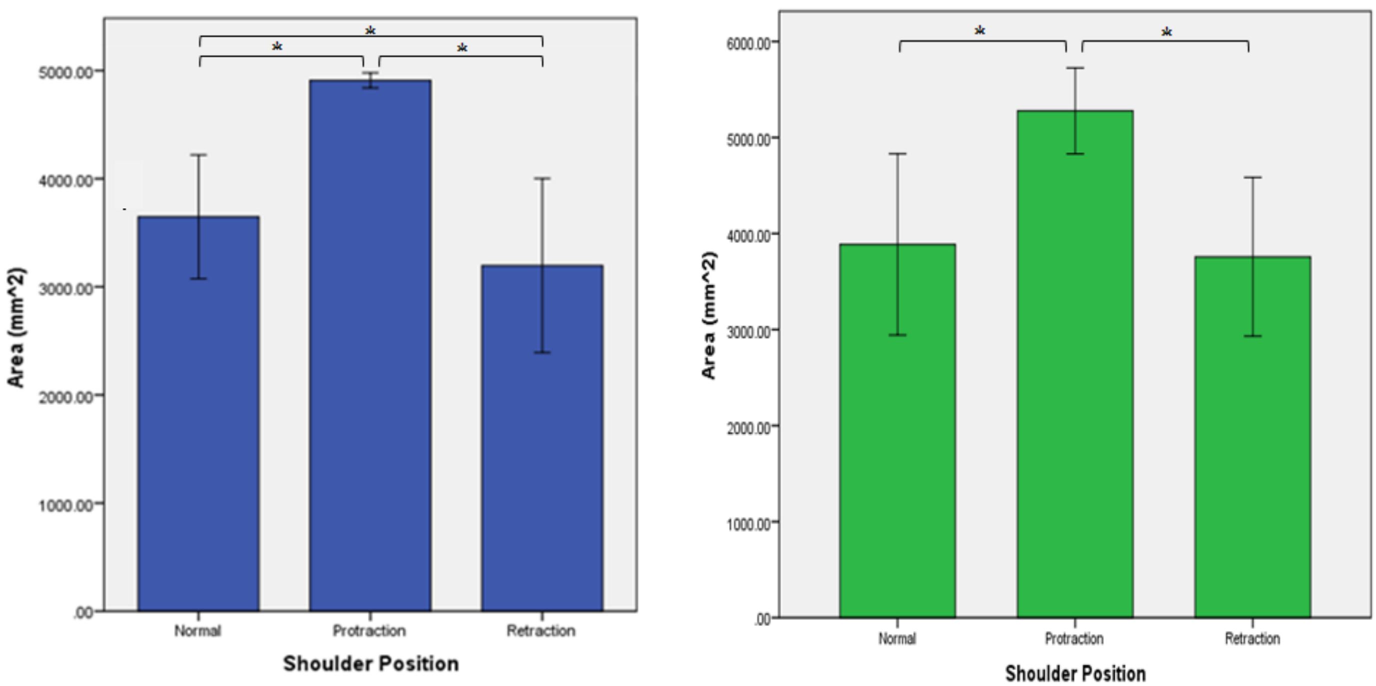

Figure 24A/B Changes in the supraclavicular triangular area observed with shoulder position on the left shoulder side (Left, A) and right shoulder side (Right, B).

* represents significance ($p < 0.05$)

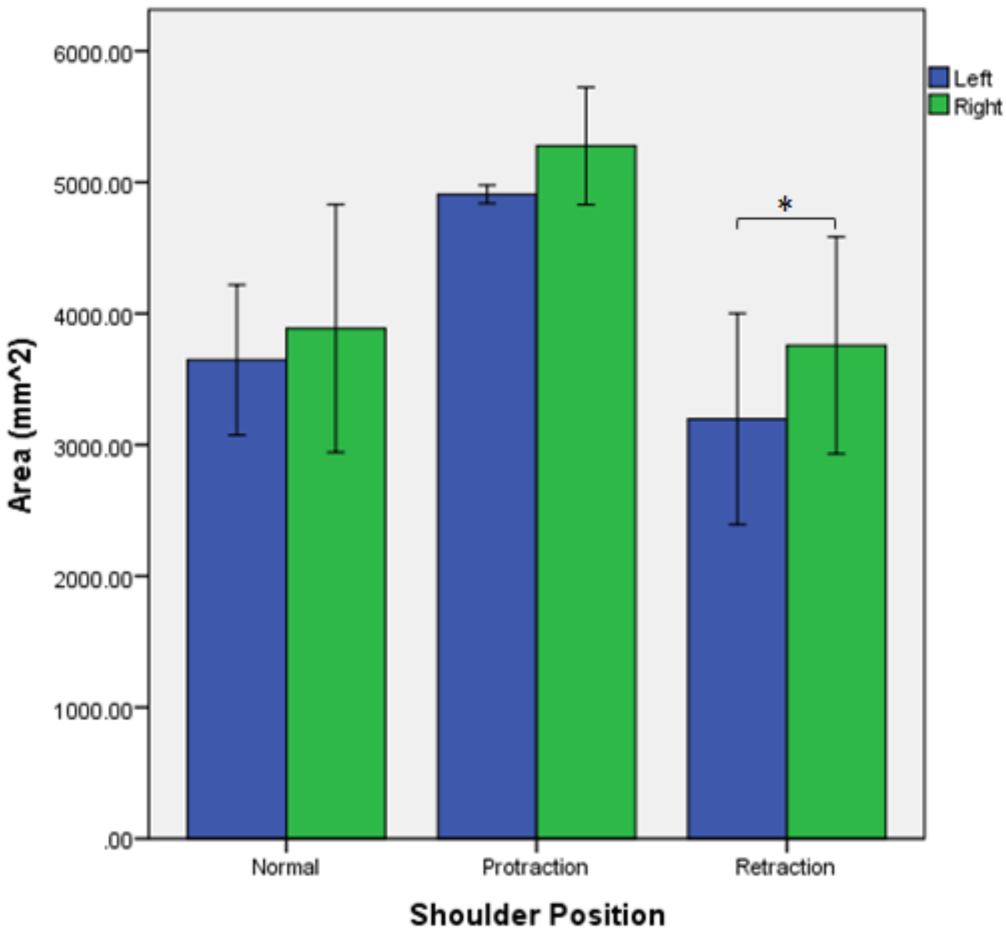

Figure 25 Changes in the supraclavicular triangular area between left and right sides observed with shoulder positioning.

* represents significance ($p < 0.05$)

4.3.2 Differences between #1945 and #1956

To examine for dimensional differences in position between cadaver dissections #1945 and #1956, descriptive statistics were performed on each dissections (Table 10) on SPSS. Using the calculated means, the percentage changes between each position were calculated in Microsoft Excel (Table 11). In sample #1945, protraction resulted in a 20.2% increase from normal (L=20.0%, R=20.3%), retraction resulted in 5.4% decrease from normal (L=5.8%, R=5.0%), and protraction resulted in a 27.1% increase from retraction (L=27.4%, R = 26.7%). In sample #1956, protraction resulted in 56.6% increase from normal (L=53.7%, R=56.6%), retraction resulted in 10.8% decrease from normal (L=20.9%, R=0.7%), and protraction resulted in 77.5% increase from retraction (L=94.3%, R=60.6%).

Table 10 Left and right means±SD of window dimensions in shoulder manipulations of the supraclavicular triangle in both cadavers (#1945 above, #1956 below)

#1945 Descriptive Statistics

	N	Mean	Std. Deviation	Minimum	Maximum
LNormal	3	4136.54	147.86	4043.44	4307.04
LProtracted	3	4964.67	20.065	4946.91	4986.44
LRetracted	3	3895.96	8.15	3889.05	3904.95
RNormal	3	4703.73	47.35	4674.34	4758.36
RProtracted	3	5658.56	110.39	5533.06	5740.66
RRetracted	3	4467.69	60.87	4404.91	4526.46

#1956 Descriptive Statistics

	N	Mean	Std. Deviation	Minimum	Maximum
LNormal	3	3158.18	66.19	3089.79	3221.94
LProtracted	3	4853.84	35.18	4817.83	4888.14
LRetracted	3	2497.84	70.22	2417.63	2548.29
RNormal	3	3069.57	142.09	2957.88	3229.51
RProtracted	3	4897.03	89.83	4844.71	5000.77
RRetracted	3	3048.63	186.84	2848.48	3218.45

Table 11 Change in supraclavicular dimensions observed between shoulder positions of left and right sides in both samples. Negative change% represents an increase in area; positive change% represents a decrease in area

	Sample #1945				Sample #1956			
	positioning	mean (mm^2)	Δ position	change	positioning	mean (mm^2)	Δ position	change
Left	Normal (N)	4136.5	N-P	-20.0%	Normal (N)	3158.2	N-P	-53.7%
	Protraction (P)	4964.7	N-R	5.8%	Protraction (P)	4853.8	N-R	20.9%
	Retraction (R)	3896.0	P-R	27.4%	Retraction (R)	2497.8	P-R	94.3%
Right	Normal (N)	4703.7	N-P	-20.3%	Normal (N)	3069.6	N-P	-59.5%
	Protraction (P)	5658.6	N-R	5.0%	Protraction (P)	4897.0	N-R	0.7%
	Retraction (R)	4467.7	P-R	26.7%	Retraction (R)	3048.6	P-R	60.6%

4.3.3 Differences between AB, AC and BC dimensions

Table 12 Significance values from post hoc Tukey's test following a one way ANOVA examining differences of AB, AC and BC dimensions between shoulder positions in both samples. †From Wilcoxon signed ranks test following a non-parametric analysis. *significance was observed $p<0.05$

#1945				**#1956**			
Dimensions	Comparison of shoulder position		Significance* (p<0.05)	Dimensions	Comparison of shoulder position		Significance* (p<0.05)
AB	Normal	Protract	0.004*	AB	Normal	Protract	0.000*
	Protract	Retract	0.088		Protract	Retract	0.000*
	Normal	Retract	0.275		Normal	Retract	0.846
AC	Normal	Protract	0.448	AC†	Normal	Protract	0.028*
	Protract	Retract	0.190		Protract	Retract	0.028*
	Normal	Retract	0.822		Normal	Retract	0.345
BC	Normal	Protract	0.001*	BC	Normal	Protract	0.000*
	Protract	Retract	0.000*		Protract	Retract	0.000*
	Normal	Retract	0.136		Normal	Retract	0.138

Significant differences were observed for the AB dimensions between normal-protract movements in both cadavers (*p*=0.004; 0.000), and protract-retract movement in #1956 (*p*=0.000). With the AC dimension, significant differences were only observed in cadaver #1956 between normal-protract (*p*=0.028) and protract-retract (*p*=0.028). Significances for BC dimensions were observed in normal-protract (*p*=0.001; 0.000) and protract-retract (*p*=0.000; 0.000) movements in both cadavers #1945 and #1956, respectively.

4.4 Discussion

4.4.1 Rationale on the selection of landmarks

The landmark points used in this study to measure the supraclavicular triangle were A) sternoclavicular joint, B) costotransverse joint of T1 and 3) acromioclavicular joint. The primary reason these structures were selected to represent the triangular points of the supraclavicular triangle was that they were easy to identify in dissection, presented little variation in position, and were fixed bony landmarks. Points A, B, and C were relatively superficial in location and were dissected with ease in both cadavers. Soft tissue landmarks like the anterior scalene muscle or the inferior belly of omohyoid have been reported to present significant variation in position (Hirokawa, 2010; Rozing, 1993) and may have led to a misrepresentative measurement of the SCT. All in all, fixed bony landmarks structures, rather than mobile, variable and soft tissues were selected to encompass all structures of interest in the supraclavicular triangle and to overcome any ambiguity in its borders reported in literature. It was also thought that these landmarks points would be best representative of the changes that would occur in the SCT with manipulations of the shoulder position during protraction and retraction.

4.4.2 Changes in the SCT Dimensions

The three dimensions of the SCT measured were:

- AB (sternoclavicular-to-costotransverse joint)
- AC (sternoclavicular-to-acromioclavicular joint), and
- BC (costotransverse-to-acromioclavicular joint)

AB dimension demonstrated significant increases from its size in normal in both cadavers, and also from retracted dimension in #1956. Interestingly, both protraction and retraction increased AB relative to normal. It is known that the clavicle acts as a pivot to accommodate the movements of the shoulder girdle at its acromioclavicular and sternoclavicular joints, which may induce an anterior movement of the clavicle at its proximal attachment to the manubrium, however, the increases in dimension for retraction remains to be explored (Moore et al., 2013). Presently, this study cannot fully explain the biomechanical reasons behind the contradictory increase in AB dimension in both protraction and retraction movements of the shoulder. However, it is evident that protraction may lead to the greatest increase in the AB dimension and increase the anteroposterior diameter between the clavicle and the transverse process of the T1 vertebra. Further studies will be required to elucidate the biomechanical reasoning behind this opposing finding.

No changes were expected with AC dimension between bodies, as AC dimension represented the fixed, proximal to distal length of the clavicle. No significance was observed in the AC dimensions of #1945 and this finding supported the notion that AC dimension represents a fixed, unchanging length of the clavicle. However, AC dimensions from #1956 presented significant differences between Normal-Protraction and Protraction-Retraction which is inconsistent with the findings from #1945. This discrepancy may be explained by the property of osteological structures to withstand strain and bend without fracturing. In particular, biomechanical studies examining bending properties of the human clavicle reported some degree of flexibility of the clavicle with applied strain (Kemper et al., 2009). Due to the observation that #1956 was of smaller physique than #1945, it may be reasonable to infer that the clavicle was also thinner in diameter and bent more readily with protraction and retraction in comparison to the thicker clavicle of #1945.

The most change in measurement occurred in the BC dimension where the most significant difference was observed between both cadavers during normal-protraction and protraction-retraction. Anatomically, the scapula is only supported medially by soft tissue and present an avenue where changes can occur in the BC dimension. In addition, the approximate fixed lengths of AB and AC dimensions result in the changes in the angle ∠ABC and the subsequent alterations to the BC dimension, which may have been the primary reason for the observed differences in SCT area across shoulder positioning.

4.4.3 Changes in the Supraclavicular Triangle Area

Statistical analysis of all changes in SCT areas in both samples displayed that there was a significant difference observed between all shoulder positions of both sides (p=0.028), with the exception of right normal to right retracted (p=0.173). Furthermore, we expected to observe no significant differences between SCT areas of the left and right side, however, there was a significant difference observed between left retraction and right retraction.

Significant differences in SCT area between normal-protraction, protraction-retraction, and normal-retraction may present the finding that shoulder positioning does significantly change the exposure area of the supraclavicular window. Protraction produced the highest exposure of the window in comparison to the normal and retraction windows, and retraction produced the least exposure. The clinical significance of this finding will be discussed below. Similar to the left side changes, we expected similar results on the right side, however, the finding that there was no significant change in the right normal-right retraction, and significant difference between left retracted and right retracted causes some confusion. The inconsistency presented above may quite possibly be explained by the difference in body size between cadavers. Cadaver #1945 was significantly larger in size compared to #1956 and the width between the scapulae may have been wider in 1945 than in 1956. The paper towel stack used was of a fixed width, and when it was placed between the vertebrae between the scapulae for retraction, it's possible that the width of the towel significantly overlapped one of the scapulae allowing retraction in the left side but not the right in 1956 (L-Retraction to R-Retraction, p=0.028). This would have resulted in right retraction area being similar in area to the right normal position, which is what was observed in this study (R-Normal to R-Retracted, p=0.173). Another source of error may have been attributed to human error in a skew placement of the towel stack along the vertebrae.

4.4.4 The effect of body size on SCT area

As mentioned previously, cadaver #1945 was significantly larger in size than #1956. Due to the fact that the towel stack used in this study was of a relatively fixed dimension (dimensions prior to placement: 10cm high x 9cm in wide; post placement: 7cm high x 9cm wide) and the cadaver size was not taken into account, it is very likely that the towel stack produced a much greater changes in the smaller physique of #1956 than in #1945. Upon examination of the % differences in the SCT area between #1945 and #1956, the latter resulted in much greater changes in area in protraction and retraction from normal in comparison to the changes observed in the former. Protraction in #1956 yielded a 53.7% change in area from normal, compared to a 20.0% change in area in #1945. Retraction resulted in a 20% decrease in area versus 5.8% in #1945. These exaggerated differences may very well be attributed to the fact that physiques of the cadavers were not taken into account with the usage of a fixed towel stack, and is an area of improvement of this study.

4.4.5 Clinical importance

The finding of the study that protraction might produce the greatest increase in the supraclavicular window in comparison to normal and retracted shoulder position may provide evidence in favor of protraction being the optimal position for maximal exposure. Conversely, retraction may result in a decrease in the SCT area compared to normal dimensions and be the least favorable for exposure of the SCT area. The increase in area of exposure varied between $9cm^2$ to $17cm^2$, ranging from a 20-54% increase in area between bodies, respectively. In reference to the diameter of an average Canadian penny (approximately $2.83cm^2$), this equates to an increase in area ranging from a little more than 3 pennies to 6 pennies. In contrast, retraction resulted in a decrease in exposure area ranging from 5.8% ($2.4cm^2$) to 21% ($6.7cm^2$) relative to normal in #1945 and #1956 respectively, an equivalent to a reduced exposure by 1 penny to a little less than 3 and a half pennies from normal, respectively.

Operations in the supraclavicular triangle which benefit from greater window exposure such as scalenectomies, first rib resections, brachial plexus surgeries and vascular surgeries of the subclavian artery may increase chances of operative success and minimize inadvertent damage due to problems that may arise with restricted visualization. However especially in vascular surgery, it is important to note that in addition to maximal exposure area, exposure depth also plays a very important part in the ease of operation. Koh et al. (2006) and Bentel et al. (2000) demonstrated that supraclavicular fossa depth was linearly associated with patient size, BMI and anteroposterior diameter. Future studies may investigate positional manipulations to reduce the depth of SCF for optimal surgical exposure of its contents, including vascular, muscular and neural contents.

4.4.6 Exclusion of Positional Manipulations

Additional shoulder manipulations of elevation and depression were excluded as a variable in this study due to the inherent difficulty in establishing a 'normal' shoulder position among fresh cadavers. However, we recognize that elevation and depression may have a role in affecting the area of the supraclavicular window, and is an additional area of potential future direction (Kang et al., 2011; Kitagawa et al., 2005). In addition, manipulations of the upper extremity, in particular, abduction and external rotation (ABER) movements may also play a role and may be an area of further research as well (Park et al., 2013; Matsumura et al., 1997). Finally, due to the stiffness of the neck despite adequate thawing of the fresh cadaver, neck rotations were also excluded, however, we recognize that it may play a role in the exposure of the SCT area (Alemanno & Vigl, 2014).

4.5 Limitations

The small number of fresh cadavers dissected in this study (L&R sides n=4) presents itself as a limitation, and may over represent the increases in area that may occur with shoulder manipulations across an increased sample size. In addition, the inherent rigidity of cadavers despite adequate duration of thawing may have also presented as a limitation in this study. In particular, the shoulders of #1956 was fixed in a slightly elevated state and may have confounded the results of this study.

4.6 Future Directions

4.6.1 Volumetric Analysis of the Supraclavicular Fossa

In the future, this study may examine the changes in the depth of the supraclavicular fossa with shoulder manipulations of elevation and depression. Studies examining this effect have reported that depression resulted in a decreased diameter of the costoclavicular space and subclavian vein, and increased the association of the subclavian vein with the subclavian artery (Kitagawa et al., 2005). Although the authors of the previous study did not explore in detail the effect of elevation/depression on the depth of the supraclavicular contents, it may be possible that the anteroposterior compression of the SCF contents may lead to an upward displacement and consequently, a more superficial exposure of the subclavian artery with shoulder depression.

Currently, we believe the best way to achieve this is by the following protocol: First, dissecting the supraclavicular fossa of a fresh cadaver following supraclavicular surgical guidelines and exposing the subclavian artery and anterior scalene muscle, in particular. Second, orienting the cadaver's SCF to be parallel to the ground (0°), which may involve positioning the cadaver to be leaning slightly posteriorly. Third, shoulder manipulations will be performed, elevating and depressing the shoulder by a certain distance relative to the height of the acromioclavicular joint. This step may involve using graded movements of the elevation and depression to examine the effect of different degrees of movements on the exposure. Lastly, injecting a gelatin + dye mixture into the SCF until the the fossa becomes filled to the brim following each movement, removing the injected mixture and measuring its weight and calculating its volume using its density. This step may be preceded by the placement of an impermeable plastic wrap to cover SCF structures and the depth of the fossa to prevent any unintended leakage of the gelatin+dye mixture into the tissues or its crevices. Koh et al. (2013) have demonstrated that the depth of the supraclavicular fossa is linearly correlated with BMI and anteroposterior diameter. This future direction may wish to measure the AP dimension (from the sternoclavicular joint to the costotransverse process of T1 vertebra) and correlate it to the findings of the depth of the SCF.

4.6.2 Graded height of manipulations

This study only examined the effect of using a fixed, one-sized towel stack (10cm height x 9cm width, which was compressed to 7cm in height under cadavers) on protraction and retraction. In the future, it may be useful to examine the effect of using towel stacks of varying height and width on the dimensions of the SCT. Examining changes that occur in the SCT with gradual increases in protraction using 5cm, 10cm, 15cm and 20cm towel stacks, for example, may provide useful information in elucidating an optimal shoulder protraction height of position for maximal supraclavicular exposure area. It may be in the best interest of this future study to examine this increase in SCT exposure area with increasing shoulder protraction height, and investigate the height that results in the maximal increase in exposure area. Similar procedure may be used to examine the effect of graded heights of retraction on the SCT exposure area.

4.6.3 Palpation methods of measuring SCT area

Division of musculature and fascia, including SCM, inferior belly of omoyhoid, platysma, deep cervical fascia of the neck may have increased the mobility of the shoulder during protraction and retraction. It is a possibility that increases in dimension observed in this study may, at least in part, be attributed to the process of dissection and not shoulder manipulation. Further studies may wish to examine this question on human volunteers by marking easily palpable surface anatomical structures of sternoclavicular joint (A), acromioclavicular joint (B) and spinous process of T1 vertebra (C) to outline the boundaries of the supraclavicular triangle. Protraction and retraction could be emulated on the volunteers, and the resulting measurements of the change in SCT area may be examined. If there is no significant difference in change between dissections observed in our study and palpation measurements from this study, we may conclude that an observable increase in area using surface landmarks is reflective of increase in area that will be observed during dissections in the operating room. The protraction and retraction in the future study may wish to incorporate graded height of shoulder manipulations, as mentioned previously.

4.7 Conclusions

This study demonstrated that the exposure area of the supraclavicular triangle present significant differences with manipulations of the shoulder in protraction and retraction movements. Boundaries of the supraclavicular triangle were set by A) sternoclavicular joint, B) costotransverse joint, and C) acromioclavicular joint to best encompass all of the important anatomical structures of the SCF and to overcome ambiguities in literature. Protraction of the shoulders produced the greatest increase in the SCT area from normal and retraction dimensions. Conversely, retraction resulted in a reduction in SCT area from normal dimensions. In this study, protraction of the shoulders presented to be the optimal shoulder position to maximize the supraclavicular window exposure and its contents, and may serve beneficial to adopt as the patient positioning of choice for supraclavicular surgeries.

Chapter 5

Overall Discussion & Conclusion

The overall study and its objectives primarily aimed to increase knowledge of vascular anatomy and vascular operative procedures. The findings of the subclavian branching pattern study presented the most common variations observed in approximately 100 CTAs, and examined differences in the prevalence of order of SCA branches. Proximal to distal along the subclavian artery, the pattern of variation with the highest prevalence was examined to be V-I-T-C-D in 13% (13/101 SCAs). This characteristic pattern was consistent with the pattern taught in some medical curricula, however, the prevalence was much lower to be considered a predominant pattern. The knowledge that V-I-T-C-D only comprises of 13% SCA variations is a key take home point to consider in surgeries of the subclavian artery. Increasing awareness of potential variations of SCA branching pattern may be an important step in reducing injuries caused by unfamiliarity of anatomical variations. Despite the knowledge of variations in the subclavian artery branching attained, sole awareness of these patterns may not be practical in subclavian surgeries without relationships to landmark anatomical structures. In particular, the preservation of vertebral artery was determined to be highly important and this led to examining the possibility of using the anterior scalene muscle as a landmark to estimate the origin of the vertebral artery. ASM is a well-known landmark to structures such as the phrenic nerve, subclavian artery and brachial plexus, and was deemed appropriate to set as the point of interest. This study demonstrated that VA originated 3cm proximal to the medial margin of ASM in approximately 95% of cases, and that ASM may serve as a reliable landmark to estimate and preserve the origin of the VA in subclavian surgeries. However, the proximal subclavian artery and the origin of the vertebral artery presents difficulty with exposure as it resides in the compact and complex region of the thoracic inlet. Surgical approaches to the proximal SCA and VA origin utilizes the supraclavicular exposure technique, which requires optimization in its operative procedure in patient positioning. This last study examined the effect of shoulder positioning of protraction and retraction on the dimensions of the SCT window. The findings of this study demonstrated that protraction maximally increased the anteroposterior measurement of the supraclavicular window at the proximal clavicle (AB dimension) in addition to maximally increasing SCT window area in comparison to the normal and retracted SCT areas. Although this study did not attempt to examine visual exposure differences, protraction of the shoulder may provide an optimal exposure of the proximal subclavian artery and vertebral origin to aid in improving visualization of the operative window and may help to reduce inadvertent injury that could occur during operation.

References

Abd, A. G., Braun, N. M., Baskin, M. I., O'Sullivan, M. M., & Alkaitis, D. A. (1989). Diaphragmatic dysfunction after open heart surgery: treatment with a rocking bed. Annals of internal medicine, 111(11), 881-886.

Alemanno, F., & Vigl, E. E. (2014). Topographical Anatomy. In *Anesthesia of the Upper Limb* (pp. 19-35). Springer Milan.

Appelboam, A., Reuben, A., Mann, C., Gagg, J., Ewings, P., Barton, A., ... & Benger, J. (2015). Postural modification to the standard Valsalva manoeuvre for emergency treatment of supraventricular tachycardias (REVERT): a randomised controlled trial. *The Lancet*, *386*(10005), 1747-1753.

Baldwin, Z. K., Chuter, T. A., Hiramoto, J. S., Reilly, L. M., & Schneider, D. B. (2008). Double-barrel technique for endovascular exclusion of an aortic arch aneurysm without sternotomy. *Journal of Endovascular Therapy*, *15*(2), 161-165.

Bergman, R. A., Thompson, S. A., Afifi, A. K., & Saadeh, F. A. (1988). Compendium of human anatomical variation: text, atlas and world literature. *Baltimore, Urban and Schwarzenberg*, *41*, 282-88.

Bhatia, K., Ghabriel, M. N., & Henneberg, M. (2005). Anatomical variations in the branches of the human aortic arch: a recent study of a South Australian population. *Folia Morphologica-Warszawa-English edition*, *64*(3), 217.

Bickerstaff, L. K., Pairolero, P. C., Hollier, L. H., Melton, L. J., Van Peenen, H. J., & Cherry, K. J. (1982). Thoracic aortic aneurysms: a population-based study. *Atherosclerosis*, *15*, 29.

Bigeleisen, P. E. (2003). Anatomical variations of the phrenic nerve and its clinical implication for supraclavicular block. British Journal of Anaesthesia, 91(6), 916–917. http://doi.org/10.1093/bja/aeg254

Cahill, D. R., & Leonard, R. J. (1999). Missteps and masquerade in American medical academe: Clinical anatomists call for action. *Clinical Anatomy*, *12*(3), 220-222.

Chaikof, E. L., Blankensteijn, J. D., Harris, P. L., White, G. H., Zarins, C. K., Bernhard, V. M., ... & Rutherford, R. B. (2002). Reporting standards for endovascular aortic aneurysm repair. *Journal of vascular surgery*, *35*(5), 1048-1060.

Chung, K. C., Yang, L. J., & McGillicuddy, J. E. (2011). *Practical management of pediatric and adult brachial plexus palsies*. Elsevier Health Sciences.

Clouse, W. D., Hallett Jr, J. W., Schaff, H. V., Gayari, M. M., Ilstrup, D. M., & Melton III, L. J. (1998). Improved prognosis of thoracic aortic aneurysms: a population-based study. *Jama*, *280*(22), 1926-1929.

Coady, M. A., Rizzo, J. A., Goldstein, L. J., & Elefteriades, J. A. (1999). Natural history, pathogenesis, and etiology of thoracic aortic aneurysms and dissections. *Cardiology clinics*, *17*(4), 615-635.

Coady, M. A., Rizzo, J. A., Hammond, G. L., Mandapati, D., Darr, U., Kopf, G. S., & Elefteriades, J. A. (1997). What is the appropriate size criterion for resection of thoracic aortic aneurysms?. *The Journal of thoracic and cardiovascular surgery*, *113*(3), 476-491.

Cousins, M. J., Bridenbaugh, P. O., Carr, D. B., & Horlocker, T. T. (Eds.). (2009). *Cousins and Bridenbaugh's neural blockade in clinical anesthesia and pain medicine*. Lippincott Williams & Wilkins.

Davies, R. R., Goldstein, L. J., Coady, M. a., Tittle, S. L., Rizzo, J. a., Kopf, G. S., & Elefteriades, J. a. (2002). Yearly Rupture or Dissection Rates for Thoracic Aortic Aneurysms: Simple Prediction Based on Size. *Annals of Thoracic Surgery*, *73*(1), 17–28. http://doi.org/10.1016/S0003-4975(01)03236-2

Dodevski, A., & Tosovska-Lazarova, D. (2012). Anatomical Features and Clinical Importance of the Vertebral Artery. *Macedonian Journal of Medical Sciences*, *5*(3), 328-335.
Edwards, J. E. (1948). Anomalies of the derivatives of the aortic arch system. *The Medical clinics of North America*, *32*, 925.

Elefteriades, J. A., & Rizzo, J. A. (2007). Epidemiology: incidence, prevalence, and trends. *Acute aortic disease. New York: Informa Healthcare*, 89-98.

Feezor, R. J., & Lee, W. A. (2009). Management of the Left Subclavian Artery during TEVAR. *Seminars in Vascular Surgery*, *22*(3), 159–164.http://doi.org/10.1053/j.semvascsurg.2009.07.007

Goodney, P. P., Travis, L., Lucas, F. L., Fillinger, M. F., Goodman, D. C., Cronenwett, J. L., & Stone, D. H. (2011). Survival after open versus endovascular thoracic aortic aneurysm repair in an observational study of the Medicare population. *Circulation*, *124*(24), 2661-2669.

Henriquez-Pino, J. a, Gomes, W. J., Prates, J. C., & Buffolo, E. (1997). Surgical anatomy of the internal thoracic artery. *The Annals of Thoracic Surgery*, *64*(4), 1041–1045.

Holt, P. J., Johnson, C., Hinchliffe, R. J., Morgan, R., Jahingiri, M., Loftus, I. M., & Thompson, M. M. (2010). Outcomes of the endovascular management of aortic arch aneurysm: implications for management of the left subclavian artery. *Journal of vascular surgery*, *51*(6), 1329-1338.

Huelke. (1958). A study of the transverse cervical and dorsal scapular arteries, (November), 233–245.

Isselbacher, E. M. (2005). Thoracic and Abdominal Aortic Aneurysms. *Circulation*, *111*(6), 816–828. http://doi.org/10.1161/01.CIR.0000154569.08857.7A

Johansson, G., Markstrom, U., & Swedenborg, J. (1995). Ruptured thoracic aortic aneurysms: A study of incidence and mortality rates. *Journal of Vascular Surgery*, *21*(6), 985–988.

Kanitsar, A., Fleischmann, D., Wegenkittl, R., Felkel, P., & Gröller, M. E. (2002). CPR-curved planar reformation. *IEEE Visualization, 2002. VIS 2002.*, 37–44. http://doi.org/10.1109/VISUAL.2002.1183754

Kasapoglu, F., & Dokuzlar, U. (2007). An unknown anatomical variation of omohyoid muscle. *Clinical Anatomy*, *20*(8), 964-965.

Kemper, A. R., Stitzel, J. D., McNally, C., Gabler, H. C., & Duma, S. M. (2009). Biomechanical response of the human clavicle: the effects of loading direction on bending properties. *J. Appl. Biomech*, 25(2), 165-174.

Klein, D. G. (2005). Thoracic aortic aneurysms. *Journal of Cardiovascular Nursing*, *20*(4), 245-250.

Lee, W. A. (2007). Endovascular abdominal aortic aneurysm sizing and case planning using the TeraRecon Aquarius workstation. *Vascular and Endovascular Surgery*, *41*(1), 61–67. http://doi.org/10.1177/1538574406296244

Lischka, M. F., Krammer, E. B., Rath, T., Riedl, M., & Ellböck, E. (1982). The human thyrocervical trunk: Configuration and variability reinvestigated. *Anatomy and Embryology*, *163*(4), 389–401. http://doi.org/10.1007/BF00305554

Loukas, M., Kinsella, C. R., Louis, R. G., Gandhi, S., & Curry, B. (2006). Surgical Anatomy of the Accessory Phrenic Nerve. Annals of Thoracic Surgery, 82(5), 1870–1875. http://doi.org/10.1016/j.athoracsur.2006.05.098

Loyd, B. J., Gilbert, K. K., Sizer, P. S., Atkins, L. T., Sobczak, S., Brismée, J. M., & Pendergrass, T. J. (2014). The relationship between various anatomical landmarks used for localizing the first rib during surface palpation. *Journal of Manual & Manipulative Therapy*, *22*(3), 129-133.

Makhoul, R. G., & Machleder, H. I. (1992). Developmental anomalies at the thoracic outlet: an analysis of 200 consecutive cases. *Journal of vascular surgery*, *16*(4), 534-545.

Matsumura, J. S., Lee, W. A., Mitchell, R. S., Farber, M. A., Murad, M. H., Lumsden, A. B., ... & Fairman, R. M. (2009). The Society for Vascular Surgery Practice Guidelines: management of the left subclavian artery with thoracic endovascular aortic repair. *Journal of Vascular Surgery*, *50*(5), 1155-1158.

Matula, C., Trattnig, S., Tschabitscher, M., Day, J. D., & Koos, W. T. (1997). The course of the prevertebral segment of the vertebral artery: anatomy and clinical significance. *Surgical neurology*, *48*(2), 131.

Moore, K. L., Dalley, A. F., & Agur, A. M. (2013). *Clinically oriented anatomy*. Lippincott Williams & Wilkins.

Nelsen, R. B. (2001). Heron's formula via proofs without words. *The College Mathematics Journal*, *32*(4), 290.

Oderich, G. S., & Ricotta, J. J. (2009). Modified fenestrated stent grafts: device design, modifications, implantation, and current applications. *Perspectives in vascular surgery and endovascular therapy*, *21*(3), 157-167.

Ouriel, K. (1998). *Atlas of vascular surgery: operative procedures* (Vol. 2). WB Saunders Company.

Owens, W. A., Gladstone, D. J., & Heylings, D. J. (1994). Surgical anatomy of the phrenic nerve and internal mammary artery. *The Annals of thoracic surgery*, 58(3), 843-844.

Poonam, S. R., & Sharma, T. (2010). Incidence of anomalous origins of vertebral artery-Anatomical study and clinical significance. *Journal of Clinical and Diagnostic Research*, *4*, 2626-31.

Reiner, A., & Kasser, R. (1996). Relative frequency of a subclavian vs. a transverse cervical origin for the dorsal scapular artery in humans. *Anatomical Record*, *244*(2), 265–268. http://doi.org/10.1002/(SICI)1097-0185(199602)244:2<265::AID-AR14>3.0.CO;2-N

Rutherford, R. B. (1993). *Atlas of vascular surgery: basic techniques and exposures*. Saunders.

Saito, N., Kimura, T., Odashiro, K., Toma, M., Nobuyoshi, M., Ueno, K., ... & Inoue, K. (2005). Feasibility of the Inoue single-branched stent-graft implantation for thoracic aortic aneurysm or dissection involving the left subclavian artery: short-to medium-term results in 17 patients. *Journal of vascular surgery*, *41*(2), 206-212.

Sanders, R. J., & Hammond, S. L. (2002). Management of cervical ribs and anomalous first ribs causing neurogenic thoracic outlet syndrome. *Journal of vascular surgery*, *36*(1), 51-56.

Schouchoff, B. (2000). Endovascular aortic aneurysm repair: an alternative approach. *Critical care nursing quarterly*, *23*(1), 35-41.

Standring, S. (Ed.). (2015). *Gray's anatomy: the anatomical basis of clinical practice*. Elsevier Health Sciences.

Su, W. D., Ohtsuka, A., Taguchi, T., & Murakami, T. (2000). Typology of the arteries in the human scalenus region, with special reference to the accessory ascending cervical artery. *Acta Medica Okayama*, *54*(6), 243–252.

Sze, D. Y., Van Den Bosch, M. a a J., Dake, M. D., Miller, D. C., Hofmann, L. V., Varghese, R., … Mitchell, R. S. (2009). Factors portending endoleak formation after thoracic aortic stent-graft repair of complicated aortic dissection. *Circulation: Cardiovascular Interventions*, *2*(2), 105–112. http://doi.org/10.1161/CIRCINTERVENTIONS.108.819722

Tan, B. K., Hong, S. W., Huang, M. H., & Lee, S. T. (2000). Anatomic basis of safe percutaneous subclavian venous catheterization. *The Journal of Trauma*, *48*(1), 82–6. Retrieved from http://www.ncbi.nlm.nih.gov/pubmed/10647570

Weiglein, A. H., Moriggl, B., Schalk, C., Künzel, K. H., & Müller, U. (2005). Arteries in the posterior cervical triangle in man. *Clinical Anatomy*, *18*(8), 553–557. http://doi.org/10.1002/ca.20143

Wiki Commons
1) Use of image permissible under the licence Creative Commons Attribution-ShareAlike 2.1 Japan (CC BY-SA 2.1JP). http://creativecommons.org/licenses/by-sa/2.1/jp/deed.en
Image has been removed of red highlight of the vertebra.
(https://commons.wikimedia.org/wiki/File:Thoracic_vertebra_2_poterior2.png)

Xenos, E. S., Abedi, N. N., Davenport, D. L., Minion, D. J., Hamdallah, O., Sorial, E. E., & Endean, E. D. (2008). Meta-analysis of endovascular vs open repair for traumatic descending thoracic aortic rupture. *Journal of vascular surgery*, *48*(5), 1343-1351.

Yamaki, K., Saga, T., Hirata, T., Sakaino, M., Nohno, M., Kobayashi, S., & Hirao, T. (2006). Anatomical study of the vertebral artery in Japanese adults. *Anatomical Science International / Japanese Association of Anatomists*, *81*(2), 100–106. http://doi.org/10.1111/j.1447-073X.2006.00133.

Yücel, a H., Kizilkanat, E., & Ozdemir, C. O. (1999). The variations of the subclavian artery and its branches. Okajimas Folia Anatomica Japonica, 76(5), 255–261.

Ziółkowski, M., Marek, J., & Oficjalska-Młyńczak, J. (1982). The omohyoid muscle during the fetal period in man. *Folia morphologica*, *42*(1), 21-30.

Appendix A

Measurements on the branch origin distances of the subclavian artery

	Age	L/R	# of branches	Length	Measurement	Typical					TCT branches				CCT branches		Acc. VA	ITA/DSA	ITA/TCT	other	other #2
	Sex					VA	ITA	TCT	CCT	DSA	IT	SSA	TCA/SSA	A.Cerv	D.Cerv	SITA					
1007 02 57	48	R	5	109	distance along subclavian	59.1	62.2	61.3	62.6	75.2											
	F					0.5422	0.57064	0.56238	0.57431	0.6899											
					diameter at origin	4.56	2.08	4.04	2.39	3											
					quadrant	S	I	A	S	SL											
1007 02 57	48	L	6	95	distance along subclavian	29.5	41.4	42.7	37.4	54.5					49.5						
	F					0.31052	0.43578	0.44947	0.39368	0.57368					0.521053						
					diameter at origin	3.74	3.19	3.81	1.98	2.34					1.31						
					quadrant	S	I	A	S	SL					S						
1196 58 00	50	R	5	135	distance along subclavian	82.1	93.4	86.3	90.5	111											
	M					0.60814	0.69185	0.63925	0.67037	0.82222											
					diameter at origin	3.41	4.79	5.2	2.85	2.67											
					quadrant	S	I	A	SP	S											
1196 58 00	50	L	6	108	distance along subclavian	51.5	64.9	63.2	71.7	86.6											56.5
	M					0.47685	0.60092	0.58518	0.66388	0.80185											0.5231481
					diameter at origin	4.07	3.11	5.35	3.56	2.45											6.33
					quadrant	S	I	A	PS	S											P
1192 92 10	47	R	6	126	distance along subclavian	67.7	70	>			64.2				75.6						
	M					0.5373	0.55555				0.50952				0.6						
					diameter at origin	5.35	2.31				1.91				1.05						
					quadrant	S	I				S				S						
1192 92 10	47	L	5	96	distance along subclavian	30.7	45.3	45.3		65.2						28.8					
	M					0.31979	0.47187	0.47187		0.67916						0.3					
					diameter at origin	4.88	3.4	3.8		3.37						1.6					
					quadrant	S	AI	A		SL						P					
1059 16 90	85	R	4	151	distance along subclavian	99.4	101	103	113												
	M					0.65827	0.66887	0.68211	0.74834												
					diameter at origin	1.9	2.63	3.38	2.36												
					quadrant	S	AI	AS	P												
1059 16 90	85	L	4	121	distance along subclavian	66.1	67.7	67.7	72.4												
	M					0.546281	0.5595	0.5595	0.59834												
					diameter at origin	3.2	2.5	5.22	4.35												
					quadrant	S	AI	A	P												
1060 84 38	58	R	5	105	distance along subclavian	65.5	66.8	66.8	71.1											75.8	
	F					0.6238	0.63619	0.63619	0.67714											0.721905	
					diameter at origin	3.38	3.36	3.3	1.9											0.933	
					quadrant	MS	AI	A	MPS											MS	
1060 84 38	58	L	4	78.3	distance along subclavian	36.9	39.9	40.5	36.9												
	F					0.47126	0.50957	0.51724	0.47126												
					diameter at origin	2.77	2.77	4.22	1.91												
					quadrant	MS	AI	A	MS												
1136 39 22	59	R	5	121	distance along subclavian	68.9	77.2	72.5	75.6	92.9											
	M					0.56942	0.63801	0.59917	0.62479	0.76776											
					diameter at origin	3.7	3.94	4.68	3.3	3.75											
					quadrant	S	I	A	S	SL											
1136 39 22	59	L	6	97.3	distance along subclavian	40.1	45.7	48.6	43.9	67.7					52.5						
	M					0.412127	0.46968	0.49948	0.45118	0.69578					0.539568						
					diameter at origin	3.42	2.97	3.86	2.63	3.04					2.5						
					quadrant	S	I	A	PS	SL					S						
1065 31 82	92	R	7	146	distance along subclavian	88.2	92.2	94.4	>	125	92.2				105	101					
	M					0.6041	0.6315	0.64657		1.32415	0.6315				0.719178	0.691781					
					diameter at origin	3.56	3.37	5.66		2.73	3.72				1.31	1.99					
					quadrant	S	I	A		SL	AS				SM	P					
1065 31 82	92	L	5	94.3	distance along subclavian	47.8	61.7	60.3							55.1						
	M					0.50689	0.65429	0.63944							0.584305						
					diameter at origin	3.19	2.18	4.7							2.35						
					quadrant	MS	I	A							MS						
1128 31 60	51	R	5	107	distance along subclavian	67	76.6	67	74.2							80.1					
	M					0.62616	0.71588	0.62616	0.69345							0.748598					
					diameter at origin	3.38	2.74	3.26	2.68							1.24					
					quadrant	S	I	AS	S							S					
1128 31 60	51	L	5	80.1	distance along subclavian	36.8	45.9	45.9	44											41.8	
	M					0.45942	0.57303	0.57303	0.54931											0.521848	
					diameter at origin	4.17	4.18	5.6	3.16											2.94	
					quadrant	S	I	A	S											PS	
1038 00 44	68	R	6	120	distance along subclavian	65	70.3	69.6	73.2		68.6										80.4
	F					0.54166	0.58583	0.58	0.61		0.57166										0.67
					diameter at origin	3.38	2.49	-	2.41		1.39										1.62
					quadrant	S	I	A	S		S										S
1038 00 44	TY EIC	left			distance along subclavian																
	female				diameter at origin																
					quadrant																
1049 15 62	69	R	5	142	distance along subclavian	63.1	68.8	70.8	75.5	84.9											
	F					0.444366	0.484	0.49859	0.53169	0.59788											
					diameter at origin	4.28	3.08	3.52	1.86	2.79											
					quadrant	MS	I	A	PS	SL											

	Age Sex	L/R	# of branches	Length	Measurement	Typical					TCT branches				CCT branches		Acc. VA	ITA/DSA	ITA/TCT	other	other #2
						VA	ITA	TCT	CCT	DSA	IT	SSA	TCA/SSA	A.Cerv	D.Cerv	SITA					
49 15 62	69	L	5	126	distance along subclavian	48.1	63.3	65.4		71.4						56.8					
	F					0.381746	0.5021	0.51904		0.56666						0.450794					
					diameter at origin	stenosed	2.31	1.95		2.53						2.93					
					quadrant	S	I	A		SL						P					
46 90 01	31	R	5	122	distance along subclavian	68.5	64.3	67.1	76.6	-										82.2	
	M					0.561475	0.527	0.55	0.62786											0.67377	
					diameter at origin	4.9	4.77	5.87	3.31											1.63	
					quadrant	S	I	A	PS											S	
46 90 01	31	L	6	97.4	distance along subclavian	40.6	45.7	47.8	48.3	73.5										55.8	
	M					0.416838	0.469	0.49076	0.49589	0.75462										0.572895	
					diameter at origin	4.76	3.8	3.41	3.71	3.54										1.37	
					quadrant	SM	AI	A	P	SP										S	
71 57 91	FOUR TY ONE	right			distance along subclavian																
					diameter at origin																
	female				quadrant																
71 57 91	FOUR TY ONE	left			distance along subclavian																
					diameter at origin																
	female				quadrant																
20 97 89	FOUR TY FOUR	right	N/A	100	distance along subclavian	56.5	58.7	?													
					diameter at origin	3.96	4.05														
	mal;e				quadrant	S	I														
20 97 89	44	L	4	83.6	distance along subclavian	41.8	49.8	46.4								39.4					
	M					0.5	0.59569	0.55502								0.471292					
					diameter at origin	4.01	3.27	4.39								1.74					
					quadrant	S	I	A								P					
85 73 42	85	R	4	116	distance along subclavian	65.3	63.6	63.6	72.5												
	F					0.562931	0.54827	0.54827	0.625												
					diameter at origin	3.56	1.44	2.75	1.28												
					quadrant	PS	AI	S	P												
85 73 42	85	L	5	95.4	distance along subclavian	41.8	45.9	49.2	51.7	64											
	F					0.438155	0.48113	0.51572	0.54192	0.67086											
					diameter at origin	2.01	2.23	2.49	1.47	2.15											
					quadrant	S	AI	A	PS	SL											
67 73 60	86	R	6	122	distance along subclavian	57.3	73.9		89.7	9.34	67.5	73.9									
	M					0.469672	0.60573		0.73524	0.07655	0.55327	0.605737									
					diameter at origin	2.93	2.34		2.83	2.51	2.04	2.52									
					quadrant	S	I		PS	SL	P	A									
67 73 60	EIGH TY ONE	left	N/A	102	distance along subclavian	41.2															
					diameter at origin	3.75															
	male				quadrant	S															
20 53 71	56	R	5	116	distance along subclavian	65.9	69.8	69.8	80.1	86.7											
	F					0.568103	0.60172	0.60172	0.69051	0.74741											
					diameter at origin	4.64	3.61	2.91	3.25	3.56											
					quadrant	S	I	A	SP	SL											
20 53 71	56	L	5	89.8	distance along subclavian	32.6	48	48	45.7	60.4											
	F					0.363029	0.53452	0.53452	0.5089	0.6726											
					diameter at origin	3.69	2.42	2.96	3.08	2.65											
					quadrant	S	AI	A	P	SL											
22 70 85	64	R	4	103	distance along subclavian	59.8	64.5	58.6	69.5												
	F					0.580583	0.62621	0.56893	0.67475												
					diameter at origin	3.58	3.94	2.87	2.93												
					quadrant	S	I	A	SP												

	Age Sex	L/R	# of branches	Length	Measurement	Typical					TCT branches				CCT branches		Acc. VA	ITA/DSA	ITA/TCT	other	other #2
						VA	ITA	TCT	CCT	DSA	IT	SSA	TCA/SSA	A.Cerv	D.Cerv	SITA					
22 70 85	64	L	5	78.2	distance along subclavian	10.9	35.8	38.3	39.5						49.8						
	F					0.139386	0.4578	0.48977	0.50511						0.636829						
					diameter at origin	2.3	2.3	4.06	3.86						2.06						
					quadrant	S	AI	A	P						S						
06 91 69	73	R	6	117	distance along subclavian	55.7	56.4	59.3	>	112					72	53.5					
	F					0.476068	0.48205	0.50683		0.95726					0.615385	0.457265					
					diameter at origin	3.13	3.48	2.81		3.7					1.36	1.92					
					quadrant	S	I	A		SL					S	S					
06 91 69	73	L	6	112	distance along subclavian	39	96.3	53	>	85.6					59.5	39.6					
	F					0.348214	0.85982	0.47321		0.76428					0.53125	0.353571					
					diameter at origin	6.66	2.9	3.74		4.26					2.97	1.59					
					quadrant	S	I	A		SL					S	P					
09 55 31	61	R	4	95.1	distance along subclavian	49	50.2	52.2	56.7												
	F					0.515247	0.52786	0.54889	0.59621												
					diameter at origin	3.24	2.39	2.59	2.13												
					quadrant	S	I	A	PS												
09 55 31	61	L	6	78.5	distance along subclavian	28	40.4	39.6	>	55.1					44.2	32.7					
	F					0.356688	0.51465	0.50445		0.70191					0.563057	0.416561					
					diameter at origin	3.8	1.95	2.77		2.53					1.59	1.58					
					quadrant	SM	I	A		SL					S	P					
94 37 84	72	R	5	127	distance along subclavian	72.3	69.9	70.6	82.6	113											
	F					0.569291	0.55039	0.5559	0.65039	0.88976											
					diameter at origin	2.78	3.99	3.61	2.46	3.03											
					quadrant	S	I	A	SP	SL											
94 37 84	72	L	6	97.7	distance along subclavian	34.3	40.3	42.5	46.4	57.4										54.5	
	F					0.351075	0.41248	0.435	0.47492	0.58751										0.55783	
					diameter at origin	4.04	3.66	2.9	2.3	2.39										1.65	
					quadrant	S	I	A	PS	PL										S	
11 17 57	63	R	5	108	distance along subclavian	50.2	64	62.1	70.3	86.5											
	F					0.464815	0.59259	0.575	0.65092	0.80092											
					diameter at origin	4.9	3.31	3.46	2.64	3.03											
					quadrant	S	I	A	SP	SL											
11 17 57	63	L	5	85.5	distance along subclavian	34.8	39	39.7	30.7	49.5											
	F					0.407018	0.45614	0.46432	0.35906	0.57894											
					diameter at origin	4.14	3.53	3.59	3.27	3.14											
					quadrant	SM	AI	A	P	SL											
67 47 05	70	R	7	124	distance along subclavian	52	78.3	>	77.3	100	65.4		71.3				66.3				
	M					0.419355	0.63145		0.62338	0.80645	0.52741		0.575				0.53467741				
					diameter at origin	3.79	1.86		1.77	1.75	2.54		3.23				3.43				
					quadrant	S	A			SL	SM		AL				S				
67 47 05	70	L	5	94.4	distance along subclavian	3.06	44.3	47.4		60.1				46.6							
	M					0.032415	0.46928	0.50211		0.63665				0.4936							
					diameter at origin	5.57	3.03	2.65		1.96				2.18							
					quadrant	LS	A	A		S				SP							
95 30 74	66	R	5	137	distance along subclavian	84.4	95.7	84.6	93.1	116											
	M					0.616058	0.69854	0.61751	0.67956	0.84671											
					diameter at origin	5.14	3.78	6.84	2.31	3.8											
					quadrant	PS	A	SA	PS	SL											
95 30 74	66	L	5	100	distance along subclavian	48.4	63.7	60.8	56	83.8											
	M					0.484	0.637	1.25619	0.87912	1.37828											
					diameter at origin	3.57	4.59	3.96	2.66	3.91											
					quadrant	SM	I	A	PS	SL											
85 28 52	51	R	5	121	distance along subclavian	77.1	82.4	78.4	78.4	88.7											
	F					0.63719	0.68099	0.64793	0.64793	0.73305											
					diameter at origin	4.39	4.2	4.54	2.71	3.63											
					quadrant	S	i	A	PS	SL											
85 28 52	51	L	6	70.3	distance along subclavian	24.9	33.9	34.7	26.6	45.5										39	
	F					0.354196	0.48221	0.49359	0.37837	0.64722										0.554765	
					diameter at origin	3.61	3.6	4.63	2.21	3.63										1.8	
					quadrant	S	I	A	P	SL										S	
29 65 39	53	R	5	117	distance along subclavian	67.2	62.9	65.5	72.6	86.3											
	F					0.574359	0.5376	0.55982	0.62051	0.7376											
					diameter at origin	4.76	4.39	3.2	2.14	3.39											
					quadrant	S	I	A	PS	SL											

	Age	L/R	# of branches	Length	Measurement	Typical					TCT branches				CCT branches		Acc. VA	ITA/DSA	ITA/TCT	other	other
	Sex					VA	ITA	TCT	CCT	DSA	IT	SSA	TCA/SSA	A.Cerv	D.Cerv	SITA					
02 38 30	58	R	5	111	distance along subclavian	63.6	78.8	77.5	85	92.6											
						0.572973	0.70991	0.69819	0.76576	0.83423											
					diameter at origin	4.04	2.95	3.6	2.6	2.81											
					quadrant	S	AIL	AS	SP	SP											
02 38 30	58	L	4	103	distance along subclavian	45.2	50.8		53.3	67.2									50.8		
						0.438835			0.51747	0.65242									0.49320388		
					diameter at origin	4.06	2.68		2.67	2.77									4.81		
					quadrant	SM	AI		P	SP									A		
96 55 34	55	R	4	123	distance along subclavian	62.3	66.1	62.5	71.1	off TCT											
						0.506504	0.53739	0.50813	0.57804												
					diameter at origin	3.88	4.14	4.7	3.13												
					quadrant	SM	IL	AS	P												
96 55 34	55	L	4	83.9	distance along subclavian	32.7	41.2	42.1	36.9	off TCT											
						0.38975	0.49106	0.50178	0.47556												
					diameter at origin	5.96	2.46	4.85	2.87												
					quadrant	M	AIL	A	P												
13 26 02	50	R	4	115	distance along subclavian	55.5	63.3	66.6		85.9											
						0.482609	0.55043	0.57913		0.74695											
					diameter at origin	4.78	4.46	3.26		2.5											
					quadrant	PSM	AIL	AS		SP											
13 26 02	50	L	3	77.6	distance along subclavian	AORTA	40.6	38.9	47.6												
							0.52319	0.50128	0.6134												
					diameter at origin		3.1	2.83	2.84												
					quadrant		AI	A	SP												
96 55 41	65	R	4	139	distance along subclavian	70	70	78.5	77.7												
						0.503597	0.50359	0.56474	0.55899												
					diameter at origin	5.73	4.03	4.38	3.24												
					quadrant	S	AL	AM	SP												
96 55 41	65	L	4	131	distance along subclavian	57.2			58.7	101.1									66.4		
						0.436641			0.44809	0.77175									0.50687022		
					diameter at origin	1.87			4.34	2.96									6.96		
					quadrant	S			P	S									A		
67 04 80	71	R	4	134	distance along subclavian	79.5	84.9	83.2	90.3												
						0.593284	0.63358	0.62089	0.67388												
					diameter at origin	3.57	2.6	3.24	1.06												
					quadrant	SM	IL	A	SP												
67 04 80	71	L	4	107	distance along subclavian	40	54.8	55.3		67.8					55	55					
						0.373832	0.51215	0.51682		0.63364					0.514019	0.514019					
					diameter at origin	4.6	3.5	3.82		3.66					2.3	1.83					
					quadrant	S	AIL	A		S					S	P					
84 57 29	74	R	4	112	distance along subclavian	58.3	71.2	71.2	62.9	TCT											
						0.520536	0.63571	0.63571	0.5616												
					diameter at origin	3.75	3.1	5.29	2.16												
					quadrant	SM	AI	AS	SP												
61 42 48	74	R	5	116	distance along subclavian	58.4	60.8	63.3	79.4	101											
						0.503448	0.52413	0.54569	0.68448	0.87069											
					diameter at origin	2.52	3.58	2.87	2.15	3.2											
					quadrant	M	AL	A	SP	SP											
61 42 48	74	L	5	84.9	distance along subclavian	33.7	41.9	46.1	55.3	71.6											
						0.396938	0.49352	0.54299	0.65135	0.84334											
					diameter at origin	3.15	4.39	3.55	2.22	3.11											
					quadrant	S	AI	A	P	SP											
56 47 10	67	R	5	152	distance along subclavian	88.5	92	97.5	108.7	117.1											
						0.582237	0.60526	0.64144	0.71513	0.77039											
					diameter at origin	4.74	3.07	2.55	3.04	3.64											
					quadrant	M	AL	A	SPM	S											
56 47 10	67	L	4	118	distance along subclavian	51.1	61.4	off ITA	60.2	83.9											
						0.433051	0.52033		0.51016	0.71101											
					diameter at origin	4.96	4.17		2.29	3.44											
					quadrant	S	I		P	S											
95 48 93	81	R	5	131	distance along subclavian	77	118	70.9	80.2	OFF TCT	68.4										
						0.587786	0.90076	0.54122	0.61221		0.52213										
					diameter at origin	5.11	3.51	4.03	3.08		3.37										
					quadrant	P	A	AS	P		S										
95 48 93	81	L	4	101	distance along subclavian	39.8	53.2	53.2	55.4	OFF CCT											
						0.394059	0.52673	0.52673	0.54851												
					diameter at origin	3.4	3.7	4.09	3.29												
					quadrant	SP	AI	A	P												
39 13 25	80	L	4	95.6	distance along subclavian	36.8	44.6	50.2		95											
						0.384937	0.46652	0.5251		0.99372											
	male				diameter at origin	6.17	4.19	6.42		2.97											
80 40 58	74	R	4	119	distance along subclavian	75.3	86.6	88.6	92.3											124	
						0.632773	0.72773	0.74453	0.77563											1.042017	
	male				diameter at origin	6.71	4.67	7.14	6.01											2.35	
	Age	L/R	# of branches	Length	Measurement	Typical					TCT branches				CCT branches		Acc. VA	ITA/DSA	ITA/TCT	other	other
	Sex					VA	ITA	TCT	CCT	DSA	IT	SSA	TCA/SSA	A.Cerv	D.Cerv	SITA					
16 88 16	81	R	5	133	distance along subclavian	83.9	81.4	83.9	95.7	117.3											
						0.630827	0.61203	0.63082	0.71954	0.88195											
					diameter at origin	5.15	3.6	3.16	2.56	2.98											
					quadrant	M	AL	A	P	S											
16 88 16	81	L	4	81	distance along subclavian	32			38.7	63.4									38.7		
						0.395062			0.47777	0.78271									0.47777777		
					diameter at origin	4.02			2.35	2.79									2.79		
					quadrant	M			SP	S									A		
24 92 93	55	R	3	107	distance along subclavian	66.5	73.57	77.6													
						0.621495	0.68757	0.72523													
					diameter at origin	4.43	4.34	6.12													
					quadrant	M	I	A													
24 92 93	55	L	3	79.6	distance along subclavian	AORTA	33	41												31	
							0.41457	0.51507												0.389447	
					diameter at origin		4.47	4.92												2.58	
					quadrant		I	A												S	
79 79 98	72	R	5	144	distance along subclavian	75	82.31	91.5	94.8	99.5											
						0.520833	0.56944	0.63541	0.65833	0.69097											
					diameter at origin	5.9	3.5	4.27	3.45	3.25											
					quadrant	SP	AL	A	S	S											
79 79 98	72	L	4	103	distance along subclavian	37.5	45.6	49.5	49.5												
						0.364078	0.44271	0.48058	0.48058												
					diameter at origin	5.35	3.54	3.77	4.24												
					quadrant	M	AL	A	SP												
88 66 55	53	R	4	118	distance along subclavian	59.6	100.3	67.66	72.34												
						0.505085	0.85	0.57339	0.61305												
					diameter at origin	3.8	3.31	3.19	2.65												
					quadrant	S	M	A	SP												
88 66 55	53	L	5	94.3	distance along subclavian	38.1	46.8	47.1	45.3	72.4											
						0.40403	0.49628	0.49947	0.48038	0.76776											
					diameter at origin	4.06	2.9	4.44	2.39	2.79											
					quadrant	M	AL	A	SP	L											
62 34 70	64	R	5	135	distance along subclavian	82.2	88.9	89.4	98.9	106.2											
						0.608889	0.65851	0.66222	0.73259	0.78666											
					diameter at origin	3.51	5.1	4.3	2.14	2.09											
					quadrant	S	AIL	A	SP	SP											
62 34 70	64	L	4	134	distance along subclavian	62.5	74.3		66.75	106.4									74.3		
						0.462963			0.49444	0.78814									0.55037037		
					diameter at origin	4.54	4.07		2.71	2.97									10.1		
					quadrant	S	AI		P	S									AI		
00 36 90	76	R	4	121	distance along subclavian	60.4		64.4	70.6	86.1		66.7									
						0.499174		0.53223	0.58347	0.71157		0.551239									
					diameter at origin	3.3		2.5	2.9	2.71		3.77									
					quadrant	S		S	P	SP		AIN									
00 36 90	76	L	5	94.7	distance along subclavian	OM AOR	40.6		42.7	63.3	40.6			48.7					40.6		
									0.45089	0.66842	0.42872			0.514256					0.42872228		
					diameter at origin		3.15		2.55	3.29	1.51			1.67					4.38		
					quadrant		AI		SP	P	ASM			S					AI		
10 32 30	42	R	5	104	distance along subclavian	54.1	58.8	59	63.5	88.4											
						0.520192	0.56538	0.5673	0.61057	0.85											
					diameter at origin	4.25	3.74	2.62	2.95	2.41											
					quadrant	S	AIL	AS	S	S											
10 32 30	42	L	5	90.1	distance along subclavian	36.1	42	42.8	40.4	69.5											
						0.400666	0.46614	0.47502	0.44839	0.77136											
					diameter at origin	3.73	3.6	3.21	2.46	2.41											
					quadrant	S	AL	AS	SP	S											
85 15 15	85	R	5	143	distance along subclavian	95.2	106	96.4	111.1	108											
						0.665734	0.74125	0.67412	0.77692	0.75524											
					diameter at origin	3.44	4.22	3.14	2.68	3.3											
					quadrant	PM	AI	S	P	S											
85 15 15	85	L	4	136	distance along subclavian	43.5	55.9	52.1	53.8												
						0.319853	0.41102	0.38308	0.39558												
					diameter at origin	5.55	7.69	4.64	2.67												
					quadrant	PM	A	S	P												
21 91 24	57	R	5	90.7	distance along subclavian	49.2	54.4	54.1	58.7	76.2											
						0.542448	0.59977	0.59647	0.64718	0.84013											
					diameter at origin	4.43	3	4.68	2.62	1.66											

	Age	L/R	# of branches	Length	Measurement	Typical					TCT branches				CCT branches		Acc. VA	ITA/DSA	ITA/TCT	other	oth
	Sex					VA	ITA	TCT	CCT	DSA	IT	SSA	TCA/SSA	A.Cerv	D.Cerv	SITA					
1180 40 58	74	L	3	109	distance along subclavian	48.6	60.2	58.2													
						0.445872	0.55229	0.53394													
	male				diameter at origin	3.09	4	6.8													
1143 81 61	60	R	5	122	distance along subclavian	74.5	81.5	75.9		95.2				84.1							
						0.610656	0.66803	0.62213		0.78032				0.6893							
	male				diameter at origin	5.36	4.49	4.34		4.01				2.89							
1195 77 67	56	R	5	131	distance along subclavian	83.4	74	78.7												96.7	1
						0.636641	0.56488	0.60076												0.738168	0.7
	male				diameter at origin	6.93	4.49	6.02												3.4	[illegible]
1195 77 67	56	L	4	104	distance along subclavian	40.5	52.2	55.2	57.8												
						0.389423	0.50192	0.53069	0.55576												
	male				diameter at origin	5.47	3.3	5.75	2.02												
1188 13 38	19	L	3	88.3	distance along subclavian	30.7	36.2	37.1													
						0.347678	0.40996	0.42015													
	female				diameter at origin	5.32	2.56	4.31													
1190 10 95	53	R	5	116	distance along subclavian	81.6	66.1	70	87.4											73.8	
						0.703448	0.56982	0.60344	0.75344											0.636207	
	male				diameter at origin	4.4	3.66	4.97	3.39											2.8	
1190 10 95	53	L	4	93.5	distance along subclavian	45.7	41		42.8	67.2											
						0.48877	0.4385		0.45775	0.71871											
	male				diameter at origin	4.67	4.82		3.57	3.08											
1151 49 28	89	R	5	143	distance along subclavian	73	70.35	78.1			63.5			82.5							
						0.51049	0.49195	0.54615			0.44405			0.5769							
	female				diameter at origin	4.76	3.46	4.24			2.86			2.13							
1151 49 28	89	L	4	89.9	distance along subclavian	32.7	35.7	35.7	61.3					47					35.7		
						0.363737			0.68186					0.5228					0.39710789		
	female				diameter at origin	6.79	3.2	3.96	3.06					2.95					4.68		
1190 17 35	77	R	4	134	distance along subclavian	68	73.5	86.9	95.7												
						0.507463	0.5485	0.6485	0.71417												
	female				diameter at origin	2.83	2.72	2.91	2.59												
1190 17 35	77	L	3	119	distance along subclavian	48.8		64.1										58.4			
						0.410084		0.53865										0.4907563			
	female				diameter at origin	5.74	3.71	3.62		3.39								5.79			
1190 64 27	44	R	5	103	distance along subclavian	48	53.3	59.1	57.7	63.8											
						0.466019	0.51747	0.57378	0.56019	0.61941											
	female				diameter at origin	4.1	2.7	3.1	1.9	2.17											
1190 64 27	44	L	4	83.1	distance along subclavian	50	59.7	59.7	75.1												
						0.601685	0.71841	0.71841	0.90373												
	female				diameter at origin	3.3	3.2	2.24	2.29												
1061 84 97	53	R	5	136	distance along subclavian	58.6	75.8	81.2	87	108.9											
						0.430882	0.55735	0.59705	0.63976	0.80073											
	female				diameter at origin	4.3	3.3	2.4	2.48	2.86											
1061 84 97	53	L	4	114	distance along subclavian	49.4				75.9									55	58.7	
						0.433333				0.66578									0.48245614	0.514912	
	female				diameter at origin	4.35	2.56	3.45		2.4									3.81	2.2	
1021 82 51	52	R	5	115	distance along subclavian	55.3	59.5	60.6	67.9	88											
						0.48087	0.51739	0.52695	0.59043	0.76521											
					diameter at origin	5.13	2.85	4.62	3.15	3.18											
1179 48 37	67	R	4	128	distance along subclavian	70.1	77.1	78.8	100												
						0.547656	0.60234	0.61562	0.78125												
					diameter at origin	5.21	3.42	8	4.41												
1179 48 37	67	L	3	101	distance along subclavian	54.2	54.4	59.7													
						0.536634	0.53861	0.59108													
					diameter at origin	5.5	2.93	5.42													
1000 42 87	75	R	5	141	distance along subclavian	87	98	92.73	110.2											97.2	
						0.617021	0.69503	0.65766	0.78156											0.689362	
					diameter at origin	3.09	1.62	4.11	2.72											2.31	

Appendix B

Sequentially ordered branch origins of the subclavian artery (from Appendix A)

PIN	Age	L/R	Typical					TCT branches				CCT branches		Acc. VA	ITA/DSA	ITA/TCT
	Sex		VA	ITA	TCT	CCT	DSA	IT(3a)	SSA(3b)	TCA/SSA(3c)	A.Cerv(3d)	D.Cerv(4b)	SITA(4a)			
1007 02 57	48	R	1	3	2	3	4									
	F															
		L	1	3	4	2	6					5				
1196 58 00	50	R	1	4	2	3	5									
	M															
		L	1	3	2	4	5									
1192 92 10	47	R	2	3				1				4				
	M															
		L	2	3	3		4						1			
1059 16 90	85	R	1	2	3	4										
	M															
		L	1	2	2	3										
1060 84 38	58	R	1	2	2	3										
	F															
		L	1	2	3	1										
1136 39 22	59	R	1	4	2	3	5									
	M															
		L	1	3	4	2	6					5				
1065 31 82	92	R	1	2	3		6	2				5	4			
	M															
		L	1	4	3							2				
1128 31 60	51	R	1	3	1	2							4			
	M															
		L	1	3	3	2										
1038 00 44	68	R	1	4	5	3		2								
	F															
1038 00 44	IXTY EIGH	left														
	female															
1049 15 62	69	R	1	2	3	4	5									
	F															
		L	1	3	4		5						2			
1046 90 01	31	R	3	1	2	4										
	M															
		L	1	2	3	4	5									
1171 57 91	OURTY ON	right														
	female															
		left														
1120 97 89	OURTY FOU	right														
	male															
1120 97 89	44	L	2	4	3								1			
	M															
1085 73 42	85	R	2	1	1	3										
	F															
		L	1	2	3	4	5									

Note: Yellow highlighted values represent vessel origins arising within 0.5mm

PIN	Age	L/R	Typical					TCT branches				CCT branches		Acc. VA	ITA/DSA	ITA/TCT
	Sex		VA	ITA	TCT	CCT	DSA	IT(3a)	SSA(3b)	TCA/SSA(	A.Cerv(3d)	D.Cerv(4b)	SITA(4a)			
1067 73 60	86	R	1	3		4		2	3							
	M															
1067 73 60	EIGHTY ON	left														
	male															
1020 53 71	56	R	1	2	2	3	4									
	F															
		L	1	3	3	2	4									
1122 70 85	64	R	2	3	1	4										
	F															
		L	1	2	3	4						5				
1006 91 69	73	R	2	3	4		6					5	1			
	F															
		L	1	6	3		5					4	2			
1009 55 31	61	R	1	2	3	4										
	F															
		L	1	4	3		6					5	2			
1194 37 84	72	R	3	1	2	4	5									
	F															
		L	1	2	3	4	5									
1011 17 57	63	R	1	3	2	4	5									
	F															
		L	2	3	4	1	5									
1167 47 05	70	R	1	5		4	6	2		3						
	M															
		L	1	2	4		5				3					
1195 30 74	66	R	1	3	1	2	4									
	M															
		L	1	4	3	2	5									
1185 28 52	51	R	1	3	2	2	4									
	F															
		L	1	3	4	2	5									
1029 65 39	53	R	3	1	2	4	5									
	F															
		L	1	2	3	4	5									
1116 88 16	81	R	2	1	3	4	5									
	F															
		L	1	>	>	2	3									
1024 92 93	55	R	1	2	3											
		L	AORTA	2	3											
1079 79 98	72	R	1	2	3	4	5									
		L	1	2	3	3										
1088 66 55	53	R	1	4	2	3										
		L	1	3	4	2	5									

PIN	Age	L/R	Typical					TCT branches				CCT branches		Acc. VA	ITA/DSA	ITA/TCT
	Sex		VA	ITA	TCT	CCT	DSA	IT(3a)	SSA(3b)	TCA/SSA(	A.Cerv(3d)	D.Cerv(4b)	SITA(4a)			
1079 79 98	72	R	1	2	3	4	5									
		L	1	2	3	3										
1088 66 55	53	R	1	4	2	3										
		L	1	3	4	2	5									
1062 34 70	64	R	1	2	3	4	5									
		L	1	3	3	2	4									
1000 36 90	76	R	1	3	2	4	5									
		L	AORTA	1	1	2	4	1			3					
1110 32 30	42	R	1	2	2	3	4									
		L	1	3	4	2	5									
1085 15 15	85	R	1	3	2	5	4									
		L	1	4	2	3										
1021 91 24	57	R	1	3	2	4	5									
		L	1	4	2	3	5									
1102 38 30	58	R	1	3	2	4	5									
		L	1			3	4									2
1196 55 34	55	R	1	3	2	4										
		L	1	3	4	2										
1113 26 02	50	R	1	2	3		4									
		L	AORTA	2	1	3										
1196 55 41	65	R	1	1	3	2										
		L	1			2	4									3
1167 04 80	71	R	1	3	2	4										
		L	1	2	3		4									
1084 57 29	74	R	1	3	3	2										
1161 42 48	74	R	1	2	3	4	5									
		L	1	2	3	4	5									

PIN	Age	L/R	Typical					TCT branches				CCT branches		Acc. VA	ITA/DSA	ITA/TCT
	Sex		VA	ITA	TCT	CCT	DSA	IT(3a)	SSA(3b)	TCA/SSA(	A.Cerv(3d)	D.Cerv(4b)	SITA(4a)			
1156 47 10	67	R	1	2	3	4	5									
		L	1			2	4									3
1095 48 93	81	R	2	4	1	3										
		L	1	2	2	3										
1039 13 25	80	L	1	2	3		4									
	male															
1180 40 58	74	R	1	2	3	4										
		L	1	3	2											
1143 81 61	60	R	1	3	2		5				4					
	male															
1195 77 67	56	R	3	1	2											
	male	L	1	2	3	4										
1188 13 38	19	L	1	2	3											
	female															
1190 10 95	53	R	4	1	2	5		3								
	male	L	3			2	4									1
1151 49 28	89	R	3	2	4			1			5					
	female	L	1			4					3					2
1190 17 35	77	R	1	2	3	4										
	female	L	2		3										1	
1190 64 27	44	R	1	2	3	4	5									
	female	L	1	2	2	3										
1061 84 97	53	R	1	2	3	4	5									
	female	L	1				4				3					2
1021 82 51	52	R	1	2	3	4	5									
1179 48 37	67	R	1	2	3	4										
		L	1	1	2											
1000 42 87	75	R	1	3	2	4										

Appendix C

Measurements of the subclavian artery branching origin distances for interrater reliability

Patient PIN	Branch Name	Examiner 1 (Juwan)	Examiner 2 (Oonagh)
1161 42 48	L VA	38.95%	39.69%
	R VA	49.37%	50.34%
1095 48 93	L VA	35.54%	39.41%
	R VA	61.18%	58.78%
1180 40 58	L VA	43.04%	44.59%
	R VA	58.26%	63.28%
1156 47 10	L VA	47.92%	43.31%
	R VA	52.18%	58.22%
1195 77 67	L VA	40.50%	38.94%
	R VA	54.34%	63.66%
1161 42 48	L ITA	46.96%	49.35%
	R ITA	53.60%	52.41%
1095 48 93	L ITA	46.73%	52.67%
1180 40 58	L ITA	58.14%	55.23%
	R ITA	68.18%	72.77%
1156 47 10	L ITA	56.42%	52.03%
	R ITA	54.55%	60.53%
1195 77 67	L ITA	53.07%	50.19%
	R ITA	55.12%	56.49%
1161 42 48	L TCT	49.60%	54.30%
	R TCT	56.58%	54.57%
1095 48 93	L TCT	48.71%	52.67%
	R TCT	58.75%	54.12%
1180 40 58	L TCT	58.14%	53.39%
	R TCT	65.04%	74.45%
1156 47 10	R TCT	58.08%	64.14%
1195 77 67	L TCT	53.07%	53.08%
	R TCT	55.58%	60.08%
1161 42 48	L CCT	57.73%	65.14%
	R CCT	68.74%	68.45%
1095 48 93	L CCT	52.18%	54.85%
	R CCT	66.91%	61.22%
1156 47 10	L CCT	51.50%	51.02%
	R CCT	62.76%	71.51%
1195 77 67	LCCT	58.81%	55.58%
1161 42 48	L DSA	76.52%	84.33%
	R DSA	74.50%	87.07%
1156 47 10	L DSA	70.42%	71.10%
	R DSA	70.51%	77.04%

Appendix D

Measurements of the distance of anterior scalene muscle to the origin of the vertebral artery

PIN #	L/R	VA-ASM distance †	SCA length*	VA Origin Distance* †	VA Origin Distance (% of SCA)	ASM position on SCA (mm)	ASM position on SCA (%)
1029 65 39	L	9.43	92	42.7	46.4	52.1	0.567
	R	9.43	117	67.2	57.4	76.6	0.655
1194 37 84	L	19.6	97.7	34.3	35.1	53.9	0.552
	R	12.8	127	72.3	56.9	85.1	0.670
1011 17 57	L	11.5	85.5	34.8	40.7	46.3	0.542
	R	19.4	108	50.2	46.5	69.6	0.644
1116 88 16	L	10.3	81	32	39.5	42.3	0.522
	R	13.6	133	83.9	63.1	97.5	0.733
1167 47 05	L	47.3	94.4	3.06	3.2	50.4	0.533
	R	25.8	124	52	41.9	77.8	0.627
1122 70 85	L	45.6	78.2	10.9	13.9	56.5	0.723
	R	4.71	103	59.8	58.1	64.5	0.626
1088 66 55	L	21.3	94.3	38.1	40.4	59.4	0.630
	R	10.7	118	59.6	50.5	70.3	0.596
1062 34 70	L	15.5	134	62.5	46.6	78.0	0.582
	R	11.2	135	82.2	60.9	93.4	0.692
1085 15 15	L	24	136	43.5	32.0	67.5	0.496
	R	28.5	143	95.2	66.6	123.7	0.865
1021 91 24	L	12	91.9	40.6	44.2	52.6	0.572
	R	8.59	90.7	49.2	54.2	57.8	0.637
1102 38 30	L	20.5	103	45.2	43.9	65.7	0.638
	R	19.7	111	63.6	57.3	83.3	0.750
1196 55 34	L	14.1	83.9	32.7	39.0	46.8	0.558
	R	10.9	123	62.3	50.7	73.2	0.595
1196 55 41	L	18.2	131	57.2	43.7	75.4	0.576
	R	11.3	139	70	50.4	81.3	0.585
1167 04 80	L	25	107	40	37.4	65.0	0.607
	R	10.2	134	79.5	59.3	89.7	0.669
1161 42 48	L	18.6	84.9	33.7	39.7	52.3	0.616
	R	16.9	116	58.4	50.3	75.3	0.649
1156 47 10	L	13.1	118	51.1	43.3	64.2	0.544
	R	14	152	88.5	58.2	102.5	0.674
1095 48 93	L	20.3	101	39.8	39.4	60.1	0.595
	R	4.69	131	77	58.8	81.7	0.624
1195 77 67	L	18.2	104	40.5	38.9	58.7	0.564
	R	11.8	131	83.4	63.7	95.2	0.727
1113 26 02	L	43.4	77.6	AORTA	0.0	43.4	0.559
	R	15.1	115	55.5	48.3	70.6	0.614
1024 92 93	L	46	79.6	AORTA	0.0	46.0	0.578
	R	9.44	107	66.5	62.1	75.9	0.710
1000 36 90	L	50.8	94.7	AORTA	0.0	50.8	0.536
	R	12.7	121	60.4	49.9	73.1	0.604
1143 81 61	L*	-	-	-	-	-	-
	R	13.1	122	74.5	61.1	87.6	0.718
1188 13 38	L	9.5	88.3	30.7	34.8	40.2	0.455
	R*	-	-	-	-	-	-
1190 10 95	L	7.81	93.5	45.5	48.7	53.3	0.570
	R	3.91	116	76.6	66.0	80.5	0.694
1151 49 28	L	14.3	89.9	32.7	36.4	47.0	0.523
	R	17.5	143	73	51.0	90.5	0.633
1190 64 27	L	25.4	83.1	50	60.2	75.4	0.907
	R	15.6	103	48	46.6	63.6	0.617
1061 84 97	L	18	114	49.4	43.3	67.4	0.591
	R	28.9	136	58.6	43.1	87.5	0.643
1179 48 37	L	17.5	101	54.2	53.7	71.7	0.710
	R	21.1	128	70.1	54.8	91.2	0.713
1000 42 87	L*	-	-	-	-	-	-
	R	14.4	141	87	61.7	101.4	0.719
1060 84 38	L	0	78.3	36.9	47.1	36.9	0.471
	R	10.3	105	65.5	62.4	75.8	0.722
1136 39 22	L	17.9	97.3	40.1	41.2	58.0	0.596
	R	5.97	121	68.9	56.9	74.9	0.619
1065 31 82	L	11.9	94.3	47.8	50.7	59.7	0.633
	R	12.9	146	88.2	60.4	101.1	0.692
1128 31 60	L	16	80.1	36.8	45.9	52.8	0.659
	R	7.04	107	67	62.6	74.0	0.692
1038 00 44	L	20.1	83.9	24.6	29.3	44.7	0.533
	R	16.2	120	65	54.2	81.2	0.677
1049 15 62	L	21.7	126	48.1	38.2	69.8	0.554
	R	13.7	142	63.1	44.4	76.8	0.541
1046 90 01	L	15.7	97.4	40.6	41.7	56.3	0.578
	R	6.87	122	68.5	56.1	75.4	0.618
1171 57 91	5	-	-	-	-	-	-
	R	9.72	84.6	37.1	43.9	46.8	0.553
1120 97 89	L	9.37	83.6	41.8	50.0	51.2	0.612
	R	9.45	100	56.5	56.5	66.0	0.660
1085 73 42	L	15.8	95.4	41.8	43.8	57.6	0.604
	R	9.12	116	65.3	56.3	74.4	0.642
1067 73 60	L	20.1	102	41.2	40.4	61.3	0.601
	R	20.3	122	57.3	47.0	77.6	0.636
1020 53 71	L	23.4	89.8	32.6	36.3	56.0	0.624
	R	15.6	116	65.9	56.8	81.5	0.703
1006 91 69	L	23.2	112	39	34.8	62.2	0.555
	R	20.2	117	55.7	47.6	75.9	0.649
1009 55 31	L	13.1	78.5	28	35.7	41.1	0.524
	R	6.6	95.1	49	51.5	55.6	0.585
1195 30 74	L	10.5	100	48.4	48.4	58.9	0.589
	R	16.6	137	84.4	61.6	101.0	0.737
1185 28 52	L	9.93	70.3	24.9	35.4	34.8	0.495
	R	9.45	121	77.1	63.7	86.6	0.715
1007 02 57	L	18.9	95	29.5	31.1	48.4	0.509
	R	6.88	109	59.1	54.2	66.0	0.605
1196 58 00	L	17.8	108	51.5	47.7	69.3	0.642
	R	13.3	135	82.1	60.8	95.4	0.707
1192 92 10	L	21.7	96	30.7	32.0	52.4	0.546
	R	12.4	126	67.7	53.7	80.1	0.636
1059 16 90	L	8.77	121	66.1	54.6	74.9	0.619
	R	13.7	151	99.4	65.8	113.1	0.749
1110 32 30	L	14.4	90.1	36.1	40.1	50.5	0.560
	R	8.59	104	54.1	52.0	62.7	0.603
1079 79 98	L	22.1	103	37.5	36.4	59.6	0.579
	R	18.1	144	75	52.1	93.1	0.647

Legend
Yellow: Extremely proximal origin of VA
Orange: Extremely distal origin of VA
Purple: CTA missing

† the sum of these values was used to calculate ASM position on SCA

* values taken from Appendix A

Appendix E

Measurements of the supraclavicular triangle from fresh cadavers #1945 and #1956

1945

	LEFT				RIGHT			
	trial	A-B	A-C	B-C	trial	A-B	A-C	B-C
normal	1	81.77	143.34	106.47	1	81.13	144.55	115.49
	2	79.78	143.36	103.64	2	80.73	145.48	117.97
	3	78.29	143.6	105.81	3	81.67	146.01	114.82
protraction	1	83.62	142.98	118.71	1	87.42	143.74	134.5
	2	82.37	143.61	120.17	2	87.21	144.07	133.47
	3	82.39	143.17	121.19	3	86.51	143.8	129.6
retraction	1	79.95	143.35	100.62	1	83.85	145.95	107.82
	2	81.17	143.1	99.35	2	83.99	146.77	106.54
	3	80.76	143.7	99.73	3	84.41	145.87	108.22

1956

	LEFT				RIGHT			
	trial	A-B	A-C	B-C	trial	A-B	A-C	B-C
normal	1	93.31	147.70	76.71	1	92.20	147.80	79.67
	2	93.18	147.20	78.32	2	92.20	150.22	77.59
	3	93.60	147.88	77.50	3	90.67	147.87	78.42
protraction	1	99.02	140.83	97.35	1	94.65	143.85	105.71
	2	99.04	140.69	98.07	2	94.07	143.90	103.22
	3	99.31	140.72	98.45	3	94.43	143.52	102.78
retraction	1	95.60	149.00	68.60	1	90.53	147.86	76.37
	2	94.63	147.89	67.53	2	91.52	147.65	78.23
	3	94.33	148.42	69.62	3	91.38	148.65	80.77

Curriculum Vitae

Name:	Juwan Ryu
Post-secondary Education and Degrees:	Western University London, Ontario, Canada 2014-2016 M.Sc. The University of Western Ontario London, Ontario, Canada 2009-2014 B.MSc.
Honours and Awards:	Dean's Honor List 2009, 2011, 2012, 2013 Western Graduate Research Scholarship 2014-2016
Related Work Experience	Teaching Assistant Western University 2014-2016 - Mammalian Histology - Gross Anatomy for Physical Therapy - Human Physiology - Gross Anatomy for Medicine Years 1 & 2